NTNU

Norwegian University of
Science and Technology

Parameter Estimation and Control of a Dual Gradient Managed Pressure Drilling System

Bård Arve Valstad

Master of Science in Engineering Cybernetics
Submission date: June 2009
Supervisor: Ole Morten Aamo, ITK

Norwegian University of Science and Technology
Department of Engineering Cybernetics

Problem Description

In MPD it is important to control the downhole pressure accurately within given narrow pressure margins for a set of normal operations. However, the availability of downhole pressure measurements during drilling is often not so good. Therefore, the current solution is to estimate this pressure with a hydraulic model that has several unknown parameters. The objective of this work is to continue the development of models and estimation schemes.

1) Give an overview of dual MPD, and motivation for the thesis.

2) Consider to extend of the model developed in the project work with compressibility and more flexible friction modeling.

3) Derive an augmented Kalman filter for online estimation of unknown parameters with the following premises:

a - Pressure at bit is measured continuously
b - Pressure at bit is measured every 20-30 seconds

4) Compare pressure drop calculations for simplified model versus WeMod

5) Perform the simulations with both air and water in the riser

6) If time permits: Develop a controller for pressure control, and simulate relevant cases in WeMod

Assignment given: 12. January 2009
Supervisor: Ole Morten Aamo, ITK

Summary

The increasing demand for oil and gas in the world, and the fact that most of the easily accessible reservoirs are in production or already abandoned, result in a need to develop new resources. These may be new reservoirs that have previously been considered uneconomical or impossible to develop, or extended operation of existing fields. Developing smaller reservoirs, means that more wells have to be drilled per barrel, which gives both more and eventually greater challenges as more and more wells are drilled because the wells has to be drilled further and into more difficult formations. Mature fields are drained, which leads to lowering of reservoir pressure and therefore tighter pressure margins for drilling.

Because of the challenges with deep water drilling and depleted reservoirs, there is a need to precisely control the pressure profile in the well during drilling in such formations. Some of the parameters that are needed to control the well precisely are not easily obtained during drilling, and an estimation of these will therefore be crucial to be able to use a model to control the well. The transmission of measurements from a well is also often either delayed or absent during periods of drilling, which will cause problems for the control of the well. It is therefore required that an estimation scheme is able to estimate the pressure in the well for the time interval between the updates of the measurements from the well. The conventional method for transmitting measurements from the bottom of the well is by mud pulse telemetry which is pressure waves transmitted through the drilling mud. These measurements will be delayed, so accurate real-time measurements will never be available.

To estimate the bottom hole pressure, a extended kalman filter was evaluated. This filter is based on a simple mathematical model derived for the drilling process. The states in the filter is height of mud in the riser, mud weight and different friction factors for the well. The filter is tested when the measurements are continuous available, with delayed update of the bottom hole measurement, and for cases where one of the measurements are absent. A simple controller to control the bottom hole pressure is implemented to control the pressure for reference tracking and during a simulated pipe connection. During simulations, it was not possible to achieve convergence for the friction factor for normal flows, and this led to errors in the other states. The friction factor would only converge to its true value during very high flows during the nominal testing, which led to the other states also achieving their correct values. The problem in estimating the friction factor applied to all different forms for friction parameters. The kalman filter was tested against an artificial well simulated in WeMod, and gave decent estimates of the bottom hole pressure except for at low flows.

Preface

This master thesis has been written in my 10th and final semester of my master of technology studies at the Department of Engineering Cybernetics, Faculty of Information Technology, Mathematics and Electrical Engineering at the Norwegian University of Science and Technology. I would like to thank my supervisor Professor Ole Morten Aamo at NTNU for his guidance and help. I would also like to thank co-supervisor Dr. John-Morten Godhavn at StatoilHydro for answering my questions regarding the thesis and for the feedback he has given me on my work. Finally I would like to thank Øyvind Breyholtz at the International Research Institute of Stavanger for helping me with matters regarding WeMod and Øyvind Stamnes at NTNU.

Contents

1 Background **1**

1.1 Pressure Problems . . . 2

1.1.1 Pressure Control . . . 2

1.2 Drilling Fluids . . . 4

1.3 Measurement of Bottom Hole Pressure . . . 5

1.3.1 Wired drill pipe . . . 5

1.3.2 Estimation . . . 6

1.4 Managed Pressure Drilling . . . 6

1.5 Dual Gradient Drilling . . . 6

2 Patents **9**

2.1 AGR . . . 9

2.2 Ocean Riser System . . . 10

2.3 Hollow Glass Spheres . . . 10

2.4 Mud Dilution with gas . . . 11

2.5 Mud Dilution with liquid . . . 11

3 Modeling **13**

3.1 Equations for the AGR system . . . 13

3.2 Equations for the ORS system . . . 15

4 Friction **17**

4.1 Friction AGR . . . 17

4.2 Friction ORS . . . 17

4.3 Piecewise linear models for friction . . . 19

5 Derivation of the Kalman Filter **21**

5.1 Augmented model for the AGR system . . . 21

5.2 Augmented model for the ORS system 22

6 Nominal testing **25**

6.1 AGR model 25

6.2 Testing of the model with higher flow 29

6.3 ORS system 32

6.4 Delayed measurement 35

6.4.1 AGR system with delayed measurement 35

7 WeMod simulations **39**

7.1 Continuous measurement update 39

7.1.1 AGR simulations 40

7.1.2 ORS simulations 43

7.2 Delayed measurement update 46

7.2.1 AGR simulation 46

7.2.2 AGR simulation with higher flow 50

7.2.3 ORS simulation 53

7.3 Use of different filters for different flows 62

8 Control **65**

8.1 Control of the AGR system 65

8.2 Control of the ORS system 68

9 Conclusions and future work **75**

9.1 Conclusions 75

9.2 Future work 76

A Kalman filter theory **79**

A.1 Discretization of model 79

A.2 Kalman filter theory 79

A.3 Discrete Kalman filter 79

A.4 Extended Kalman Filter 80

Chapter 1

Background

Oil and gas has become one of the most important resources in the world. It is used in all type of applications from fuel, cooking, lubrication and production of electricity, to production of plastic, paint, asphalt and numerous other products. The demand for oil has risen considerably in the last decades, but oil and gas is not a renewable energy source, and therefore there are limits to how much we can produce and therefore use. Most of the reservoirs which are easiest to produce are already found and many of them are abandoned or in tail production. Therefore, new wells must be drilled, and many of these are wells which previously have been seen as impossible or uneconomical to drill. Despite the investment in drilling rigs that can operate in water depths up to 3000 meters and more, much of the potential oil and gas resources in reservoirs at these depths cannot be developed without new ways to lower hydrostatic mud pressure to prevent fracturing in shallow zones. Ultra deep water drilling possess several problems, including shallow water flows, lost circulation and loss of well control. Any of these may prevent a well objective from being reached. To avoid these problems, it has been necessary to run multiple casing strings. That means that the production string may be too small for high rate wells and for horizontal or multilateral completions that might be necessary to make a discovery economic. The small margin between pore pressure and fracture gradients is at the root of these problems.

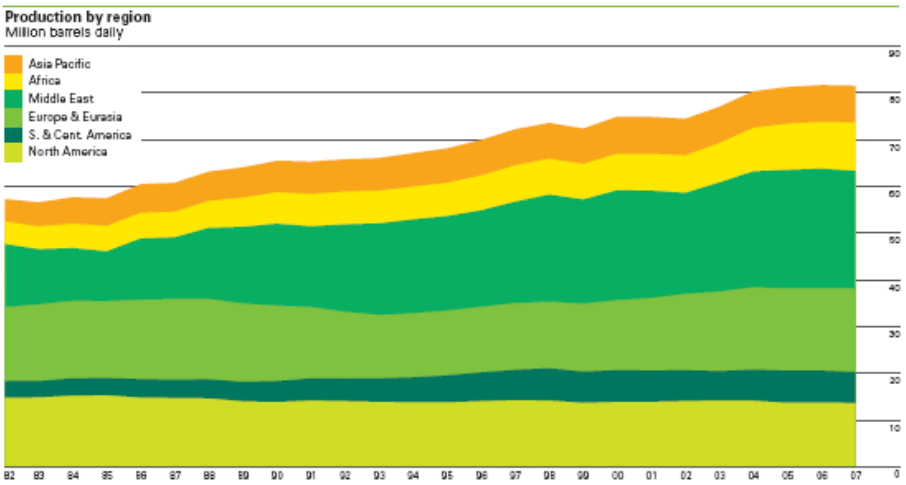

Figure 1.1: Worldwide production of oil

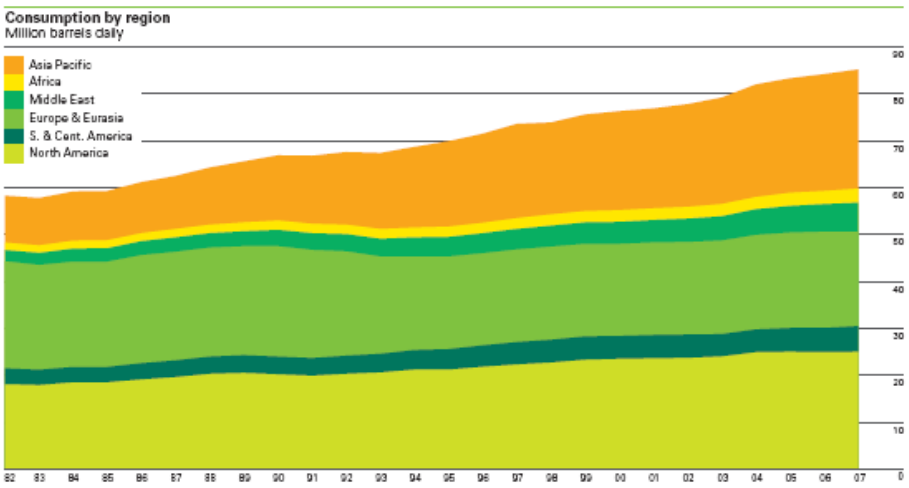

Figure 1.2: Worldwide demand for oil

1.1 Pressure Problems

All formations are porous to some degree. The pores can contain fluids such as hydrocarbons, water or a mixture of these. These fluids exert a pressure which is called pore pressure. The combined weight of formation materials and fluids in the formation which lie above any particular depth is called the total overburden pressure. The formation pressure of the fluid is the pressure which exists within the pores of a rock formation. This is called reservoir pressure within hydrocarbon reservoirs. The formation pressure must be less than the total overburden pressure for the fluid to be kept in the reservoir. Fracture pressure is the pressure at which injection of fluids will cause the rock formation to fracture hydraulically. The pressure which causes a well to deform as a result of differential pressure acting form outside to inside of the well is called collapse pressure. The collapse pressure is relatively high when the well is perfectly circular, but can decrease significantly if the well is slightly oval. The relations between these pressures are

$$p_{collapse} < p_{reservoir} < p_{fraction}$$

1.1.1 Pressure Control

In order to overbalance the pore pressure, drilling fluid with adequate density is circulated into the bore hole [2]. If the pressure in the annulus exceeds the fracture gradient, the following problems can occur: First and most dangerous is that if only a short string of casing has been set, a fracture can extend to the surface causing a blow-out around the rig. The second problem resulting from fracturing the formation is the possibility of a down hole blow out. This means that the fluids flow into other formations and not to the surface, which can lead to obstructions in the well bore, damage on reservoir and loss of fluids. If the pressure in the well is lower than the collapse pressure, this can lead to a case where the walls of the well falls into the well, which can cause problems with stuck and broken pipes. A result of a twist-off of the pipe can be that the well has to be drilled again.

The goal for the pressure in the well in ordinary drilling operations will be defined by

$$p_{collapse} < p_{reservoir} < p_{well} < p_{fraction}$$

Drilling with a pressure in the well above the reservoir pressure, is a method denoted as over-balanced drilling. This leads to some loss of fluids from the well bore to the reservoir. This loss will usually be small as long as the pressure in the well is kept below the fraction-pressure. If the pressure in the well is less than in the reservoir so that

$$p_{collapse} < p_{well} < p_{reservoir} < p_{fraction}$$

there will be an influx from the reservoir to the well. This is called underbalanced drilling and causes a lowering of the mud weight. The mud is said to be "gas cut", "salt water cut" or "oil cut" depending on the fluids mixing with the mud. If the influx is large, the problem is known as a kick or in severe cases, blow outs can occur. The causes for influx to the well is:

- Drilling mud density is too low. The hydrostatic pressure in the well becomes lower than the formation pressure.
- Swabbing occurs when the drill string is being pulled upward in the well. This can for instance happen when a joint of pipe is added or when a bit is changed.
- The drilling mud level in the annulus gets too low, with the result that the pressure in the well is lowered. The low mud level may be because the hole is insufficiently filled during a trip or because of mud losses into the formation.
- The bit grinds up porous rocks. This risk is not the same since as soon drilling has ceased, there is no more influx.

Risk of a kick or the fact that a kick is occurring can be indicated by several signs. These can be summarized as:

- Sudden increase in rate of penetration, which can occur if the bit penetrates a porous or fractured formation or the differential pressure between the pressure exerted by the column of mud in the well and the formation pressure decreases.
- If the volume of mud used to replace the volume of steel when the drill pipe is tripped out of the well is less than the volume of steel, this can indicate a fluid kick.
- Loss of mud to the formation around the well lowers the pressure in the well and can lead to a kick.
- Gas mixed with the mud can be considered as a sign for a kick, but can have several causes.
- An increase in fluid level at the surface can indicate a fluid kick in the well.

U-tubing is an effect that occurs because the pressure in the annulus at the wellhead is significantly less than the pressure inside the drill string at the same depth. This is caused by the fact that the dual gradient only exists in the annulus, whereas the drill string is filled with mud from the surface to total depth. This will result in mud flowing from the drill string out to the annulus until the pressure is the same in the annulus and the drill string when the mud pump at the drill string stops. To prevent this, a drill string valve (DSV) is developed to shut in the well when the mud pump has stopped. This means that the mud will stay in the drill string, and the fluids in the annulus will be separated from the fluids in the drill string. The DSV is essentially a pressure-balanced drill pipe float with a very large spring. In operation, the basic effect is to shut a valve in the drill pipe at any point below the sea floor when circulation stops, and open it when circulation starts. At drilling circulation rates, the DSV is held open with a very small pressure drop.

1.2 Drilling Fluids

Drilling fluids are often divided into three categories [3]. These are

- Non water based
- Water based
- Pneumatic

Non water based fluids consist of synthetic fluids, and diesel and mineral oil. Water based fluids include colloidal clay, clay and polymer and polymer fluids. The last category, pneumatic fluids, includes dry gas, mist, foam and gasified mud. Drilling fluids has several functions in the well [4] [5]. These can be summarized as

- Transporting cuttings to the surface
- Suspending the cuttings when circulation is stopped
- Cooling and lubricating the bit and drill string
- Consolidating the walls of the hole
- Preventing inflows of formation fluids into the well
- Acting as a drilling parameter
- Transmitting power to down hole motor
- Providing geological information
- Minimize corrosion of the drill string, casing and tubing
- Controlling the pressure in the well
- Making measurements possible

Transporting the cuttings which are removed below the bit is essential for a mud system. The fluid velocity in the annulus must exceed the downward falling rate of the cuttings. Mud weight, viscosity, suspension and gelation properties of the mud affect its carrying properties. Laminar and turbulent flow regimes also exhibit different lifting capabilities. When circulation of the drilling fluid is stopped during for instance a pipe connection, the cuttings are no longer carried upwards in the annulus. It is then the thixotropix properties of the mud that **keeps the cuttings suspended** by gelling. During drilling, a considerable amount of heat is generated due to friction. Mud can help **transmit this heat to the surface** as well as **lubricate the well bore**. Mud filters into permeable formations and deposits a **film of colloidal particles** on the walls of the hole. This isolates the formation from the drilling fluids and can allow for longer stretches of uncased hole to be drilled because it stabilizes the formation. The drilling fluid also exerts a hydrostatic pressure that **prevents fluids from the reservoir to flow into the well** as long as the pressure in the well remains higher than the pressure of formation fluids. In such a way, the mud is considered as the first blowout preventer to control pressures down hole. The choice of type and properties of drilling mud also governs the instantaneous rate of penetration by the mud's capacity to sweep the area in the bottom of the well clean. In some applications like directional drilling, a down hole motor is incorporated in the drill string to rotate only the bit an

nothing else. **The motor is driven by the flow rate of mud** pumped through the drill string. Cuttings, traces of fluids or gases and changes in pH, temperature, chloride content etc,. **gives valuable information and indications on how the drilling is proceeding.** Additives such as scavengers can be added to the mud to **prevent corrosion of drill string, casing and tubing.** Many reservoirs where drilling occurs contains toxic gases, and these present dangers to metal components from hydrogen embrittlement, blistering and stress cracking. Mud is essential to **control the pressure in the well** between given limits by alteration of different parameters for the mud like mud weight and viscosity. The mud also **transmits measurements** through pressure waves created down hole as described in the next section.

1.3 Measurement of Bottom Hole Pressure

To control the pressure within given margins, the present pressure has to be known. Traditionally, the pressure in the bottom of the well is transferred to the surface with mud pulse telemetry. Shock waves are generated in the MWD-tool (measurement while drilling) and transferred through the mud up the drill string, and is interpreted by a computer on the surface. The pulses created are either:

- Negative pulses created by reducing the stand pipe pressure by directing mud from inside the drill string and out to the annulus section through a valve.
- Positive pulses created by blocking the mud flow through the drill string. When the mud is blocked, a pressure increase can be noted at the surface.
- Continuous waves is generated by alternately blocking and opening for mud flow through the drill string. This give a sinusoidal wave where information is given by the variation in phase.

This method for transmission of measurements of (among others) bottom hole pressure has been used since the sixties, and although it has evolved, the bit rate is still low. This means that the operator has to be selective when deciding which measurements to transfer to the surface. Mud pulse has the severe limitation that it cannot run without the mud pump running. This means that it is not possible to obtain pressure readings from the bottom hole assembly (BHA) while tripping unless mud is circulated. This is a problem since most of the kicks, especially in weak formations, occur during tripping. If is is chosen to circulate to get pressure reading, this would add to the swabbing when tripping in, and could lead to fracturing. Therefore, circulating while tripping is time consuming because tripping must be done very slowly in order not to fracture the formation. The fact that flow is needed for measurements, the low bandwidth and that measurements are time delayed, has motivated people to try to obtain data from the well in different ways. One of these is the wired drill pipe.

1.3.1 Wired drill pipe

Wired drill pipe [6] gives the opportunity to obtain a much more detailed picture of the conditions in the well. The wired drill pipe consist of drill pipes with a cable for data transmission mounted inside. Inductive connections transfer the signal between the pipes. The increased amount of data obtained from the well can lead to better steering of the bit, faster detection of kick and loss off circulation, increased bit performance and rate of penetration among others. But more important in a managed pressure drilling context is the possibility of measurement of not only

bottom hole pressure, but also pressure and other readings along the entire drill string. In addition, the measurements can be obtained continuously and in real-time, and they are also available even when there are no circulation. This can lead to greater control of the well.

1.3.2 Estimation

Another method to acquire parameters that can be used to control the manipulated variables which in time controls the conditions in the well, is by using available measurements to calculate parameters that are not measured, or have slow update ratios like the bottom hole pressure. Several different more or less complex models have been developed to estimate the states in wells. This ranges from relative simple models which assumes one-phase flow without loss or gain in the well, to advanced multi phase flow simulators like OLGA 2000.

1.4 Managed Pressure Drilling

Managed pressure drilling (MPD) [7] [8] is an adaptive drilling process to precisely control the annular pressure profile throughout the well. The main idea is to create a pressure profile in the well to stay within close tolerances and close to the boundary of the operation envelope defined by the pore pressure, hole stability envelope and fracture pressure. Or said with other words to "walk the line" of the pressure gradients. Managing the pressure and remaining inside this pressure gradient window can avoid many drilling problems. MPD can be divided into two categories, reactive and proactive MPD. Reactive MPD includes drilling programs that are tooled up with at least a rotating control device (RCD), choke, and perhaps drill string float to safely and efficiently deal with problems that could occur down hole. Proactive MPD includes designing a casing, fluids and open hole program that precisely manages the well bore pressure profile. This category of MPD can offer the greatest benefit to the offshore drilling industry as it can deal with unforeseen problems before they occur. Several different MPD-methods exists, including

- PMCD (Pressurized Mud Cap Drilling)
- CMC (Controlled Mud Cap)
- CBHP (Constant Bottom hole Pressure
- HSE (Returns Flow Control)
- RC (Reverse Circulation)
- DG (Dual Gradient)

The focus for this thesis is Dual Gradient Managed Pressure Drilling

1.5 Dual Gradient Drilling

Deep water drilling presents both opportunities and challengees. One challenge that consistently presents itself is the difference in pressure, at the mud line, between the hydrostatic head of the mud in the riser and the formation pressure close to the mud line, which is, typically, defined by the seawater head. This pressure differential causes an operational difficulty that may, in

some cases, prevent drilling the well to its target depth using conventional riser return drilling methods. The concept of Dual Gradient drilling, using a riser filled with seawater has been proposed as a viable method of limiting this pressure imbalance and of facilitating the drilling of challenging deep water wells. Over the years, especially in the 60's and 70's by major Oil companies, many different approaches to dual gradient drilling have been studied.

One of the major requirements of dual gradient drilling, using a seawater filled riser, is the need to create an interface between the drilling mud in the well bore/wellhead and the seawater, or other fluid, in the riser. In this thesis the simulations are done for a fluid/fluid interface.

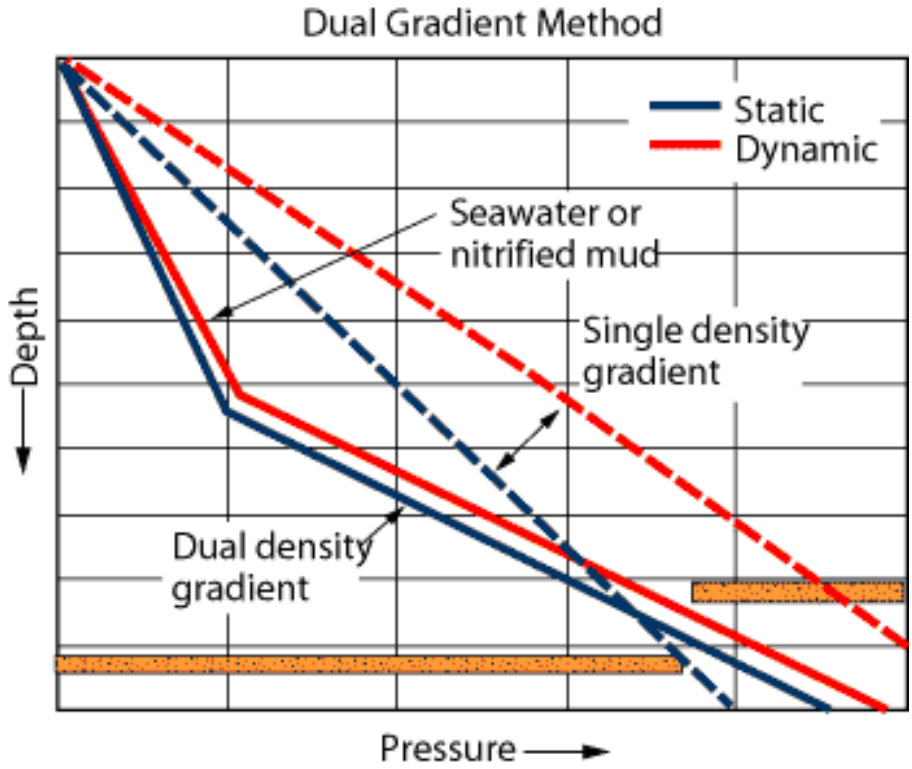

Figure 1.3: Pressure profile DG vs conventional drilling

The concept of dual gradient drilling gives many economic advantages over conventional drilling. In the case further discussed in this report, the riser is filled with seawater, and this means that less mud is needed to fill the system, which in turn leads to the possibility of using smaller rigs with smaller mud pits. A positive bi-effect of a riser filled with seawater is that the riser section is lighter, so that the riser tension is decreased. This gives smaller rigs better premises to drill in ultra-deep waters, which both lower costs and makes more rigs available for the task, thus lowering the waiting time for rigs that occurs because of the shortage of rigs capable of drilling such difficult wells. In certain sedimentary basins around the world, the difference between formation pore and fracture pressures can be limited as a result of the reduced overburden pressures. This reduced pressure may be the result of younger sediments replacing heavier overburden sediments that are not present in deep waters. As water depth increases, the probability increases that the difference between pore- and fracture-pressure is reduced. When this occurs, the maintenance of both well- and bore pressure balance and bore hole stability can present a problem, and, in some cases, limit ability to reach target depth. In order to drill wells which fall into this category in a conventional manner, additional casing strings are quite often required to minimize risk and allow drilling ahead. As a result it is possible for the bore hole size to be reduced below that which can be economically produced, and in some cases it can be impossible to reach total depth before the hole size prevents drilling ahead. By utilizing the fact that a riser

filled with seawater (or other concepts as described in chapter 2) gives the same pressure as the hydrostatic pressure from the seawater, the pressure on the formation in shallow zones is reduced in dual gradient drilling, so that fractioning of the formation is less likely. Therefore, fewer casing strings is needed, and fewer casing strings means less time used for setting casings and shorter drilling time. It also means that the final production string may have larger dimensions, giving increased production rates and thus gives the well a increased economic potential. Other benefits from this system is less use of consumables like mud in the well, lower logistics costs and less weight requirement. Since there are less mud in the riser, the probability for large spills are reduced. By controlling the pressure more tightly in the well, the chances for kicks and blowouts can be greatly reduced, which is positive both in an environmental- and safety-aspect.

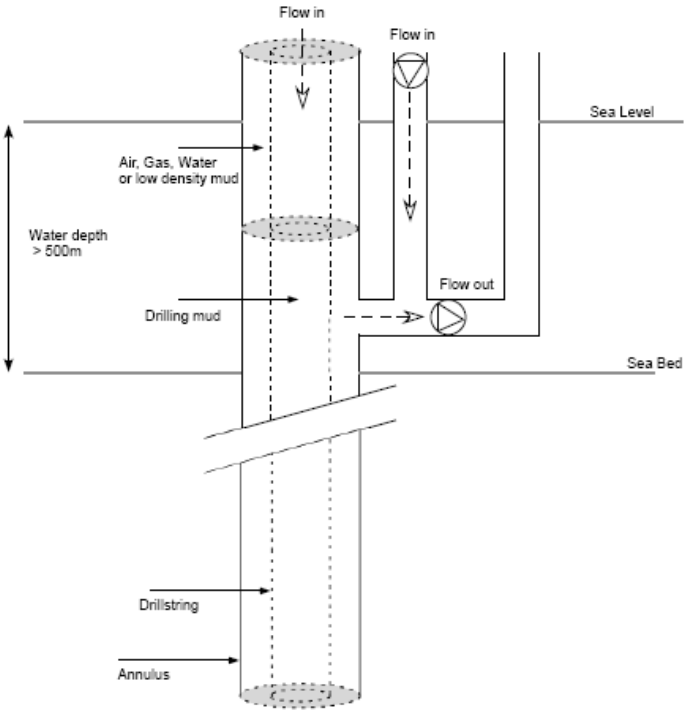

Figure 1.4: Illustration of Dual Gradient system

Chapter 2

Patents

2.1 AGR

The AGR dual gradient system is a method for controlling drilling fluid pressure during sub sea drilling. Drilling fluid is pumped down into a bore hole through a drill string, exits at the bit and flows upwards in the annulus between the drill string and the walls of the bore hole. A pump is connected to the riser near the seabed, which pumps the drilling fluid out from the annulus and up to the rig as seen in figure 1.4, but without the fill pump. The annular volume above the drilling fluid is filled with another fluid with a lower density than the drilling fluid. This characterizes the system as a "Dual Gradient System", because the two fluids with different densities exerts a pressure on the bottom hole which is different than for one of the fluids, and the fluids give two different pressure gradients. The pressure exerted by the drilling fluid at the seabed may be controlled from the drilling rig by selecting the height of the fluid coluumns, the density of the drilling fluid and the density of the riser fluid. The inlet pressure at the pump is given by

$$P_{pump} = H_1\rho_1 + H_2\rho_2 \tag{2.1}$$

where H_1 and H_2 is the height of the riser fluid and drilling fluid respectively, and ρ_1 and ρ_2 is the density of the two fluids. H_1 and H_2 will together make up the height of the riser from the pump inlet to the deck of the drilling rig. Continuous control of the fluid flowing into and out of the bore hole is obtained since the liner annulus is filled with a riser fluid, and thus it is relatively easy to detect for example drilling fluid flowing into the formation or if gas or liquid is flowing from the formation and into the well bore by monitoring the volume of the riser fluid. Also during changes of drilling fluid densities, it is possible to maintain a substantially constant pressure from the drilling fluid on the seabed. Choosing another inlet pressure to the pump, will cause the heights H_1 and H_2 to alter according to the chosen pressure. It is also possible to have the outlet from the annulus to the pump below the seabed, by coupling a pump pipe to the annulus at desired depth. To prevent the pressure from the drilling fluid to exceed desired levels, the riser may be equipped with a dump valve, which can be set to open for dumping of drilling fluid to the sea at a particular pressure.

2.2 Ocean Riser System

The system from Ocean Riser System (ORS), is called Low Riser Return and Mud-lift System (LRRS) (figure 1.4). The riser is constructed without kill- and choke lines, and is filled with air. The riser is connected to a surface blowout preventer (BOP) located on the drilling vessel. At the seabed the riser is connected to a sub sea BOP. Drilling fluid is pumped down through the drill string and exits through the bit at the bottom of the well. The drilling fluid flows upwards in the annulus region, and at a certain precaluculated depth, the drilling fluid is diverted through an outlet which is connected to a pumping system which pumps the fluid back to the rig. The level of drilling fluid in the riser is adjusted by the sub sea pumping system, so that the hydraulic pressure in the bore hole can be controlled by adjusting the liquid level in the riser in accordance to the requirements for the drilling process. As the drilling situation is dynamic, and the required pressure constantly changes, the liquid level in the riser will constantly vary. The liquid level in the riser can be anywhere between the return level for conventional drilling at the drilling rig above the surface BOP, and down to the depth of the low riser return outlet. The bottom hole pressure can in this way be controlled by regulating the liquid/air interface in the riser. Using this method, it can be possible to drill an entire well with the same density fluid. This gives possibilities for decreased costs by both reducing time spent, and reducing consumption of drilling fluids. The top sections of the well can be drilled with the same density fluid as the deepest sections by lowering the air/fluid level so that the fluid exerts a pressure equal to the seawater pressure, to not fraction the fragile formation at shallow depths. If the need to increase in mud weight appears, the level in the riser can be decreased at the same time, to reduce the pressure in the top sections, while the pressure in the bottom of the well increases. This can occur if an unexpected high pressure is encountered at the bottom of the well, and the top of the well can not support the increased pressure of heightening the fluid column in the riser to compensate for the increase in the bottom hole pressure. The LRRS also has useful properties for drilling through severely depleted reservoirs and drilling underbalanced. Instead of drilling with special fluids like foam, air or gases, the pressure exerted from the drilling fluid in the LRRS can be lowered to a level much lower than the hydrostatic pressure from water at the given depth. The ORS MPD system is in fact not a true Dual Gradient system since there is only one fluid exerting one pressure gradient in the well because the pressure above the mud column is close to atmospheric pressure. The top of the riser is evacuated and contain no pressures even during well control events.

2.3 Hollow Glass Spheres

The method for using hollow glass spheres to achieve a dual gradient, is an invention by Marurer Technology. The hollow glass spheres are used as a lightweight additive to the drilling fluid. The spheres are pumped into the riser at the bottom of the riser to reduce the density of the mud flowing in return up the annulus of the riser. The set up of the rig for this system is very similar to conventional drilling, except for the introduction of an injection point at the bottom of the riser. Hollow spheres are mixed in a slurry and pumped into the riser at the sea floor. This slurry reduces the density of the mud flowing upwards inside the riser. When the fluid from the riser containing drilling fluid, cuttings and hollow glass spheres returns to the rig, it enters a separator system. The drilling fluid, cuttings and glass spheres are separated from each other, and the glass spheres can be used again. Some of the advantages of using the hollow-spheres in achieving the dual gradient concepts are as follows: the hollow spheres can be regarded as incompressible and they produce a linear pressure gradient, they can easily and safely be mixed into the drilling fluid during drilling operations, and no equipment is required on the sea floor. Possible drawbacks for this method are breakage of the hollow-spheres and difficulties in separating the hollow-spheres

from the drilling mud.

2.4 Mud Dilution with gas

The riser dilution method with gas is very similar to the hollow-spheres method. In this system gas is used as the lightweight additive. The system consists of a supply line of gas to the bottom of the riser, and the amount of gas injected in the riser is dependent on the pressure which the column in the riser must exert at the seabed. The gas reduces the density of the return fluid in the riser just like in the hollow-sphere methods. When the mixture reaches the rig floor the gas must be separated from the drilling fluid and cuttings, so that gas and drilling fluid can be reused. The gas lift method has some problems, including high compressor costs, the fact that compressors are large so they occupy space on the drilling rig, difficulties in degassing mud before it is re-injected into the well, and the fact that gas is a compressible fluid which will lead to nonlinear pressure gradients.

2.5 Mud Dilution with liquid

The liquid lift approach is one of the latest methods of achieving dual gradient in deep waters. This system pumps drilling fluid down the drill pipe, through the nozzles in the drilling bit and then into the open hole where it picks up cuttings. The drilling fluid and cuttings then travels up the annulus and into the Blowout Preventer (BOP) stack. Just above the BOP stack is a riser charging line which runs to the drilling rig. The riser charging line introduces a low density fluid into the riser to mix with the return fluid that travels up to the drilling rig. The base fluid is introduced at the bottom of the riser, so as to achieve a riser density lesser or equal to sea water density. In offshore operations it is well know that the pressure at the sea floor is equal to sea water hydrostatic pressure. Therefore, the pressure at the beginning of the well bore is equal to sea water hydrostatic. In order to maintain the integrity of the well bore it is important that sea water density is maintained above the well bore and heavier density down the well bore. Therefore, by combining the appropriate quantities of drilling fluid with the lighter base fluid injected at the bottom of the riser, the required riser density can be attained. Equation 2.2 can be used to determine the return mud density in the riser. The diluted riser density is given by

$$\rho_R = \frac{Q_A \times \rho_A + Q_C \times \rho_C}{Q_A + Q_C} \tag{2.2}$$

where Q_A is the flow rate in the annulus, ρ_A is the mud density in the annulus, Q_C is the flow rate in the charging line, ρ_C is the density of the fluid in the charging line and ρ_R is the density in the riser. The density in the riser and the height from the rig to the seabed will determine the pressure exerted from the fluid column in the riser on the top of the fluid in the annulus. By altering the density in the riser, the bottom hole pressure and the pressure gradient from the riser fluid will change. For the liquid lift dual gradient system to be effective, it is crucial that it is possible to separate the drilling fluid from the injected liquid. The outflow from the riser to the rig must be separated continuously and reused, as a rig cannot carry enough drilling and injection fluid to drill the entire well without reuse of preciously mixed fluids.

Chapter 3

Modeling

A simple model for the system sketched in figure 3.1 was derived for both the AGR and ORS system. The flow through the main pump into the drill string is denoted q_{in}. The flow through the bit is considered equal to the flow through the main pump. In the ORS system, there is a possibility to pump mud directly into the riser, so that it is possible to heighten the level of mud in the riser quicker and without use of the main pump. The volume flow through this pump is denoted q_f. For both systems, mud is extracted from the riser and pumped up to the rig in a separate return line. The flow through the extraction pump is denoted q_{out}. The height of the mud above the extraction pump is denoted h, the height from the rig to the extraction pump is denoted h_r, while the total depth from the rig to the bottom of the well is denoted d. The level of mud in the annulus is always considered to be higher than the point of extraction. In the AGR system, there is water above the mud line, so that the hydrostatic pressure of the water column must be added to the equation. In the ORS system, the top of the riser is evacuated and contains no pressures even during well control events.

3.1 Equations for the AGR system

Using the assumption that mass is conserved in the system, gives an equation for the rate of change in the mud level h:

$$\frac{\partial V \rho_a}{\partial t} = A\dot{h}\rho_a = (q_{in} + q_{out})\rho_a \tag{3.1}$$

where V is the volume of mud in the riser, ρ_a is the density of the fluid in the annulus which is regarded constant, so this will be an average value for the density of the fluid in the annulus. The alteration in height of the mud column in the riser is then given by

$$\dot{h} = \frac{1}{A}(q_{in} - q_{out}) \tag{3.2}$$

The pressure at the extraction point is defined as

$$p_{out} = \rho_w g(h_r - h) + \rho_a g h + p_0 \tag{3.3}$$

where ρ_w is the density of the fluid in the riser above the mud line (considered seawater in the simulations in this thesis), g is the acceleration due to gravity, h_r is the height of the riser and p_0

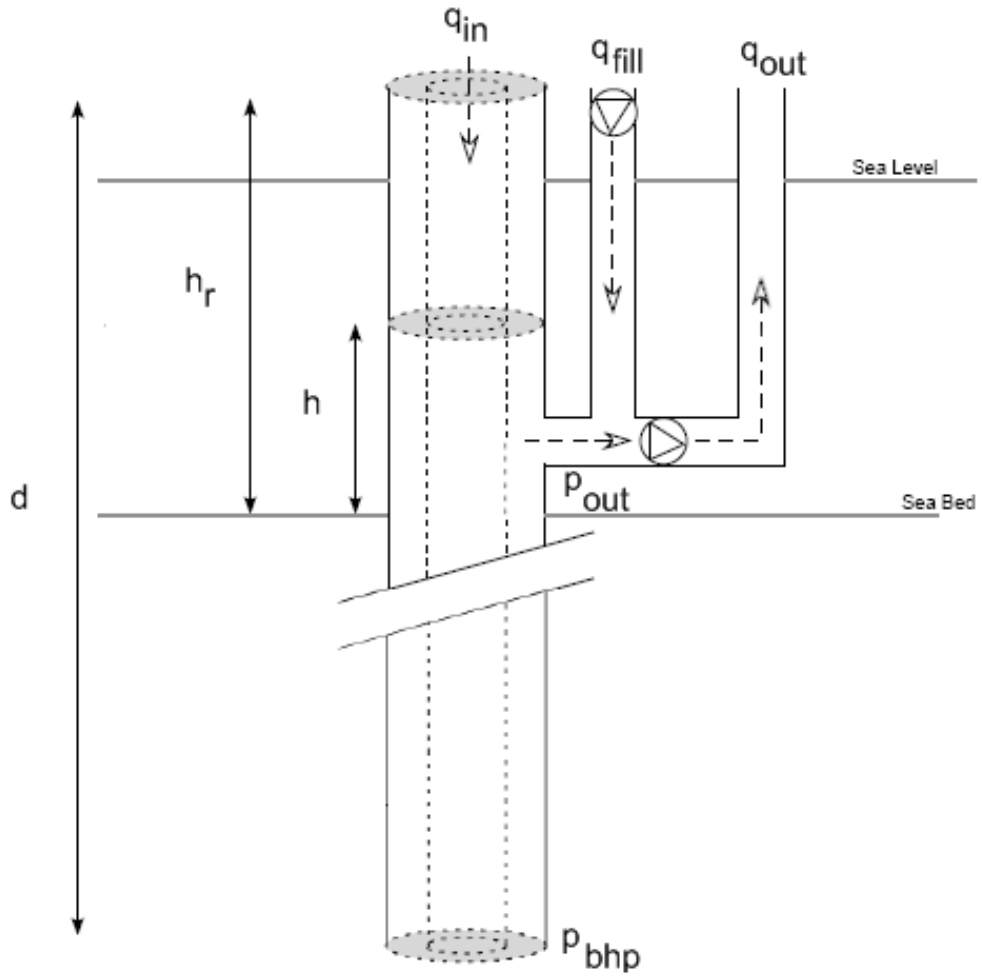

Figure 3.1: Scetch of the system modelled

is the pressure above the water column in the riser (set to atmospheric pressure). The bottom hole pressure is then given by

$$p_{bhp} = \rho_w g(h_r - h) + p_0 + \rho_a g(d + h - h_r) + F(q_{in}) \tag{3.4}$$

where $F(q_{in})$ is a term for the friction loss as a function of flow. The two types of friction terms [9] are head losses and minor losses. Head losses is a term used to describe the losses in sections consisting of straight pipes. Minor losses are losses due to pipe entrance or exit, sudden expansion or contraction, bends, elbows, tees, and other fittings, valves and gradually expansions or contractions. In this model, these two types of friction terms are gathered in one expression.

Although friction loss can be an important term in dynamic systems, it is neglected in equations 3.3 and 3.6 because the speed of the liquid is low. But in the equations for bottom hole pressure (3.4 and 3.7), the friction term $F(q_{in})$ is included. For the model used in this report, the friction loss contribution has to be estimated, but is modelled as described in chapter 4.

3.2 Equations for the ORS system

For the ORS system, the equations will be similar, but since there is air above the mudline in the riser, and there is a possibility to fill mud directly into the riser, the equations will be somewhat different:

$$\dot{h} = \frac{1}{A}(q_{in} + q_f - q_{out}) \tag{3.5}$$

Where q_f is the pump that fills mud into the annulus at aproximately the same height as the extraction pump. The pressure at the extraction pump is defined as

$$p_{out} = \rho_a g h + p_0 \tag{3.6}$$

The bottom hole pressure is then given by

$$p_{bhp} = p_0 + \rho_a g(d + h - h_r) + F(q_{in}) \tag{3.7}$$

where $F(q_{in})$ also here is a term for the friction loss as a function of flow into the well.

Chapter 4

Friction

The circulation of drilling mud will cause a friction contribution to be added to the bottom hole pressure. Different models for the friction contribution was tested, to find a model that suited the characteristics of the well best. These were first- and second order approximations of the friction loss as function of flow in the well. They can be summarized as

$$Friction = Fa_1 q^2 + Fa_2$$
$$Friction = Fa_1 q + Fa_2$$
$$Friction = Fa_1 q^2 + Fa_2 q + Fa_3$$

where Fa_1, Fa_2 and Fa_3 is constants.

4.1 Friction AGR

The friction in the annulus as a function of flow was found to be as in figure 4.1a for the AGR system. By simulation, linear friction was found most suitable to mimic the friction contribution as seen in WeMod. As seen from the figure, there will be large deviations from the linear friction model at low flows because there is a very different behaviour for the contribution at low flows. There is a possibility to change parameters for the friction at low flows, to better mimic the friction contribution deviated from the well. Another problem at low flows, is that the measurement can not be transmitted by mud pulse, so that no measurements of the bottom hole pressure can be acquired topside.

4.2 Friction ORS

The friction in the annulus as a function of flow was found to be as in figure 4.1b. Altough the characteristic of this alteration in bottom hole pressure as function of flow is more non-linear than in the AGR case, a linear function gave the best fit also here. The same problem for low flows also applies for the ORS system as the AGR system. The difference in the friction contribution to the bottom hole pressure for the two different systems is believed to result from the different characteristic of the mud used in the two systems.

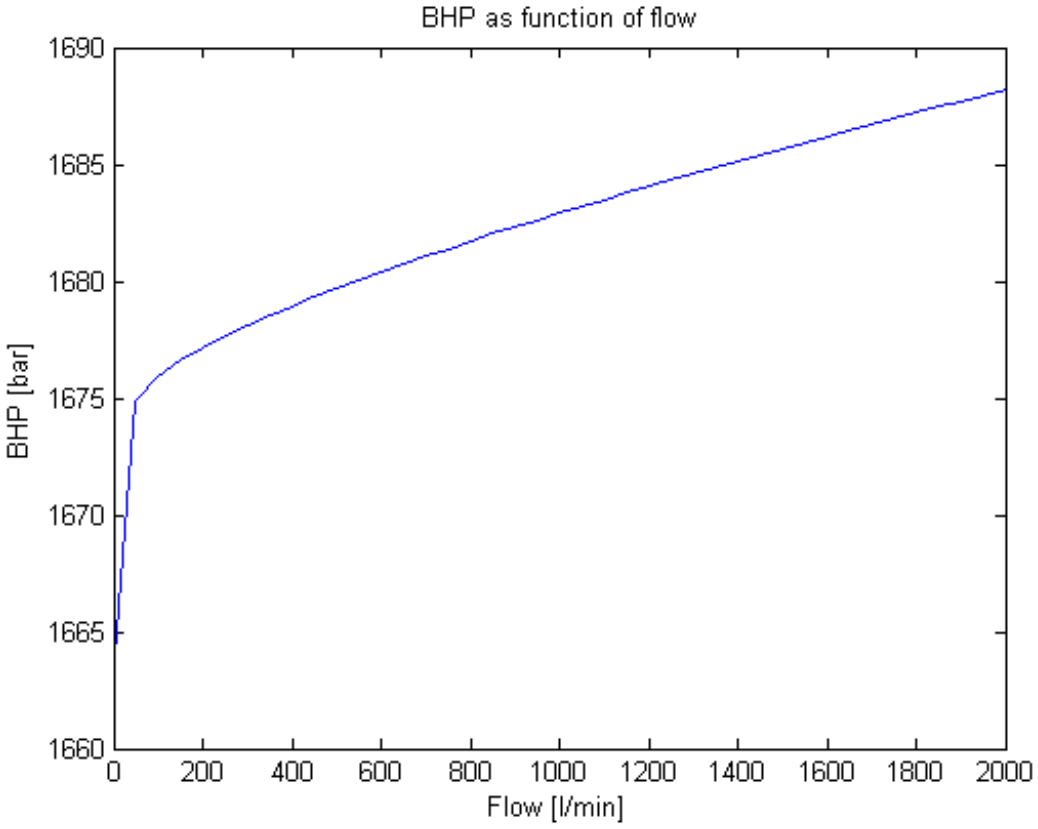

(a) BHP as function of flow in the well for the AGR system

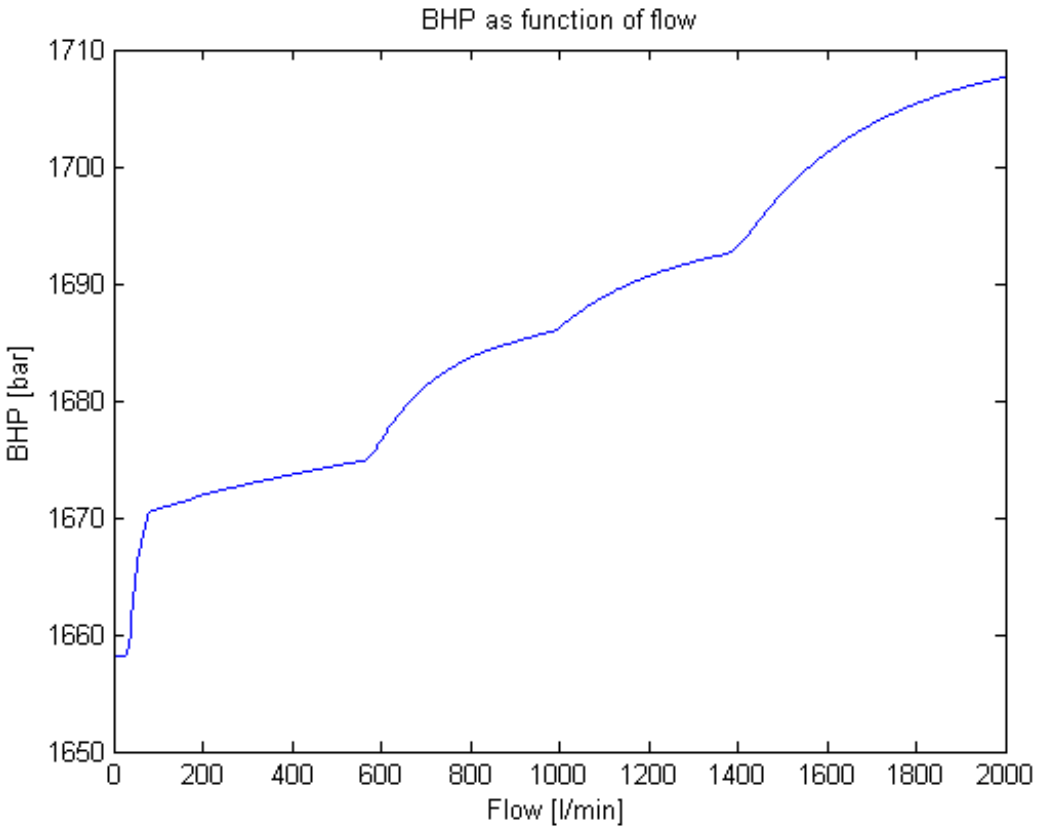

(b) BHP as function of flow in the well for the ORS system

Figure 4.1: Bottom hole pressure for increasing flow

4.3 Piecewise linear models for friction

Figure 4.2a shows how a piecewise linear friction model can be adapted to the AGR system. The difference between the linear friction model and the friction derived from simulation in WeMod is also shown in figure 4.2a. The same is shown for the ORS system in figure 4.2b. This shows that a piecewise linear model can be fitted to mimic the friction derived from WeMod without great errors. It is possible to use this simple linear model for the friction as function of flow in the simulations if the friction parameters does not converge, but they demand knowledge of the alteration in bottom hole pressure as a function of flow. The system will then be reduced to estimation of the two states mud height and mud weight, together with the pressure at the extraction pump and the bottom hole pressure. A piecewise linear model for the friction in the AGR system is attempted estimated in section 7.3, while the piecewise linear model for the friction as seen in figure 4.2a is implemented in the simulation shown in figure 7.7.

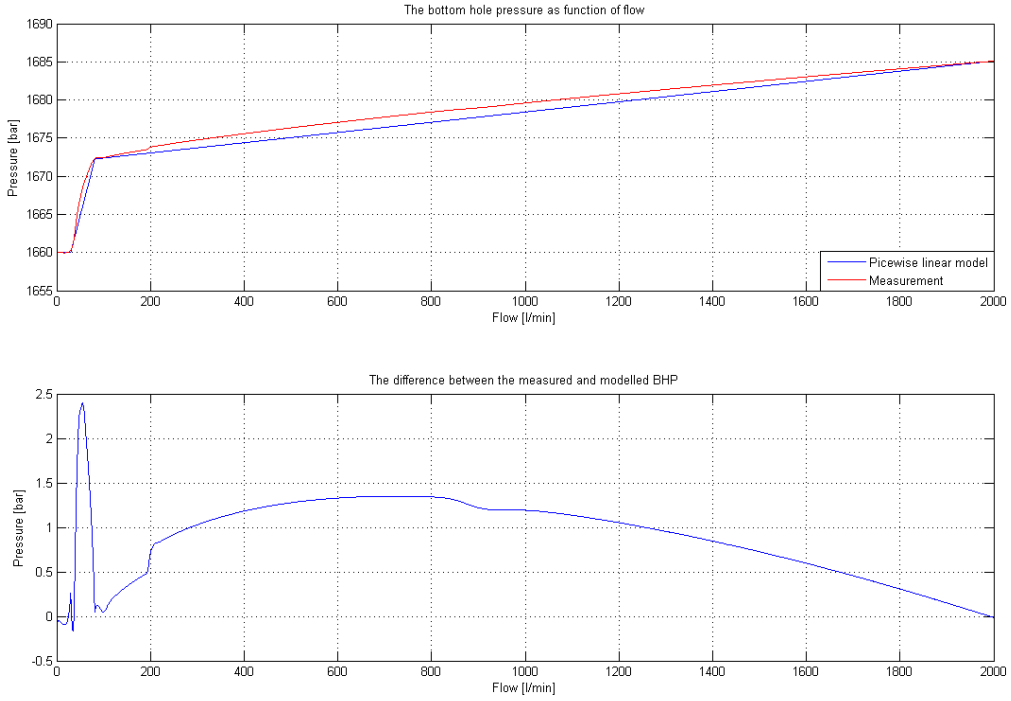

(a) AGR system

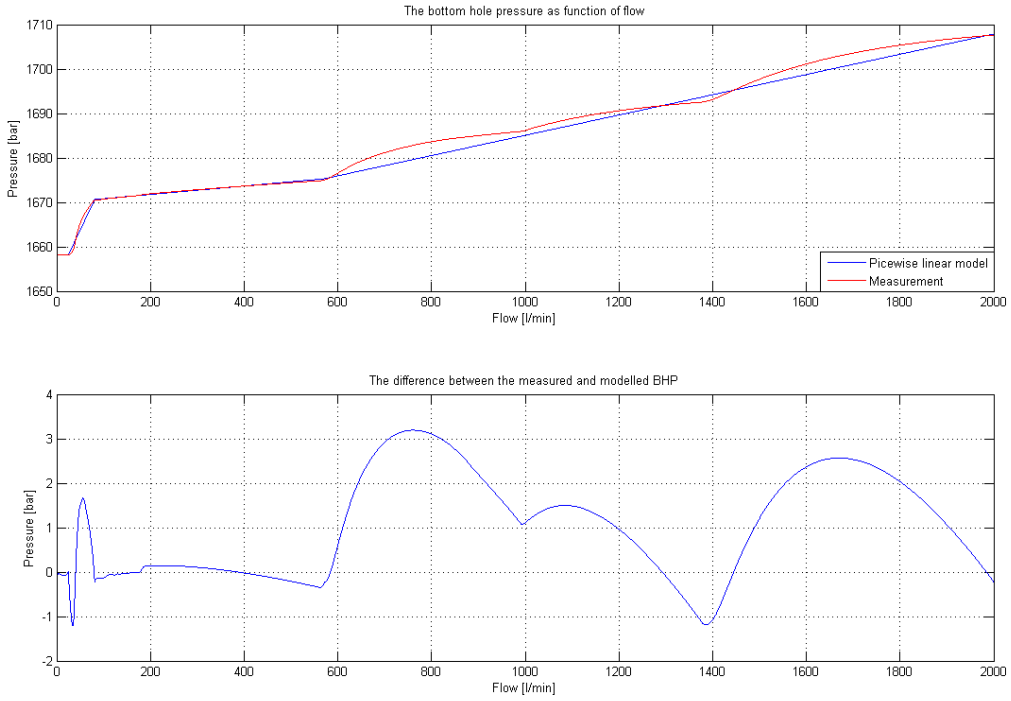

(b) ORS system

Figure 4.2: The friction from WeMod plottet against the piecewise linear models for the systems

Chapter 5

Derivation of the Kalman Filter

5.1 Augmented model for the AGR system

The details for kalman filtering can be found in appendix A. The model from chapter 3 was augmented to include the parameters that needed to be estimated. The augmented state vector was defined as

$$x = \begin{bmatrix} h \\ \rho_a \\ F_a \end{bmatrix}$$

Where F_a is the friction parameter for the linear friction as a function of flow. The friction contribution in the system is given as Fa q_{in} for simplicity. This is because it was not possible to get the friction parameters to converge as seen from chapter 6 and 7. Therefore, this model is believed to give decent estimates when the flow in the well is above a certain limit (ca 80 l/min) because the friction contribution will then be approximately linear up to the saturation point for the main pump. Other possible state space systems that have been simulated includes

$$x = \begin{bmatrix} h \\ \rho_a \\ F_{a1} \\ F_{a2} \\ F_{a3} \end{bmatrix}$$

where the friction contribution to the bottom hole pressure was given by

$$Friction = F_{a1} q_{in}^2 + F_{a2} q_{in} + F_{a3}$$

In section 7.3 an attempt to switch filters at different flows was attempted to achieve a piecewise linear friction estimation. In the simulation shown in figure 7.7 the friction is set to the piecewise approximation seen in figure 4.2a.

The augmented state space system when using 5.1 is written

$$f(x) = \begin{bmatrix} \dot{h} \\ \dot{\rho_a} \\ \dot{F_a} \end{bmatrix} = \begin{bmatrix} \frac{1}{A}(q_{in} - q_{out}) \\ 0 \\ 0 \end{bmatrix}$$

The augmented model can thus be written as

$$\dot{x} = f(x) + w \tag{5.1}$$

where **w** is a column vector which represents the process noise for the system. This noise is white noise with zero mean. The two measurement equations for the system is given by

$$h(x) = \begin{bmatrix} Y_1 \\ Y_2 \end{bmatrix} = \begin{bmatrix} \rho_w g(h_r - h) + \rho_a g h + p_0 \\ \rho_w g(h_r - h) + \rho_a g(d + h - h_r) + p_0 + F_a(q_{in}) \end{bmatrix}$$

where $F_a(q_{in})$ can be different functions of the flow in the well. Y_1 is the pressure at the extraction pump, and Y_2 is the pressure at the bottom of the well. The measurement can be written as

$$h(x) = \begin{bmatrix} Y_1 \\ Y_2 \end{bmatrix} + v$$

where v is the measurement noise in the system. Implementing these equations into the extended kalman filter algorithm as seen in appendix A gives the Jacobian matrices

$$\mathbf{F} = \frac{\partial f}{\partial x} = \begin{bmatrix} 0 & 0 & 0 \\ 0 & 0 & 0 \\ 0 & 0 & 0 \end{bmatrix}$$

$$\mathbf{H} = \frac{\partial h}{\partial x} = \begin{bmatrix} (\rho_a - \rho_w)g & gh & 0 \\ (\rho_a - \rho_w)g & (d + h - h_r)g & q_{in} \end{bmatrix}$$

$$\mathbf{L} = \frac{\partial f}{\partial w} = \begin{bmatrix} 1 & 0 & 0 \\ 0 & 1 & 0 \\ 0 & 0 & 1 \end{bmatrix}$$

$$\mathbf{M} = \frac{\partial h}{\partial v} = \begin{bmatrix} 1 & 0 \\ 0 & 1 \end{bmatrix}$$

5.2 Augmented model for the ORS system

For the ORS system, the augmented model consist of the same states, but the equation for the alteration in height consist of one more term, the fill pump q_{fill}. The augmented state space system is thus defined as

$$f(x) = \begin{bmatrix} \dot{h} \\ \dot{\rho_a} \\ \dot{F_a} \end{bmatrix} = \begin{bmatrix} \frac{1}{A}(q_{in} + q_{fill} - q_{out}) \\ 0 \\ 0 \end{bmatrix}$$

The measurement equations for the system is given by

$$\begin{bmatrix} Y_1 \\ Y_2 \end{bmatrix} = \begin{bmatrix} \rho_a g h + p_0 \\ \rho_a g(d + h - h_r) + p_0 + F_a(q_{in}) \end{bmatrix}$$

where the terms including ρ_w from the AGR system disappears because there is only air above the mud column in the riser, and there is approximately atmospheric pressure above the mud column. Y_1 is the pressure at the extraction pump, and Y_2 is the bottom hole pressure.

$$h(x) = \begin{bmatrix} Y_1 \\ Y_2 \end{bmatrix} + v$$

where v is the measurement noise in the system. The Jacobian matrices for this system will be the same, except for the H-matrix which will be

$$\mathbf{H} = \frac{\partial h}{\partial x} = \begin{bmatrix} \rho_a g & gh & 0 \\ \rho_a g & (d + h - h_r)g & q_{in} \end{bmatrix}$$

Chapter 6

Nominal testing

An augmented model to use in the extended kalman filter for the system was derived in chapter 5. The details for kalman filtering can be found in appendix A. The extended kalman filter was tested against a perfect model to test its performance. The goal for the Kalman Filter was to give an estimate for the three states h, ρ_a and F_a shown in section 5.1, which in turn gives the estimate of the two measurements available in the system. The parameters used in testing of the model for both the AGR and ORS system is shown in table 6.1, but for the ORS system there is no water in the riser, just air with atmospheric pressure.

Parameter	**Value**	**Unit**	**Description**
g	9.81	[m/s]	Gravity constant
ρ_w	1000	$[kg/m^3]$	Water density
h_r	2150	[m]	Extraction pump depth
A	0.652	$[m^2]$	Area of riser minus drill string
d	9220	[m]	Bore hole depth
p_0	1	[bar]	Atmospheric pressure
Q_{max}	2000	[l/min]	Maximum pumpflow

Table 6.1: Parameters used in simulations

6.1 AGR model

To see how the EKF derived performed on the AGR system, the EKF was implemented on the design model. Different manipulated variables was used to see how this affected the convergence of the states. The initial values for the parameters used in the simulation were set to the values in table 6.2

Parameter	**Value**	**Unit**	**Description**
h	2120	[m]	Mud height in riser
ρ_a	1850	$[kg/m^3]$	Annulus density
F_a	$3.41 * 10^7$		Friction factor

Table 6.2: Initial values for the states in the AGR simulation

The flow in the system is shown in figure 6.1. The real and estimated states are shown in figure 6.3a. Both the value for the height of mud in the riser and the value for the density in the annulus is approximately the same as the true values, but the value for the friction factor would not converge during the testing of the filter using normal values for the flow q_{in}. Since all three states does not converge to the real values, there will be some errors in the other states as well, as shown in figure 6.3b. The errors in the states are small, and will be zero when the flow into the well is zero, because the friction contribution will then be eliminated, so that the error in the friction factor does not influence the model. It is possible to get convergence for all three states, but this requires to set the manipulated variables to larger values than physically possible (section 6.2). The reason for the problem of getting the friction factor to converge, is that the value for q_{in} is so small, and the friction contribution to the pressure in the well compared to the hydrostatic pressure is so marginal. The real pressure and the pressure estimated from the estimated states at the extraction pump and in the bottom of the well is shown in figure 6.2a. Since the estimate for the two states that gives the greatest contribution to the pressure is approximately the same as the real values, the estimated pressure also converges to the real values. The error between the estimated values for the pressure and the real pressure is shown in figure 6.2b. It is clear that the estimated pressures quickly converges to the real pressure when the manipulated variables is constant, and during alteration of the variables, the error is very small.

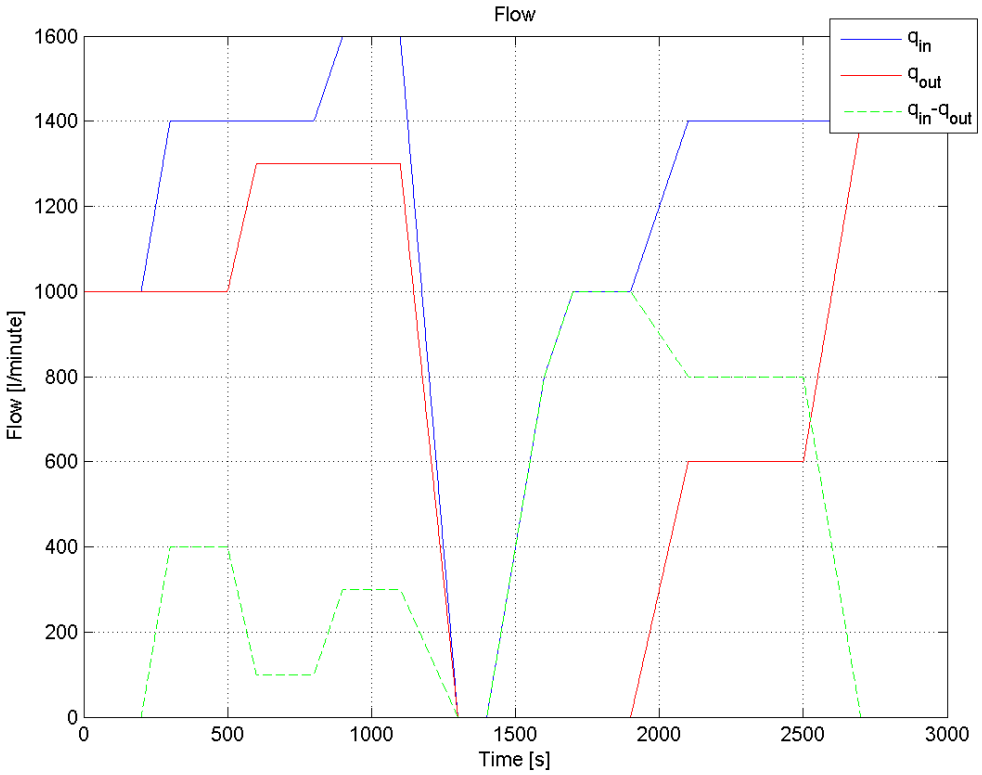

Figure 6.1: The flow in the system during simulation of the AGR system

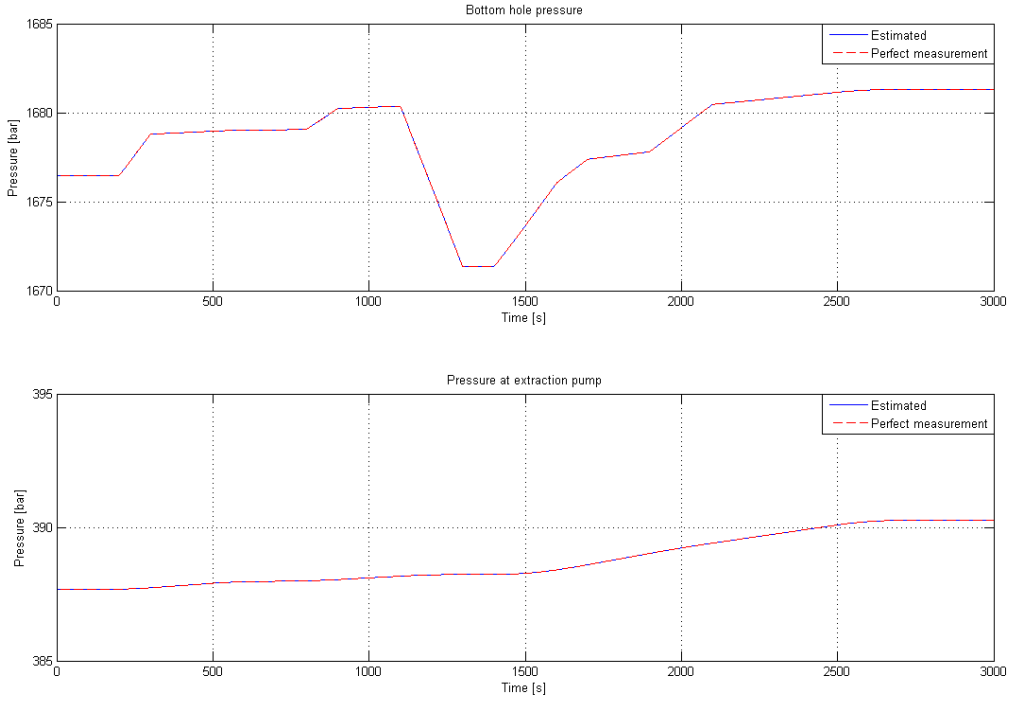

(a) The pressures in the system

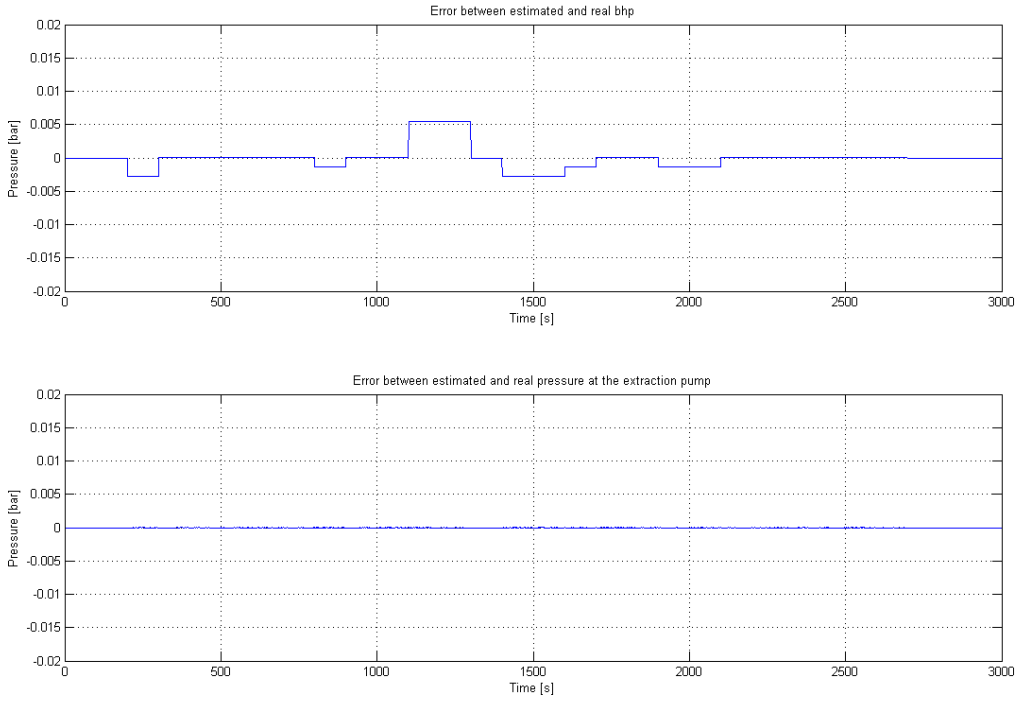

(b) The errors between estimated and real pressures

Figure 6.2: The pressures and error between the estimated and real pressures

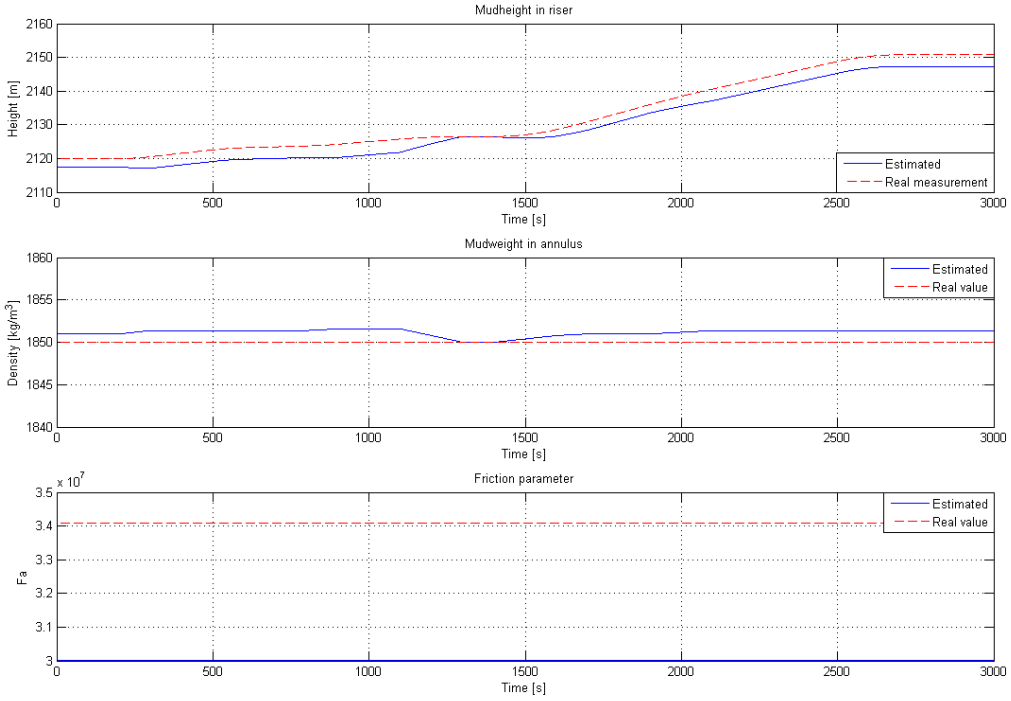

(a) The states in the system

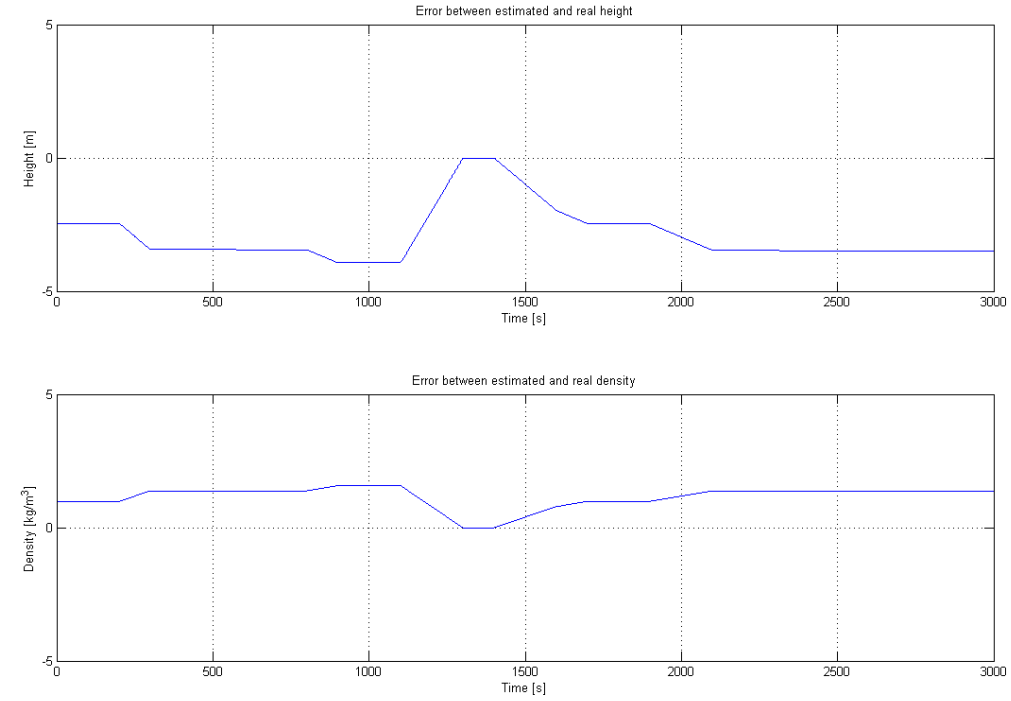

(b) The error between the estimated and real states

Figure 6.3: The states and error between the estimated and real states

6.2 Testing of the model with higher flow

All three states converge when the system is simulated with the flow in figure 6.4, but this flow is higher than physically reasonable for the well. The true and estimated states can be seen in figure 6.6a. The friction factor converges in this case because the contribution to the bottom hole pressure from the friction term is much larger compared to the hydrostatic pressure in this case. Since all states converge, the errors between the estimated and real pressure will disappear as seen in figure 6.5b. The pressure in figure 6.5a show that the pressures in the system are much higher than any physically possible pressure. This is because the friction contribution is enormous, and that the height of mud in the riser (as seen from figure 6.6a) will increase enormously because of the flow in the system. Since the flow in the well is much higher than in normal operating conditions, and greater than physically possible, this only shows that the model is believed to give better results if the friction contribution to the bottom hole pressure was greater compared to the hydrostatic pressure contribution.

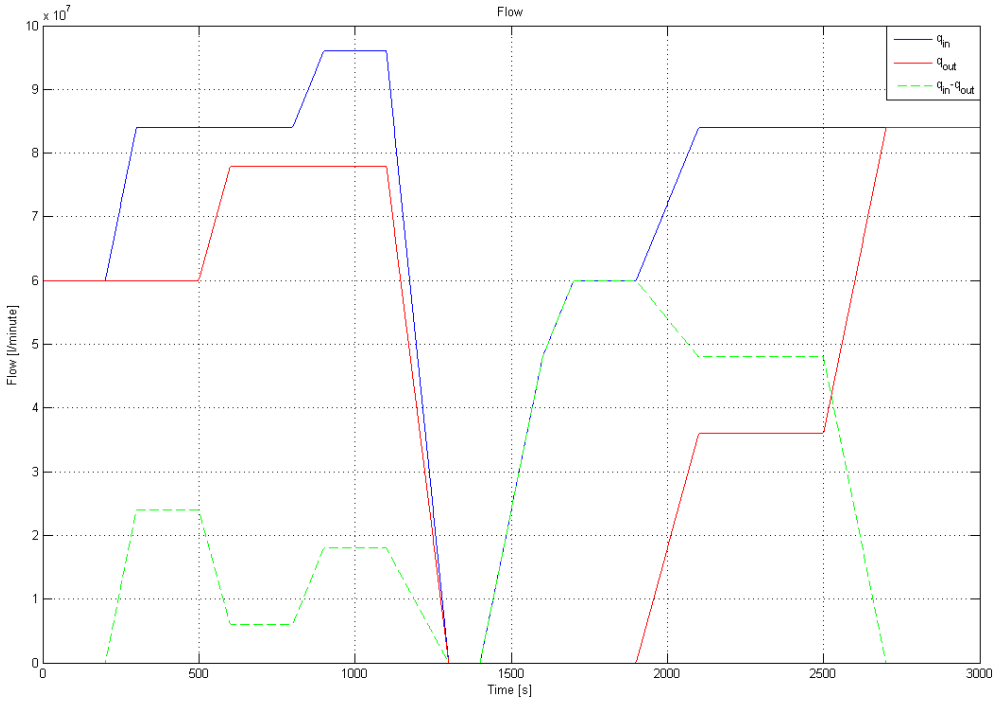

Figure 6.4: The flows in the system

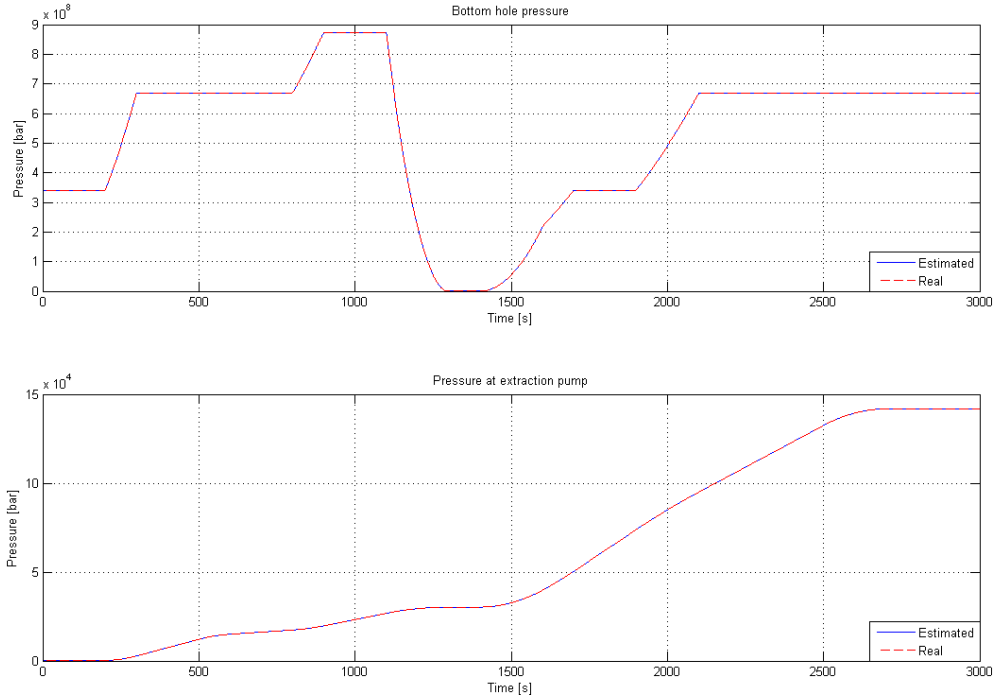

(a) The pressures in the system

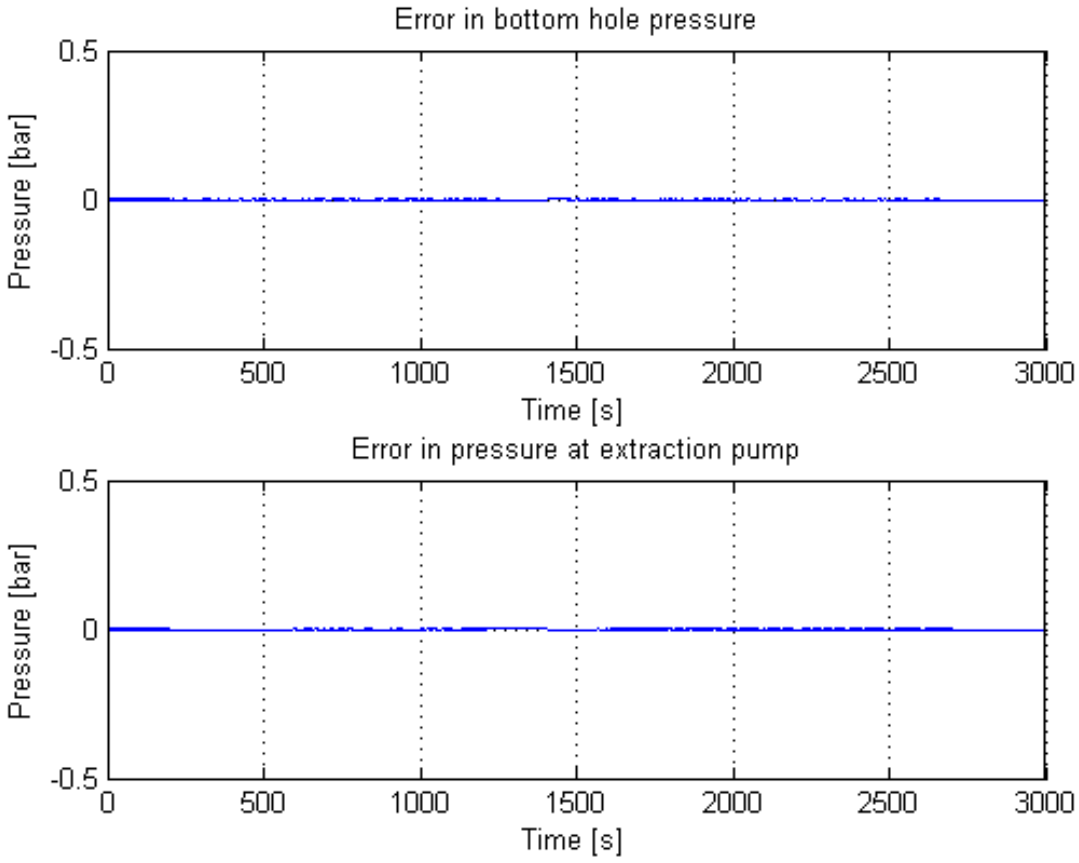

(b) The error between the estimated and real pressures

Figure 6.5: The pressures and error between the estimated and real pressures at very high flows

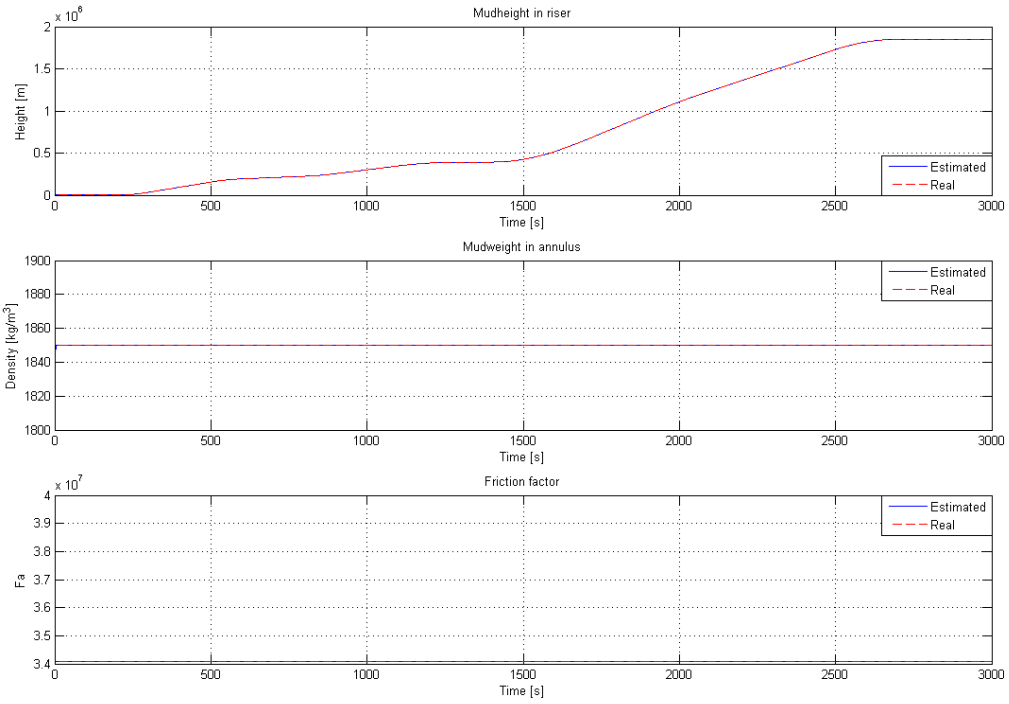

(a) The states in the system

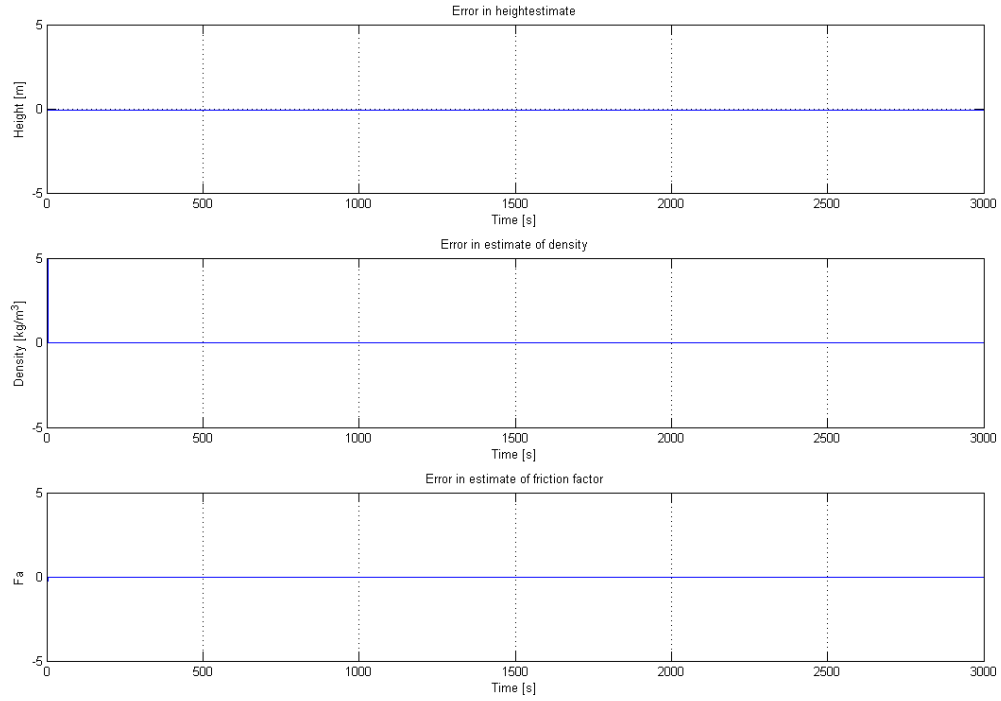

(b) The error between estimated and real states

Figure 6.6: The states and error between the estimated and real states during at high flows

6.3 ORS system

The simple model for the ORS system is very similar to the AGR system, but there is air above the mud level in the riser, and there is a fill pump to quickly heighten the level of mud in the riser.

Parameter	Value	Unit	Description
h	2020	[m]	Mud height in riser
ρ_a	1880	$[kg/m^3]$	Annulus density
F_a	$1.3 * 10^8$		Friction factor

Table 6.3: Initial values for the states in the ORS simulation

The flow in the system was set as shown in figure 6.7. The difference between the flow in the AGR and ORS system is obvious from the extra line showing q_f in figure 6.7. The real and estimated states for the ORS system are shown in figure 6.8a. Both the value for the height of mud in the riser and the value for the density in the annulus converges against the true values, but the value for the friction factor would not converge during the testing of the filter using normal values for the flow q_{in}. As in the AGR system, the friction factor will converge against its true value in the model for abnormal high flows. As seen from figure 6.8b, the two states height and mud weight do not converge to exactly the real values. This is because the friction factor does not converge, so that the friction contribution to the bottom hole pressure is wrong. The two states does however converge when the flow in the system is zero because the friction contribution will then be zero because of zero flow, which is the correct value even if the friction factor is wrong. Figure 6.9b shows that the estimated pressures is very close to the real pressures at all times. Even if the states do not converge entirely to their real values, the combination of the errors in the states give the correct estimated pressures. It is clear from the figure that the estimated pressure quickly converges to the real pressure when the manipulated variables is constant, and during alteration of the variables, the error is very small.

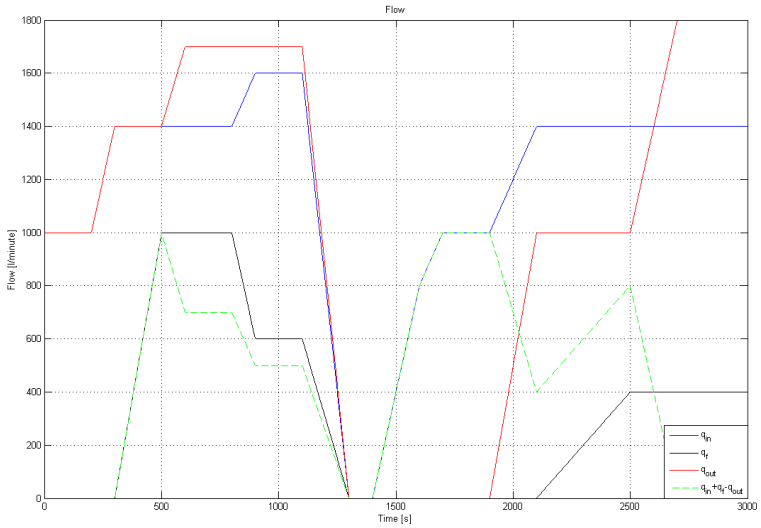

Figure 6.7: The flow in the system during simulation of the ORS system

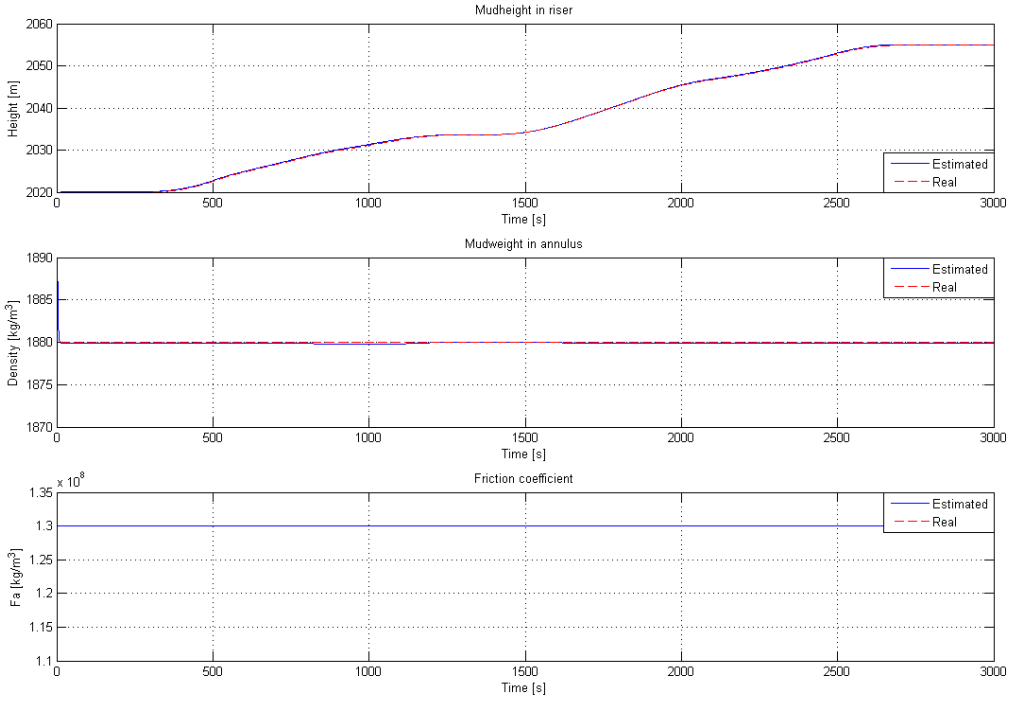

(a) The states in the ORS system

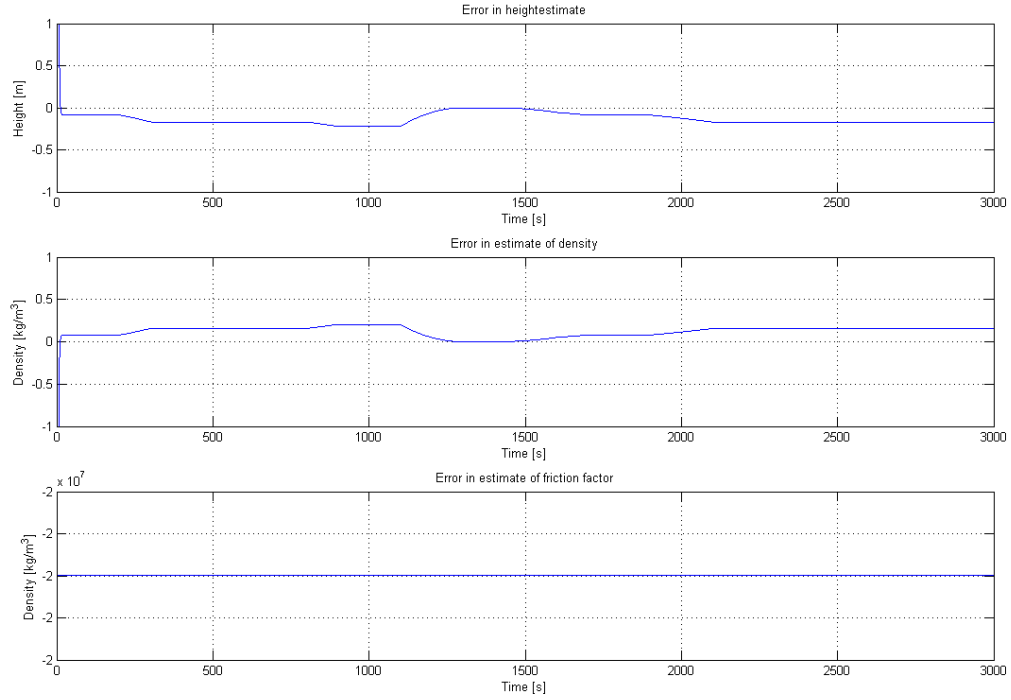

(b) The error between estimated and real states

Figure 6.8: Plot of the real and estimated states and their errors in the ORS system

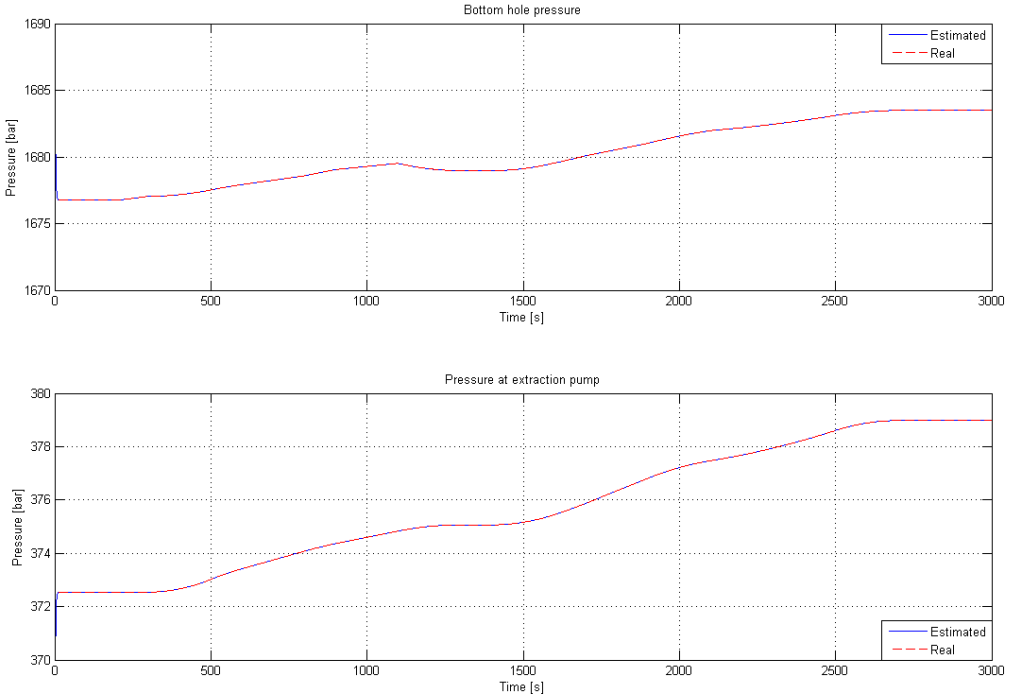

(a) The pressures in the system

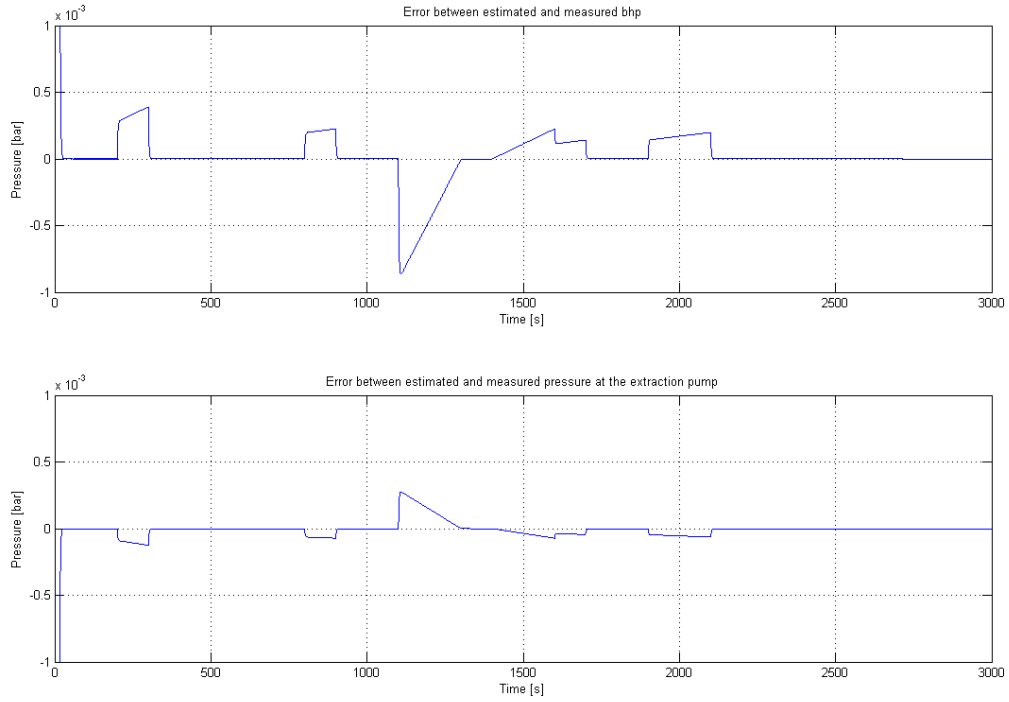

(b) The errors between estimated and real pressures

Figure 6.9: Plot of the real and estimated pressures in the ORS system

6.4 Delayed measurement

To get a more realistic approach to the measurements made in the well, the model was set up to update the measurement of the bottom hole pressure only once per thirtieth second, and this measurement was at the same time delayed with thirty seconds, reflecting the time delay for transmitting the value for the bottom hole pressure using mud pulse technology. Since the measurement for pressure at the extraction pump is above the seabed, it was expected that this reading could be transmitted by cable, so this signal is continuously available and sampled every second as before, and without time delay. This means that the kalman filter must use one measurement and one estimated measurement based on the estimated states between each measurement. When a measurement for the bottom hole pressure is obtained every thirtieth second, the Kalman filter estimates the states and the pressures for each time step since last measurement, and then gives better estimates of the states at the time the measurements arrive, and therefore more accurate estimation of the bottom hole pressure at this time step. Since the states estimated at the time of the arrival of the measurement is more precise, the estimation of the states and estimation of the bottom hole pressure will be more accurate until next delayed measurement arrives thirty seconds later, and the same procedure will be repeated until the end of the simulation. The longer the interval between measurements and the more delayed the measurements are, the more inaccurate the estimated states and estimated measurements will be. If signals from the mud pulse motor are lost, the bottom hole pressure measurement will not be updated, and the filter has to use estimated bottom hole pressure for further estimation until new measurements again are obtained through mud pulse telemetry.

6.4.1 AGR system with delayed measurement

The flow in this simulation is the same as in the simulation of the AGR system without delayed measurement for comparability (figure 6.1). Figure 6.10a shows the delayed measurements and when they are obtained, together with the plots of the estimated and real bottom hole pressure. By zooming in on the area where the alteration in the bottom hole pressure is greatest (figure 6.10b), it is possible to see that the estimated pressure is updated and given a better value each time the delayed measurement for the bottom hole pressure is obtained. The estimate of the height of mud in the riser and the mud weight, together with the real height and mud weight are shown in figure 6.11a. The last state is not shown here because it does not converge. The error between the real and estimated values for two of the states is shown in figure 6.11b, together with the difference between real and estimated bottom hole pressure. From the plots of the states, it can be seen that the estimated values for the mud height in the riser is lower than the true value, while the value for the density of the mud is higher than the true value. The estimated bottom hole pressure fits the model very well and the error between real and estimated pressure is zero at steady state flows. The reason for the lacking convergence of the states is the fact that the friction parameter does not converge, and that the measurements used to update the states are in fact estimates of the measurements, predicted forward in time from the last measurement was obtained. The states do converge at zero flow, because the friction contribution to the bottom hole pressure will then be zero, no matter the value of the friction factor.

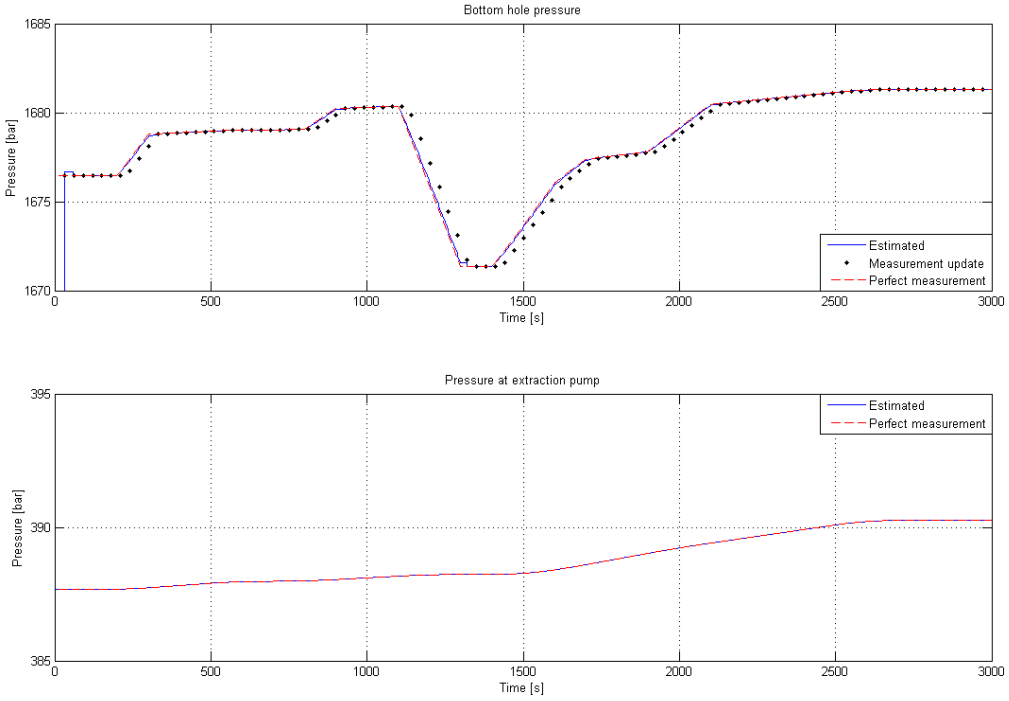

(a) The real and estimated bottom hole pressure together with the measurements obtained

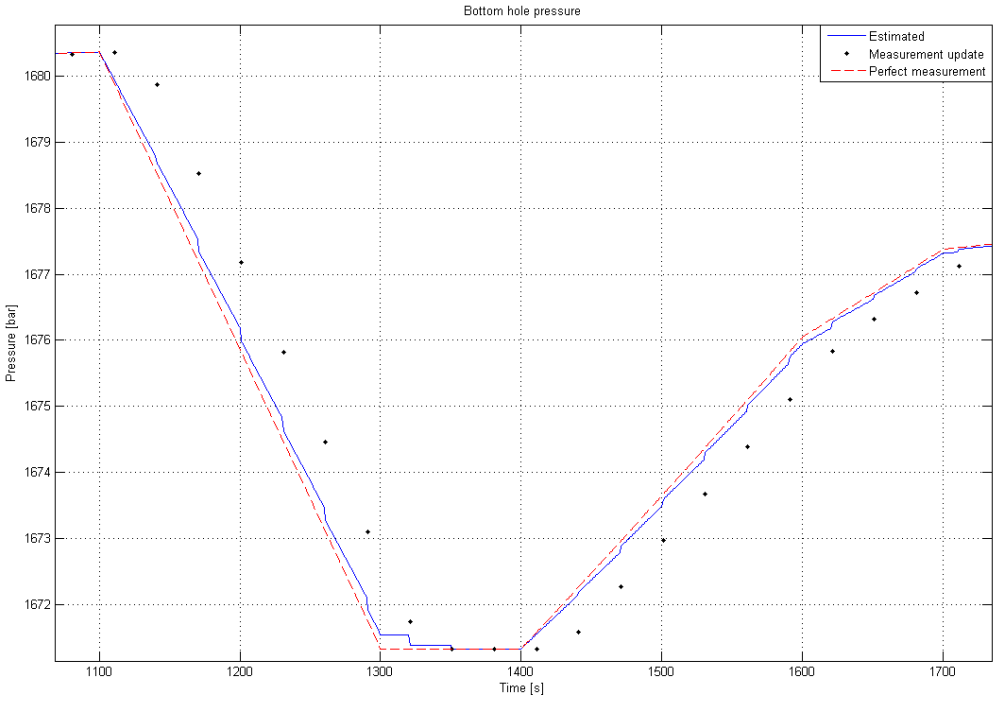

(b) A closer look at the estimated pressure versus the real pressure

Figure 6.10: The real and estimated pressures in the system

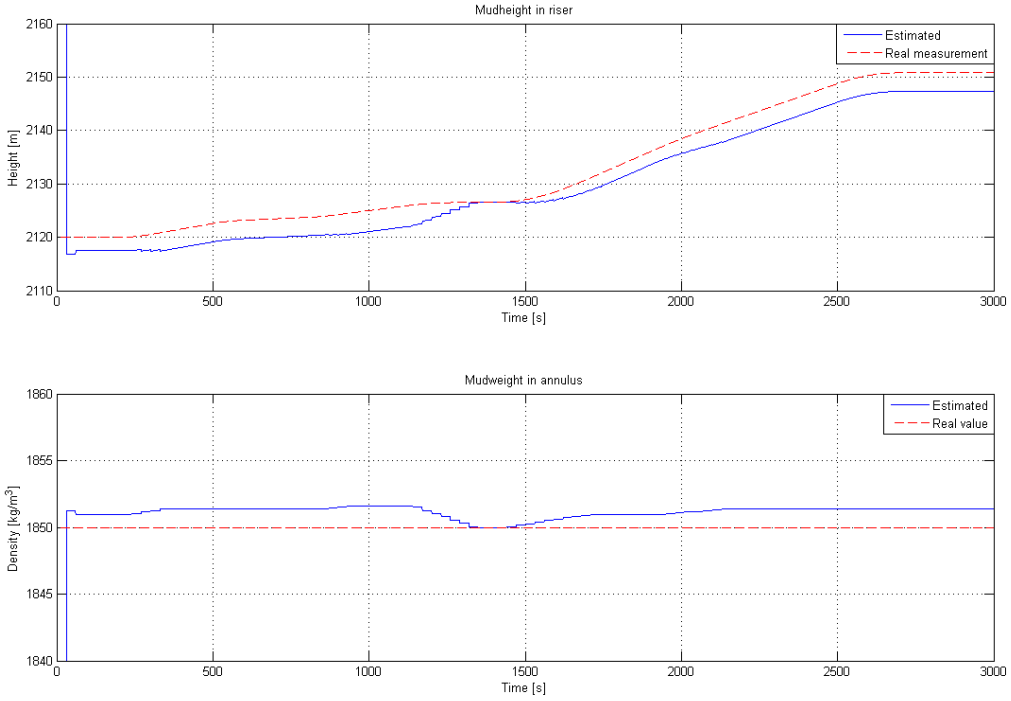

(a) The real and estimated states

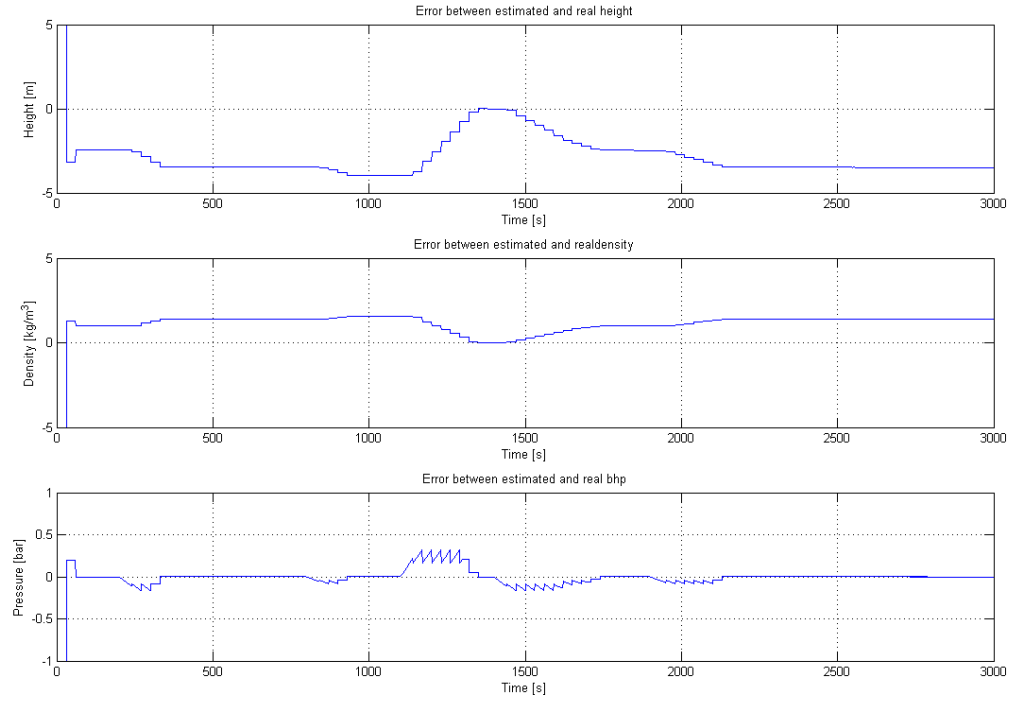

(b) The error for the states and estimated bottom hole pressure

Figure 6.11: The pressure errors and states in the simulation

Chapter 7

WeMod simulations

The filter was tested against simulations from WeMod to see how it handled unmodelled dynamics. WeMod is a well simulation software from International Research Institute of Stavanger. Through a MATLAB interface the user can change different parameters in the simulation to fit the cases the user wishes to explore. The augmented kalman filters from chapter 6 were implemented into the MATLAB code for WeMod. WeMod does not have measurements for the height of mud in the riser, and the mud weight is calculated based on temperature and pressure in the well. In the model derived, the friction term is approximated as a function dependent of the flow into the well. In WeMod, the friction is, among other factors, dependent on temperature, viscosity of the drilling mud, geometry of the drill hole and roughness. There is therefore no possibility of testing if the estimated states correspond to the true values from WeMod. But the three states is used in estimations of the two pressures that are measured, so it is possible to see if the estimated states gives the correct estimated pressures.

7.1 Continuous measurement update

The extended kalman filter was first tested against how the simplified model would behave when both measurements was available at each time step. Table 7.1 shows the parameters used in the simulations.

Parameter	**Value**	**Unit**	**Description**
g	9.81	[m/s]	Gravity constant
ρ_w	1000	$[kg/m^3]$	Water density
h_r	2150	[m]	Extraction pump depth
A	0.652	$[m^2]$	Area of riser minus drill string
d	9220	[m]	Bore hole depth
p_0	1	[bar]	Atmospheric pressure
Q_{max}	2000	[l/min]	Maximum pumpflow

Table 7.1: Parameters used in WeMod simulations

7.1.1 AGR simulations

WeMod was simulated with the same flows as the model in the nominal test in chapter 6.1. The flow in the system was thus as shown in figure 7.1a. The estimated states evolved as shown in figure 7.1b. The pressure measurements from WeMod is plotted against the estimated pressures from the estimated states in figure 7.2a. The error between the estimated and measured pressures are shown in figure 7.2b. It is clear from the plots, that the model does not give the correct values for the states, and the friction factor does not converge against the true value. Since there is no possibility in WeMod to increase the flow to levels used in the nominal testing in section 6.2, it is not possible to see if higher flows would give a correct value for the friction contribution. Since the wrong values is obtained for the friction contribution, the value for the density of the mud and the height of the mud column will also have errors which will compensate for the errors from the friction contribution, and the estimated pressures will not deviate much from the measured pressures. When the flow is ramped down to zero, the errors in the estimate of the height of mud in the riser and the density of the mud will increase. This is because the error in the friction contribution is greater at low flows since the friction contribution will alter more rapidly when the flow through the main pump is very low. There is however believed that the mud weight will be a bit lower because of the lowered pressure in the system, but the effect is probably much less than the alteration in the estimated state. The pressure estimate is very close to the mesured values, but this is not very suprisingly since both measurements are avaliable at each timestep.

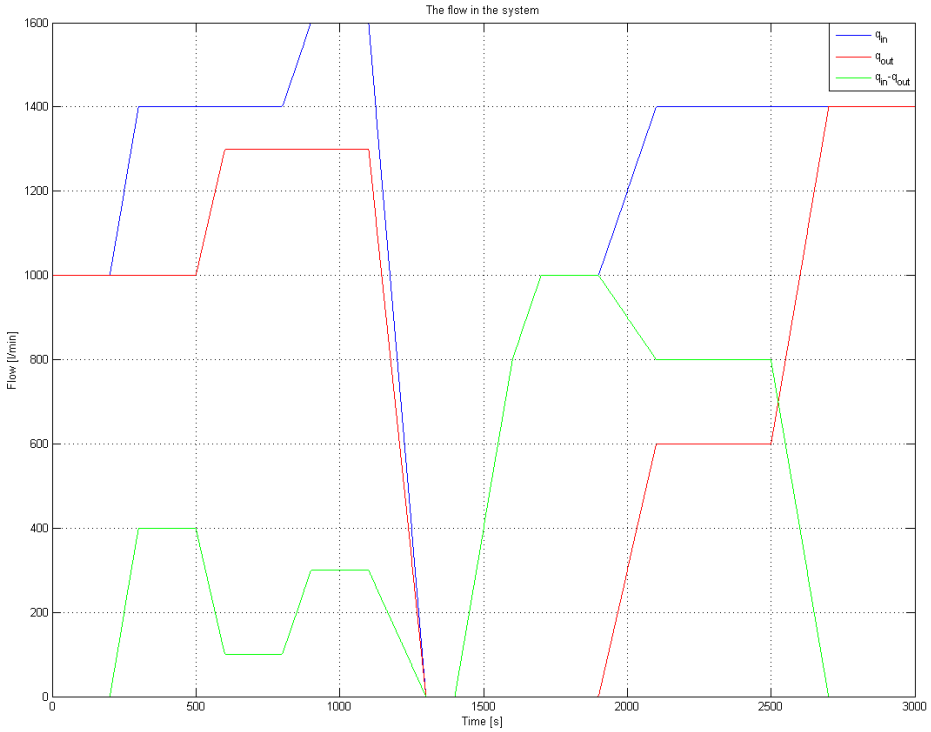

(a) The flow in the system

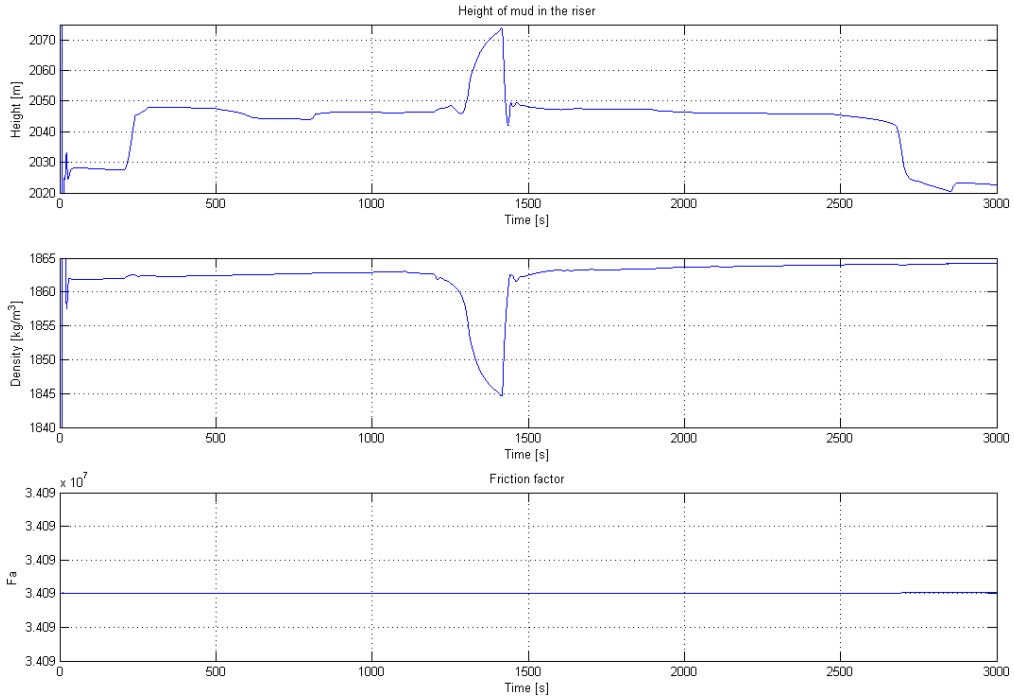

(b) The estimated states in the system

Figure 7.1: The flow in the system and the development of the states during simulation of the AGR system

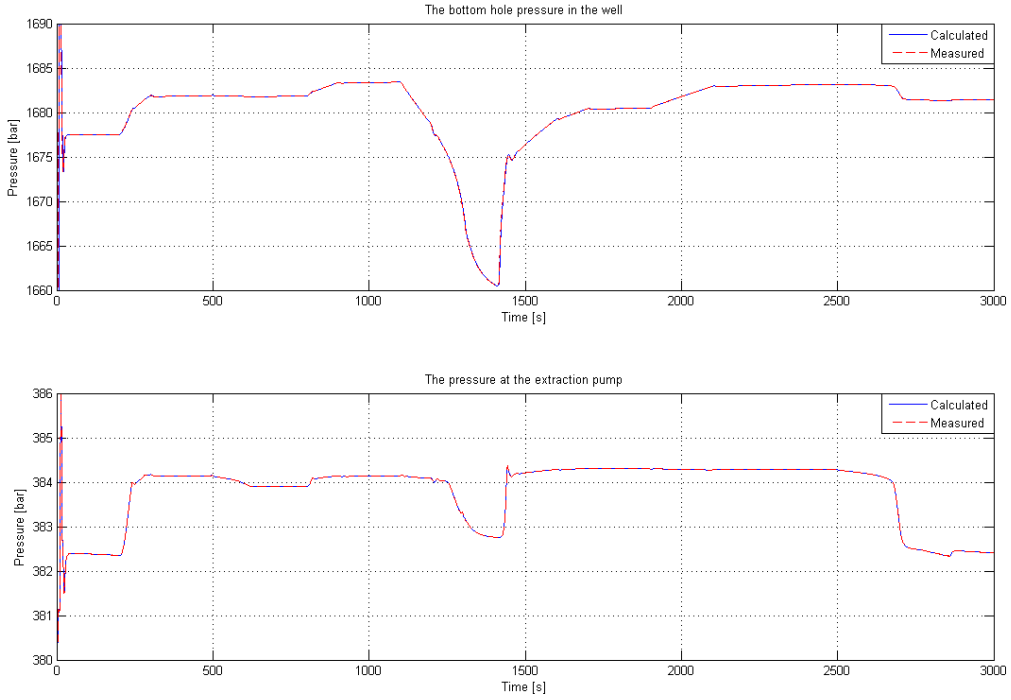

(a) The estimated and measured pressures

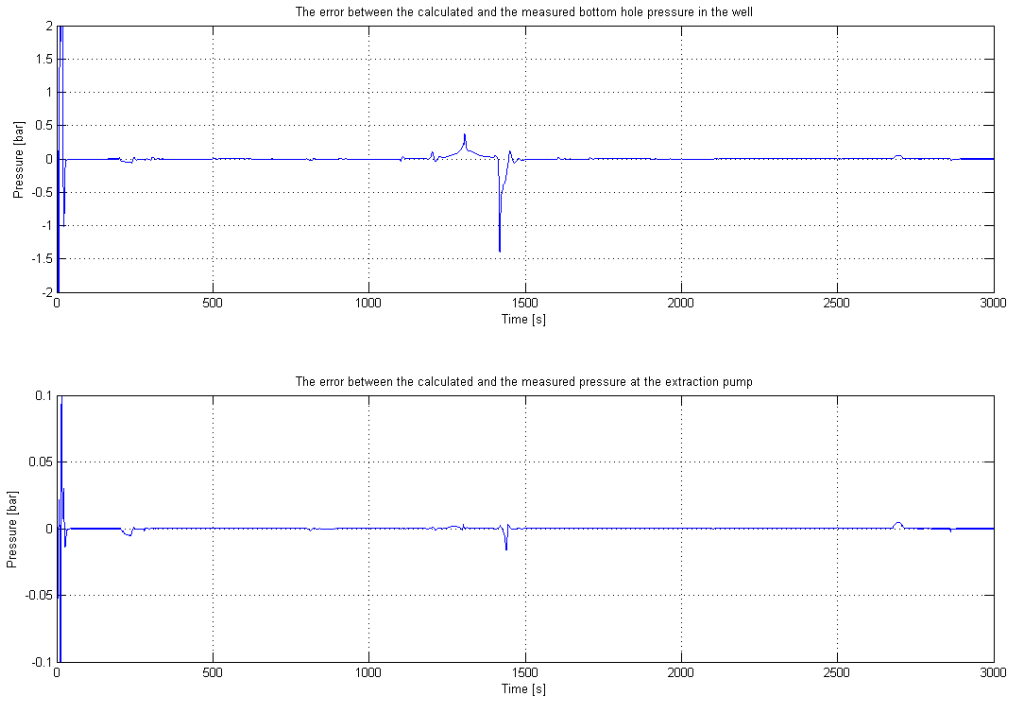

(b) The error between the estimated and measured pressures

Figure 7.2: Plot of the real and estimated pressures in the AGR system together with the errors

7.1.2 ORS simulations

The flow in the simulation of the ORS system, is shown in figure 7.3a, the same as used in the nominal testing of the system. Also for the ORS simulation, the lacking convergence of the friction factor, leads to errors in the values for height and weight of the mud in the system. This is most visible when the flows in the system approaches zero as seen in figure 7.3b, where there are great alterations of the estimate for the height of mud and the mud weight. At low flows, the alteration of the friction contribution as a function of flow increases more rapidly than at high flows as seen from chapter 4, so the value which is set as a starting point for the approximation of the friction contribution will give large errors in the bottom hole pressure estimation since the friction factor does not converge. But since the estimate of the height of the mud, and mud weight alters a lot at the same time, the estimated bottom hole pressure is still more or less the same as the measurement, even though the states are incorrect. But since both measurements is available at all times in this case, and the states does not converge to their true values, the information given from the kalman filter is of little practical use.

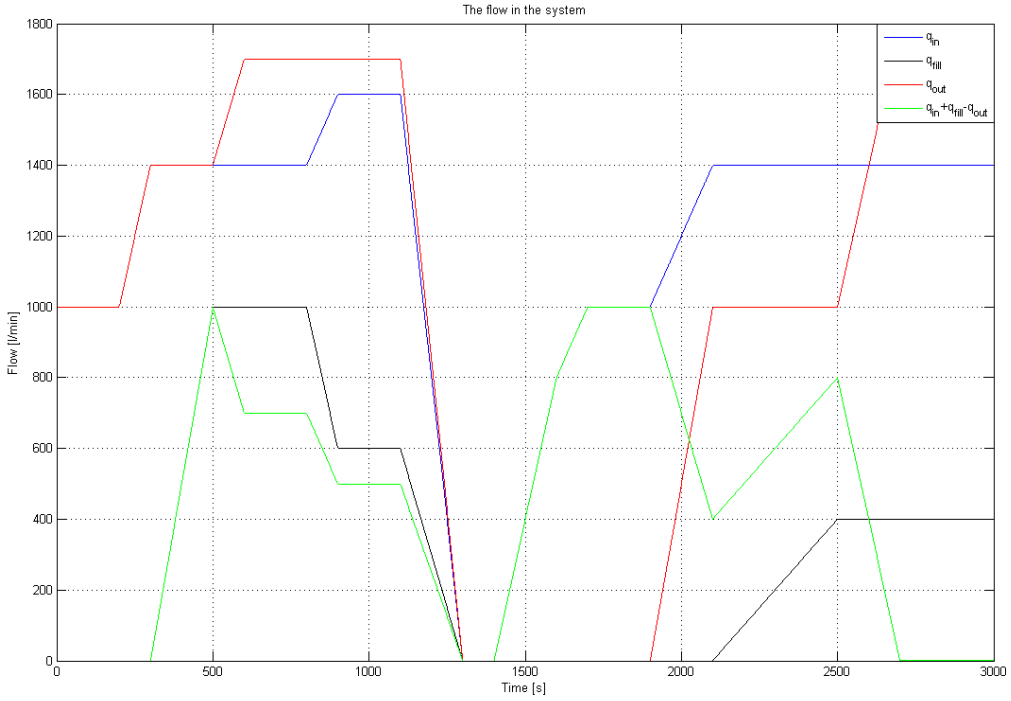

(a) The flow in the ORS system

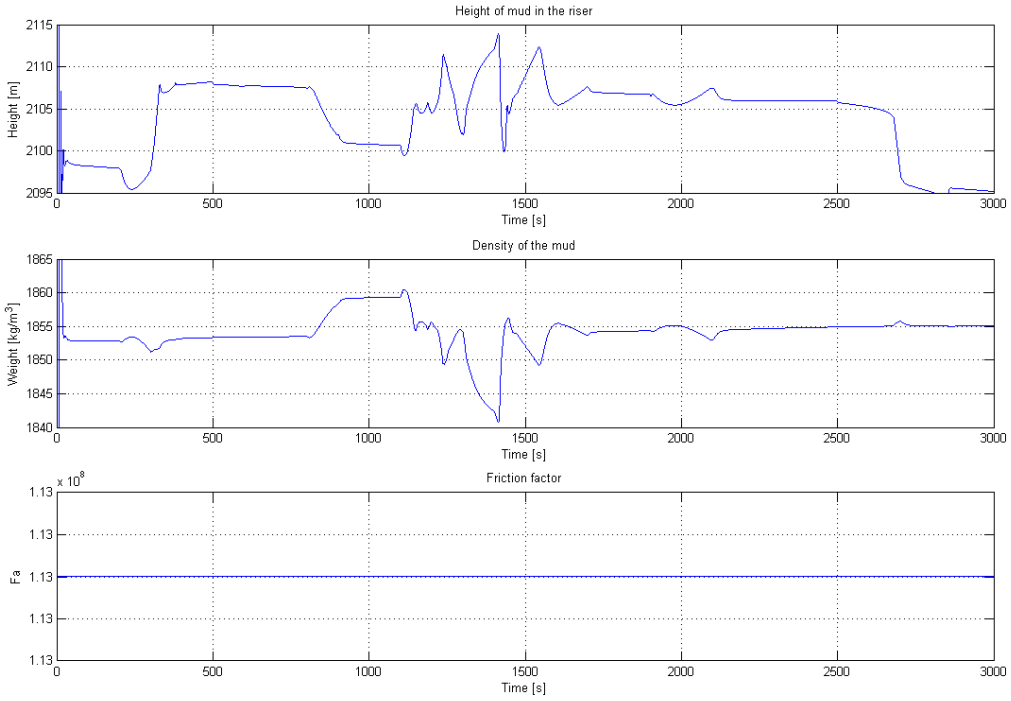

(b) The states in the ORS system

Figure 7.3: The flow in the system and the estimated states during simulation of the ORS system

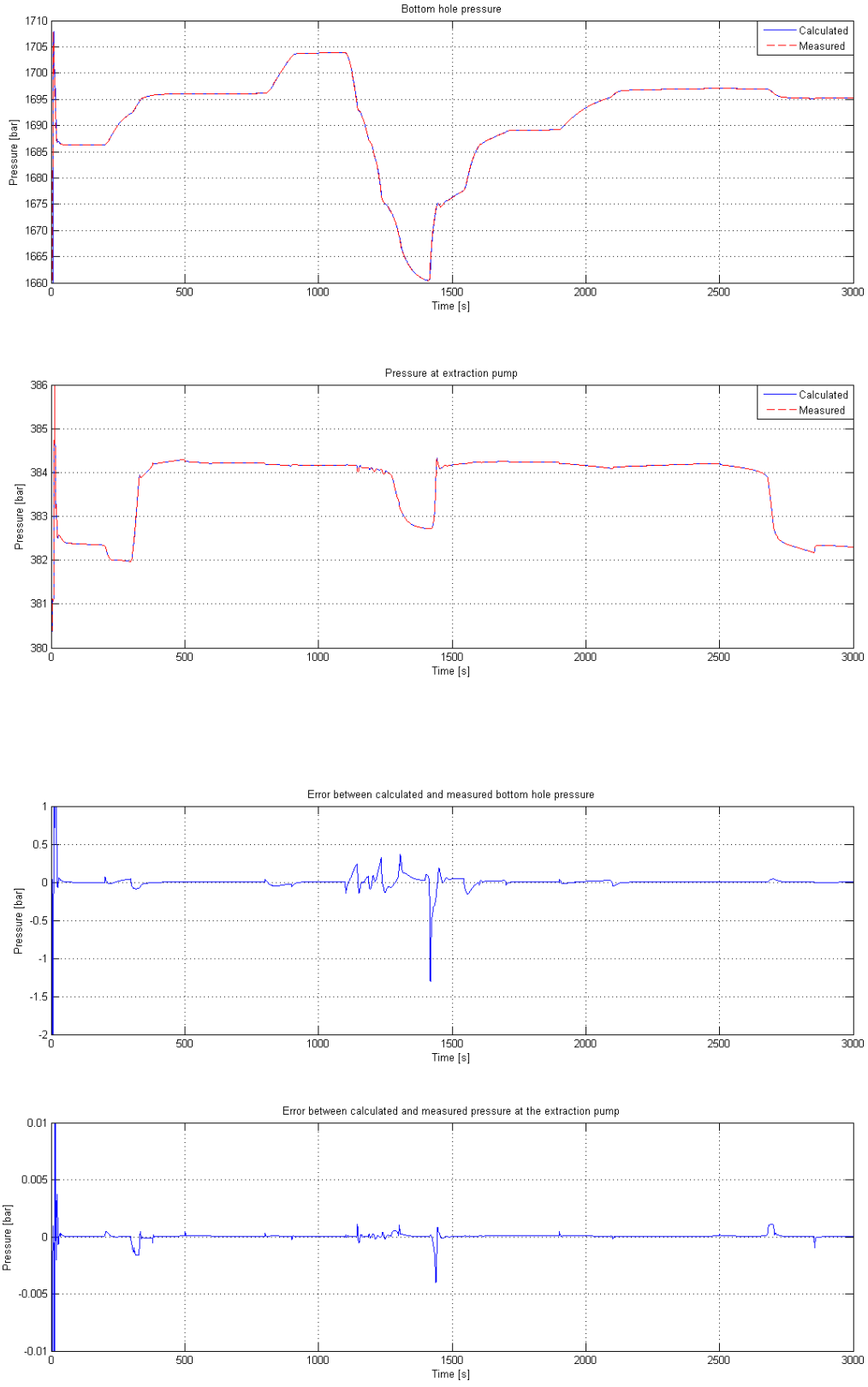

Figure 7.4: The pressures and error between estimated and measured pressures in the system

7.2 Delayed measurement update

As in the nominal testing of the kalman filter with delayed update of the bottom hole presses as in section 6.4, the measurement for the bottom hole pressure was in this simulation updated once every thirtieth second, and each measurement was thirty seconds delayed. Simulating under the same conditions as in the nominal test, will give a better overview on the performance of the kalman filter against behavior of a real well as opposed to simulation of the perfect model.

7.2.1 AGR simulation

For the first simulation of the AGR-case, the flow in figure 7.1 was used. Figure 7.6 shows the behavior of the estimated states. The estimated and measured bottom hole pressure together with the update of the measurement, and the error between the estimated and measured pressures is shown in figure 7.5. A measurement for the bottom hole pressure arrives each thirtieth second, and this is shown by the blue dots in the plot. It is clear that the model does not give satisfactory results when the flow into the well approaches zero. This is because there will be great errors in the friction term for flows below ca 80 l/min. There will also be big errors in the states at low flows, and the friction factor will not converge for this case either. When the pumps are ramped down to give zero flow in the system, the bottom hole pressure in the well will change rapidly, and the effect of the delayed measurements will be very obvious. The estimated value for the bottom hole pressure will lag behind the real pressure in the well as seen in figure 7.5a. The mud weight will decrease somewhat due to decreased bottom hole pressure, but since the estimated height increases when the pumps are ramped down, the estimated mud weight is assumed to decrease more than the true decrease in mud weight. The kalman filter was updated several times between each time step, to test if this gave better resemblance with the values from WeMod, but the performance gain was not significant. The behaviour of the two first states in this case resemble the behaviour of the states in figure 7.1b, but the alteration in the states are more violent when the measurements arrive and the estimated states are recalculated. As a result, the estimated bottom hole pressure will also change rapidly when the measurements arrive and the time horizon since last measurement is recalculated. This will give large deviations from the real pressure when the pressure alteration is violent as seen when the pumps are ramped down to achieve zero flow in the system. At higher flows, the kalman filter will give a good estimate of the bottom hole pressure as seen from this simulation and subsection 7.2.2.

The AGR case with flow as in figure 6.1 was simulated with the piecewise linear friction from figure 4.2a. This resulted in estimation of the two variables height of mud and mud weight. The resulting estimate of the bottom hole pressure is shown in figure 7.7. Unfortunately, this friction model does not give the desired improvement for the bottom hole pressure estimate at low flows.

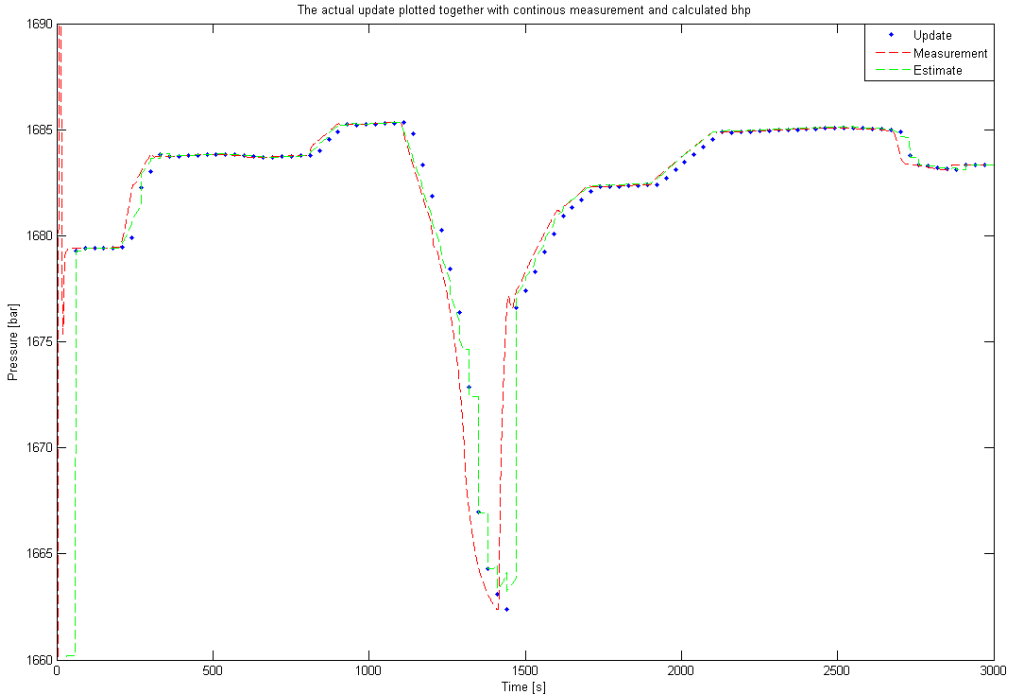

(a) Plot of the real and estimated bottom hole pressure in the AGR system

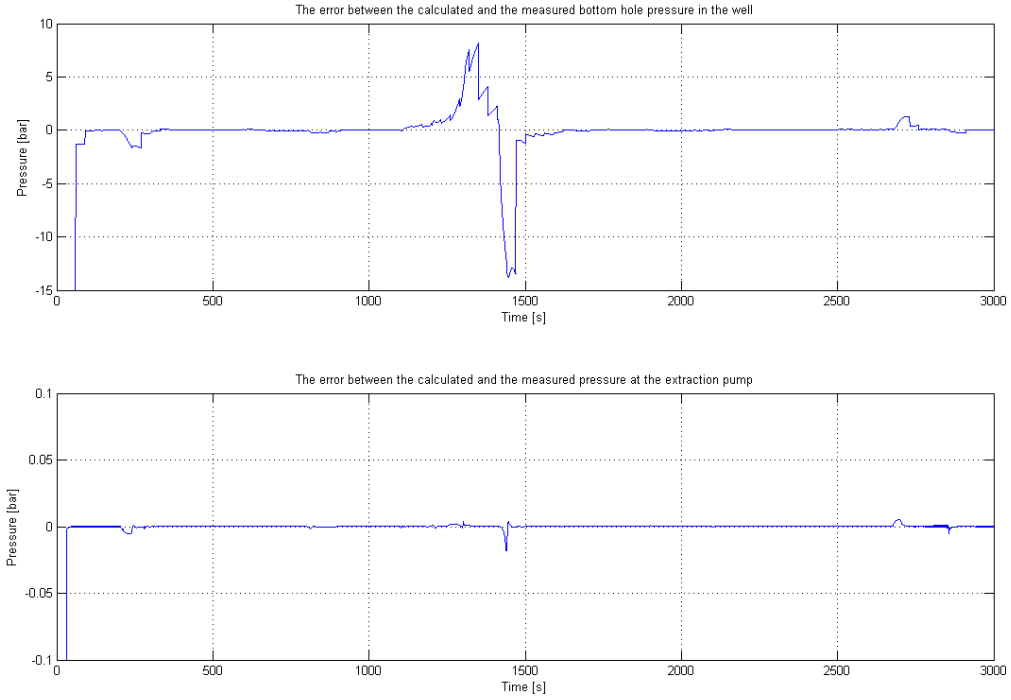

(b) Plot of the errors between the estimated and real pressures in the AGR system

Figure 7.5: Plot of the bottom hole pressure and error between estimated and measured pressures

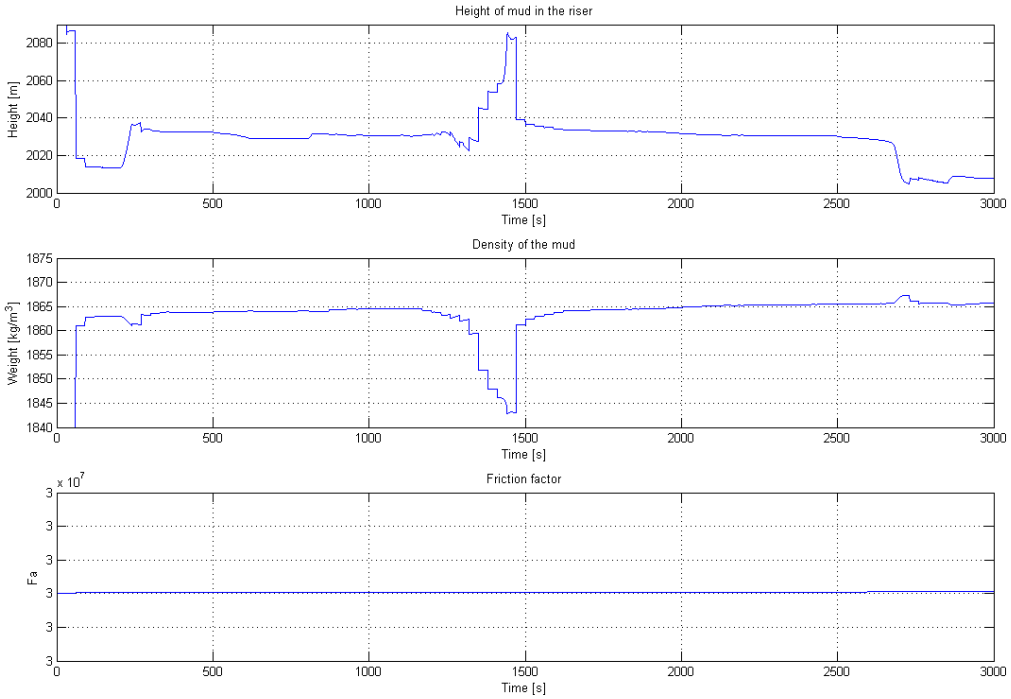

Figure 7.6: Plot of the estimated states in the AGR system

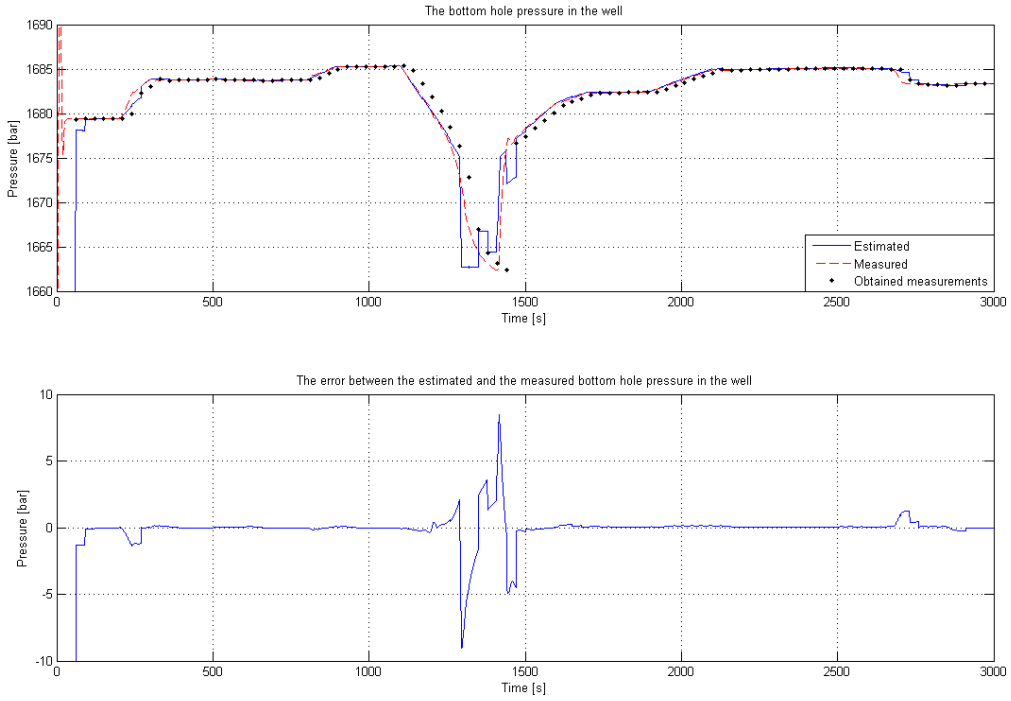

Figure 7.7: The bottom hole pressure with use of the piecewise linear friction model

Since the bottom hole pressure will be impossible to transmit by mud pulse telemetry at low flows, the kalman filters performance was tested when the measurement was delayed with 30 seconds, but at the same time was absent at flows below 400 l/min. The flow from figure 7.1a was used in this simulation also, to show the difference in estimated pressure when the measurements disappears and the kalman filter has to update the state estimate based on estimated bottom hole pressure measurement until the flow in the system is sufficient for mud pulse telemetry to work. Figure 7.8 shows the estimated and measured bottom hole pressure. The blue dots shows when measurements are obtained, and the absence of these shows that measurement is not obtained when the flow is below 400 l/min. It is clear from the plot that there will be large errors between the estimated and real pressure in this example. This is because the bottom hole pressure is rapidly changing when the measurement disappear after 1250 seconds of the simulation, so the kalman filter updates the states based on previous estimates until next measurement is obtained after 1500 seconds. Since the alteration in friction contribution is great at these low flows, the kalman filter will not be close to estimating the real pressure until the flow through the main pump raises again, and new measurements are obtained.

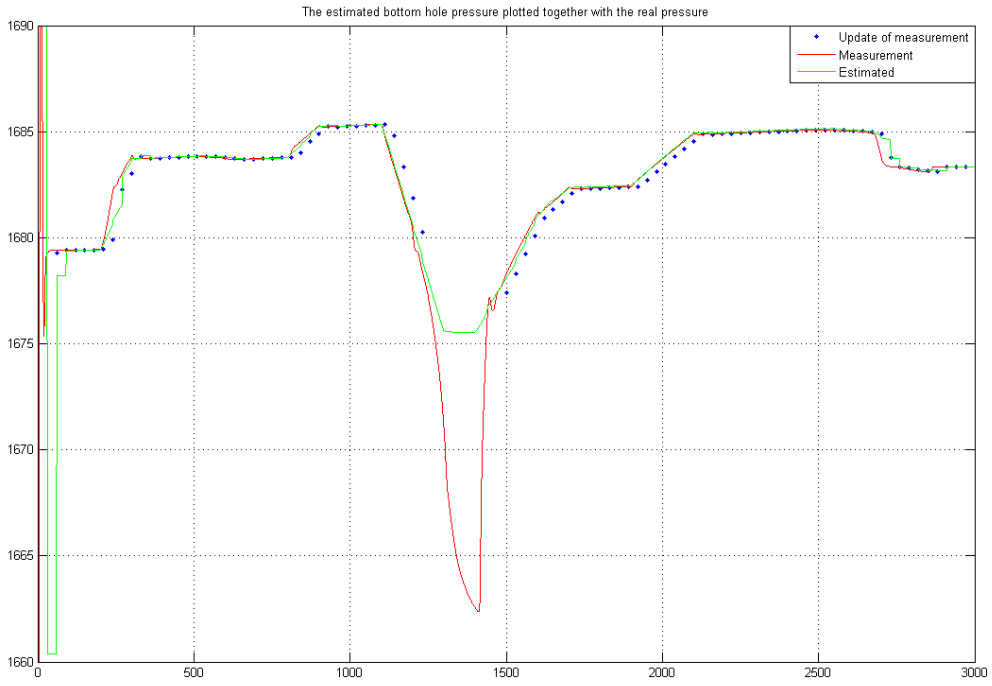

Figure 7.8: The estimated and measured bottom hole pressure when measurement is absent for low flows

7.2.2 AGR simulation with higher flow

To have a better look at the performance of the kalman filter for the AGR case at conditions where it is more likely that it will give better results, the system was simulated with the flow in figure 7.9a. By not ramping the flow too low, the problem with the error in the friction contribution to the bottom hole pressure at low flows was eliminated. The figures 7.9b, 7.10a and 7.10b shows the estimated states, the estimated and real pressures and the error between the estimated and real pressures. It is clear that at higher flows, the kalman filter gives a better estimate of the pressures in the system, even when the flows are changing rapidly. This is because the error from the friction contribution is lower than when the flow are ramped down to zero. But still, the model does not seem to give accurate estimates of the height and mud weight. The estimate of the mud weight is approximately constant, but the estimate of the mud height alters in a way that does not correspond with the flow. It is believed that the mud weight in this case is close to the average mud weight in the system, which shows that for higher flows, the kalman filter has better performance for state estimate as well as pressure estimate.

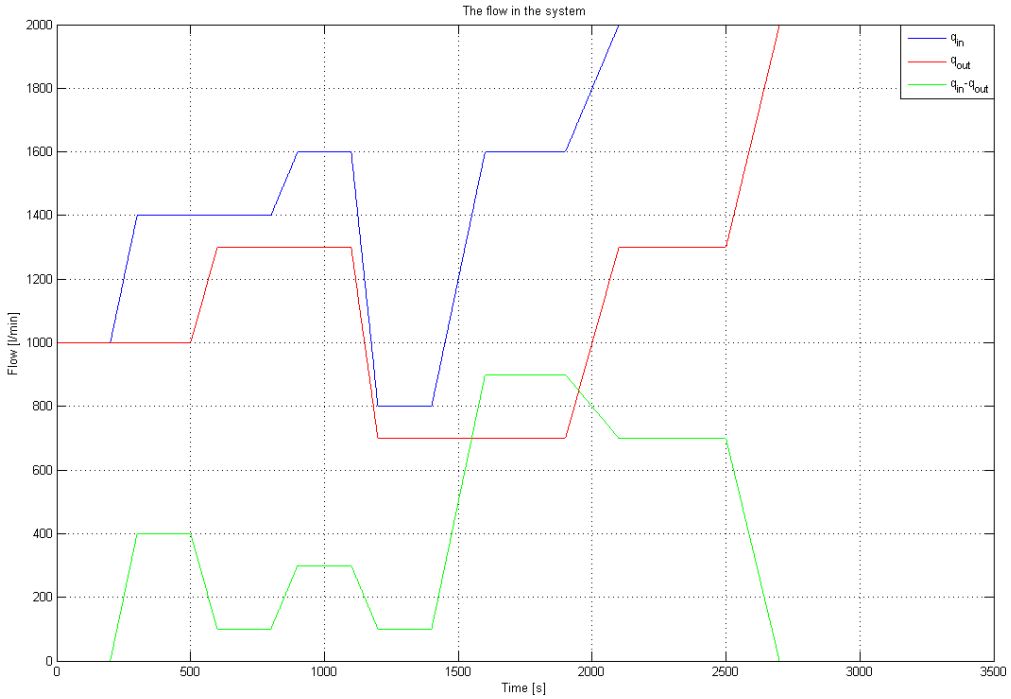

(a) The flow in the system

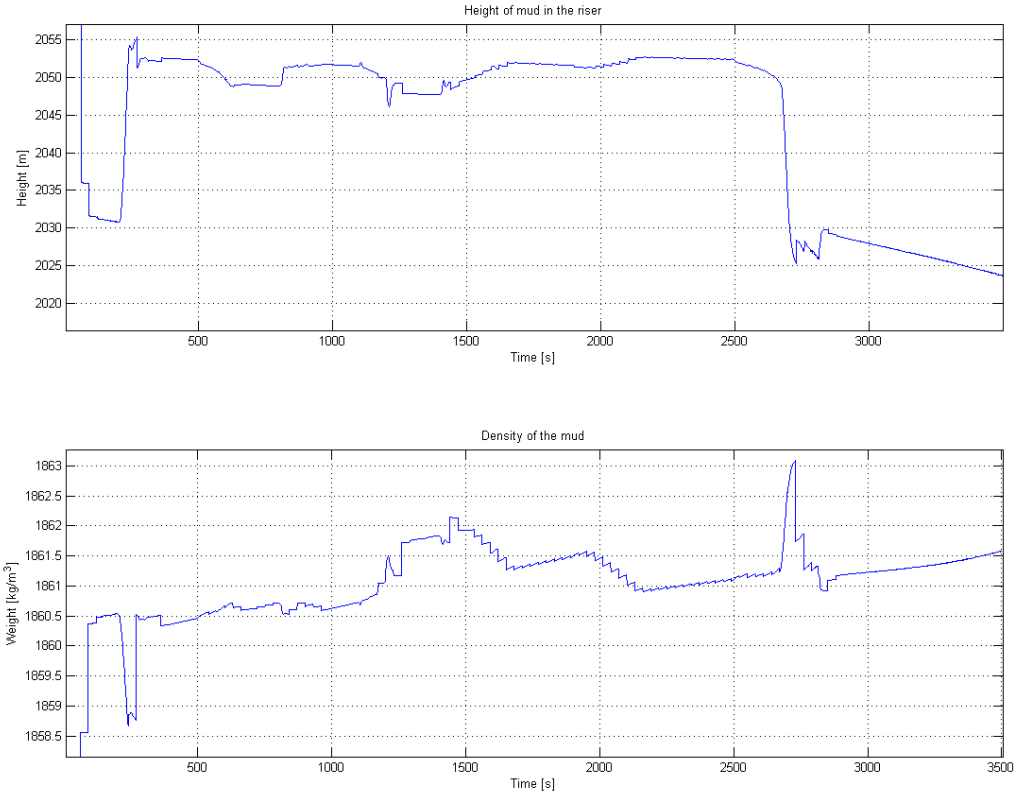

(b) Plot of the estimated states in the AGR system

Figure 7.9: The flow estimated states in the system

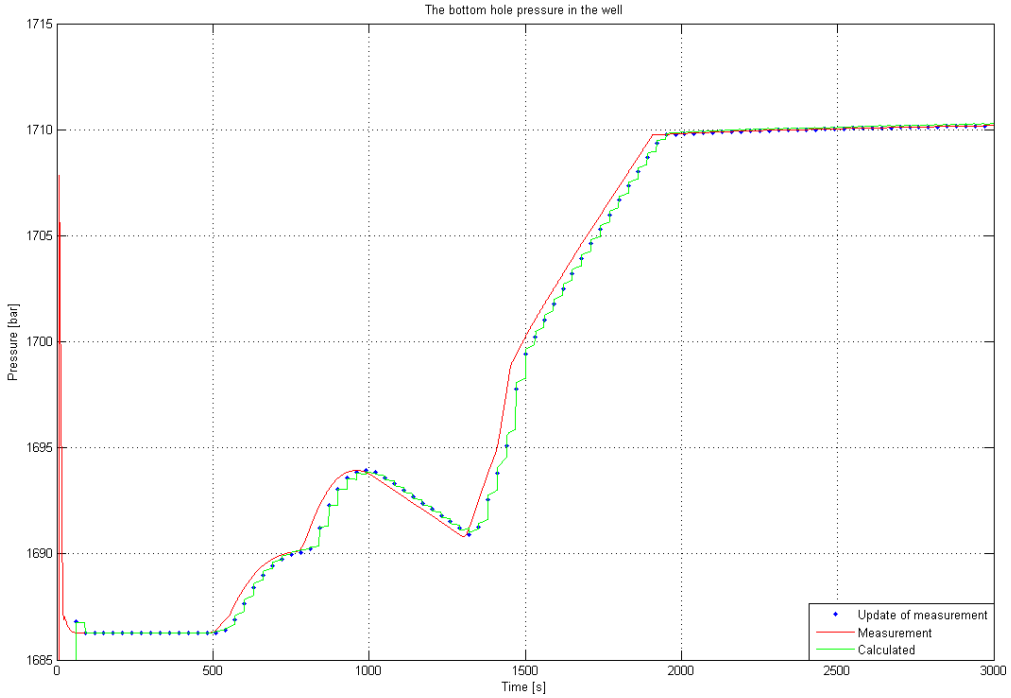

(a) Plot of the real and estimated bottom hole pressure in the AGR system

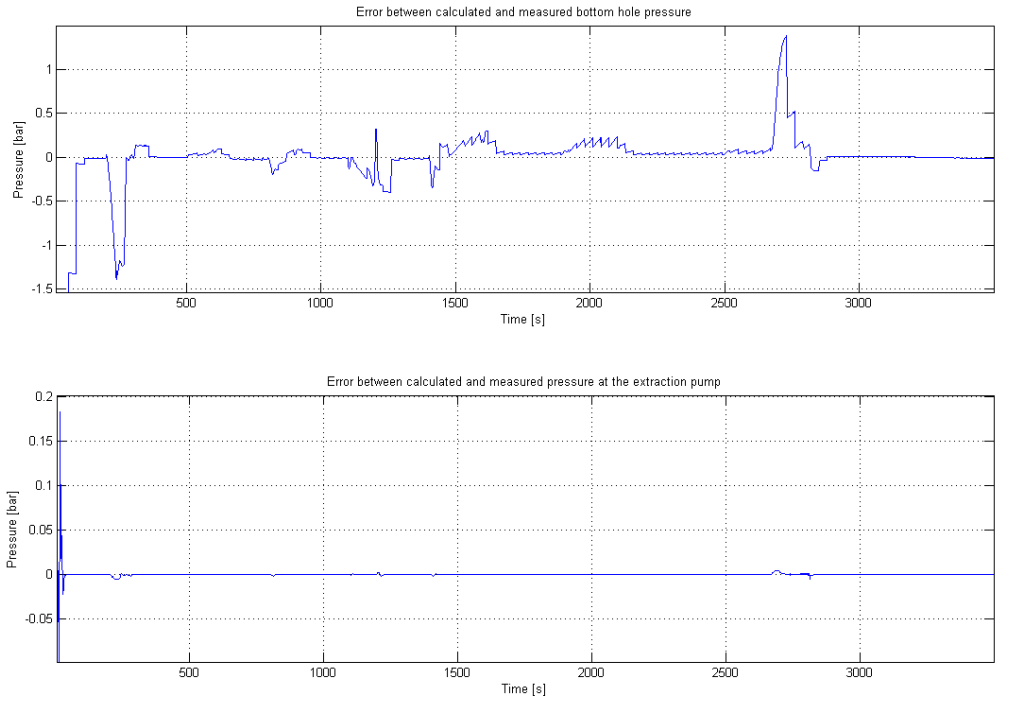

(b) Plot of the errors between the estimated and real pressures in the AGR system

Figure 7.10: Plot of the real and estimated bottom hole pressure and pressure errors in the AGR system

7.2.3 ORS simulation

The flow in the system for this simulation was as shown in figure 6.7. For the ORS system, the same problems as for the AGR system applies; the error between the estimated and measured bottom hole pressure will be large at low flows because of the error in the friction factor state. This will be somewhat compensated for in the estimated bottom hole pressure by errors in the height and mud weight states, but the error regarding the bottom hole pressure is still significant as can be seen from figure 7.12b. Since the friction factor does not converge, the other two states does not have the right values. The error is greatest when the flow in the system is ramped down to zero because this gives the greatest error for the friction contribution in the system as shown in figure 7.12b. But the error in the estimated pressure is very small when the pressure measurements are updated every second. To try to further improve the results, especially at low flows, the filter was updated several times between each update of the measurements, but this did not give a significant improvement.

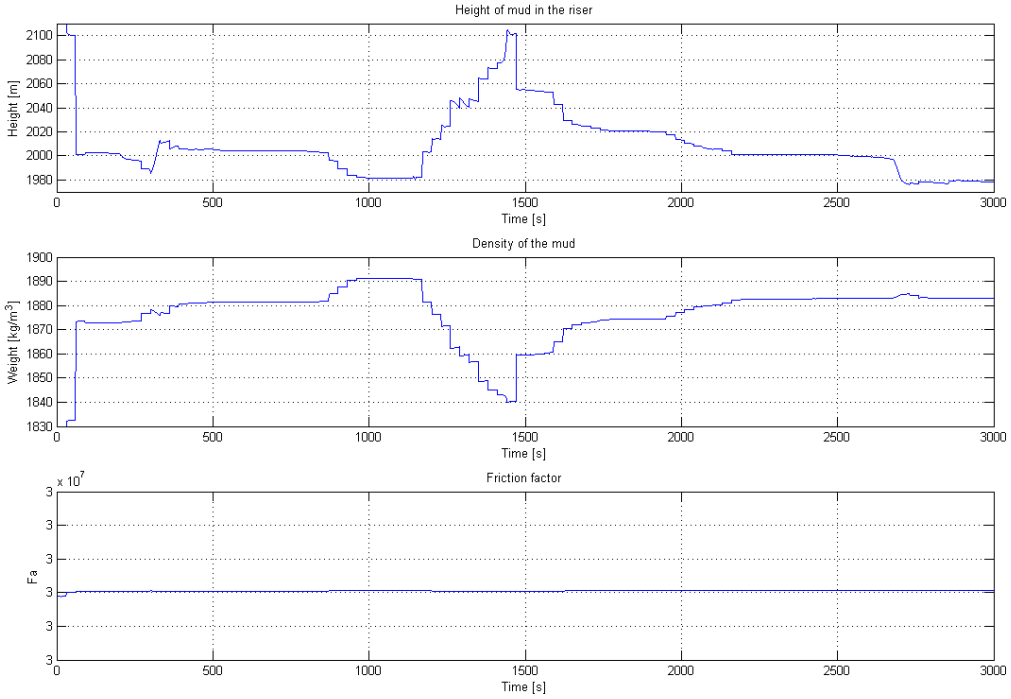

Figure 7.11: Plot of the real and estimated states in the ORS system

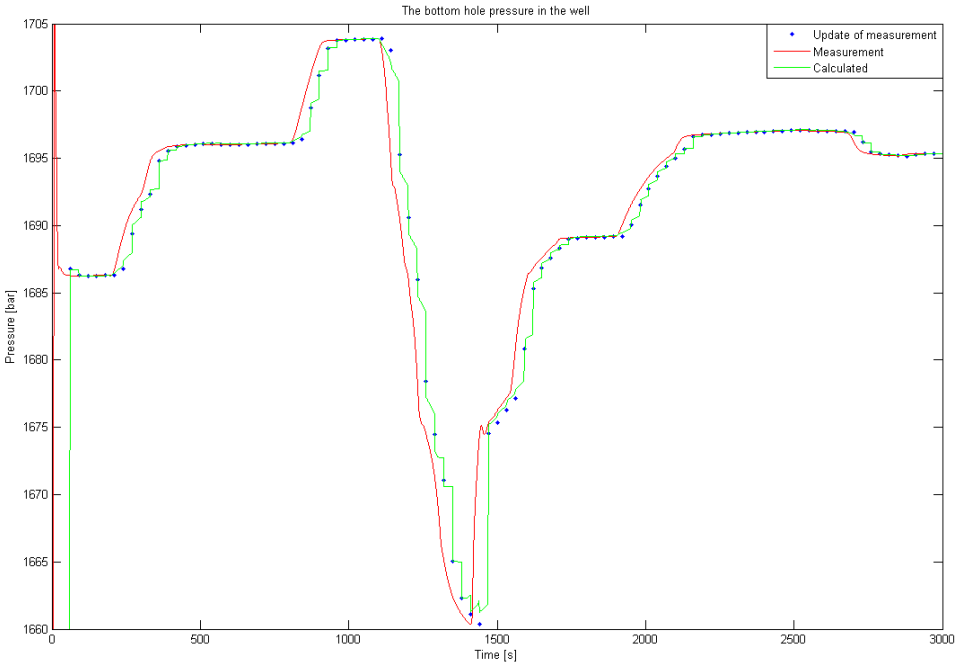

(a) Plot of the real and estimated pressures in the ORS system

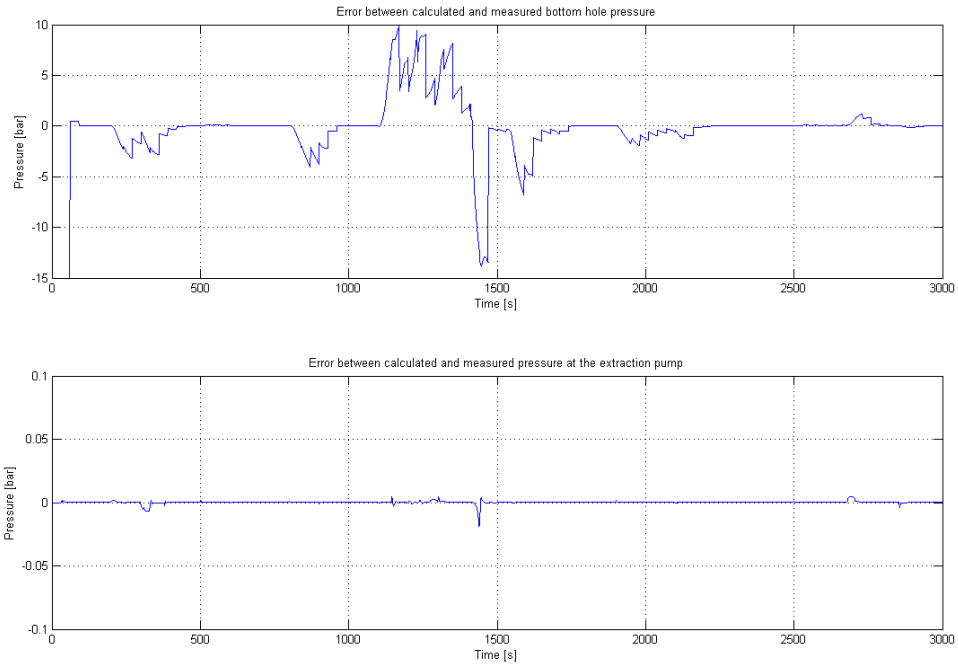

(b) Plot of the errors between the estimated and real pressures in the ORS system

Figure 7.12: The pressures and errors between estimated and real pressures

To have a better look at the performance of the kalman filter for the ORS case at conditions where it is more likely to give better results, the system was simulated with the flow in figure 7.13a. By not ramping the flow too low, the problem with the large error in the friction contribution to the bottom hole pressure at low flows was eliminated. At these flows, the error in the friction contribution will not be so significant, so the error between the estimated and real bottom hole pressure will not be so significant as seen in figure 7.14. But there are still problems for the kalman filter to estimate the real states since the friction contribution will be erroneous, and this will affects the other states. The estimate of the mud level behaves as anticipates, as it sinks when the flow out of the system is larger than the total flow in, increases as the total flow into the system exceeds the flow out of the system, and is stable when the flow into the system is equal to the flow out from the system (figure 7.13b). The mud weight increases throughout the simulation, and it is believed to increase because of the increased pressure in the well. So from the plot of the states and the pressures, it is clear that the kalman filter performs better at high flows, and the error between estimated and measured pressures will be lower than when the flow in the system is low.

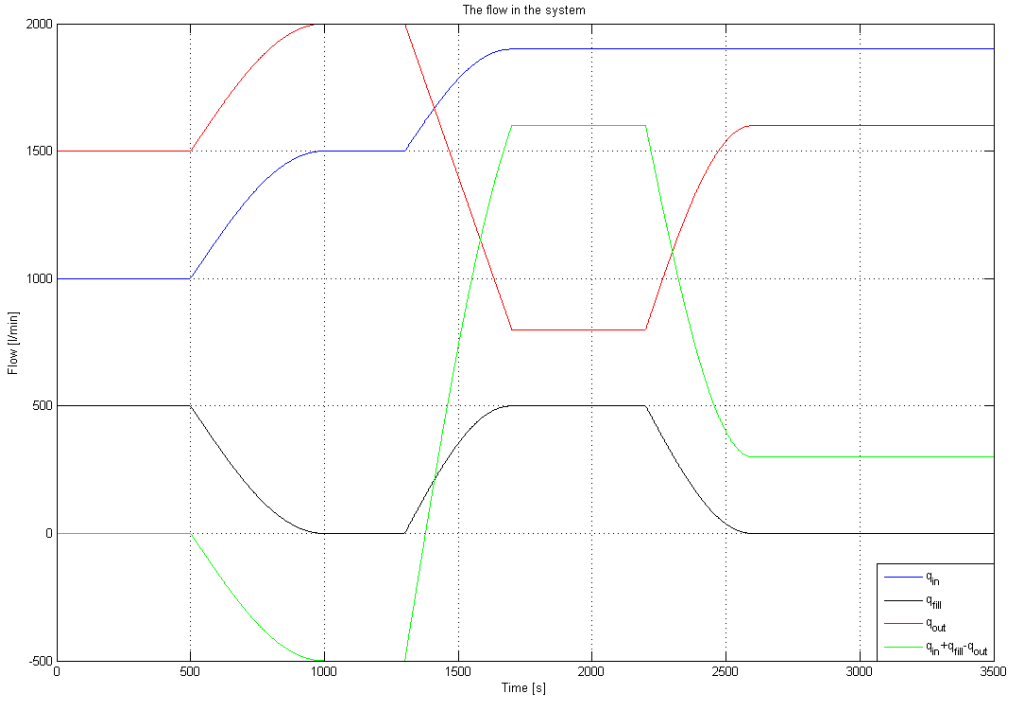

(a) The flow in the ORS system

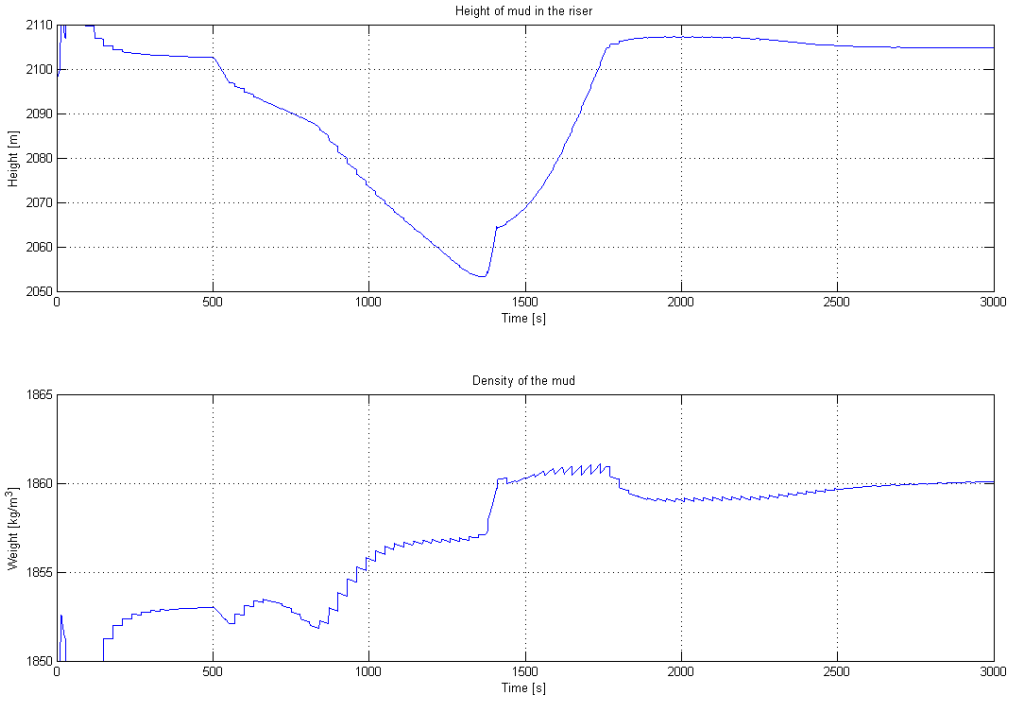

(b) The states in the ORS system

Figure 7.13: The flows and states in the ORS system

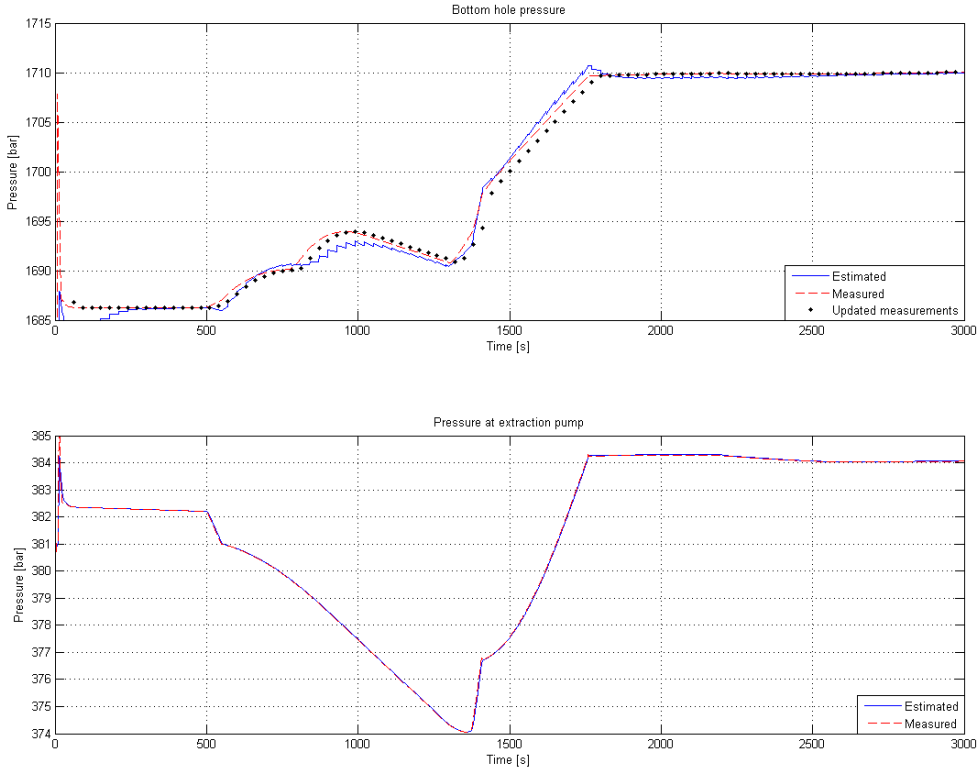

(a) The measured and estimated pressures

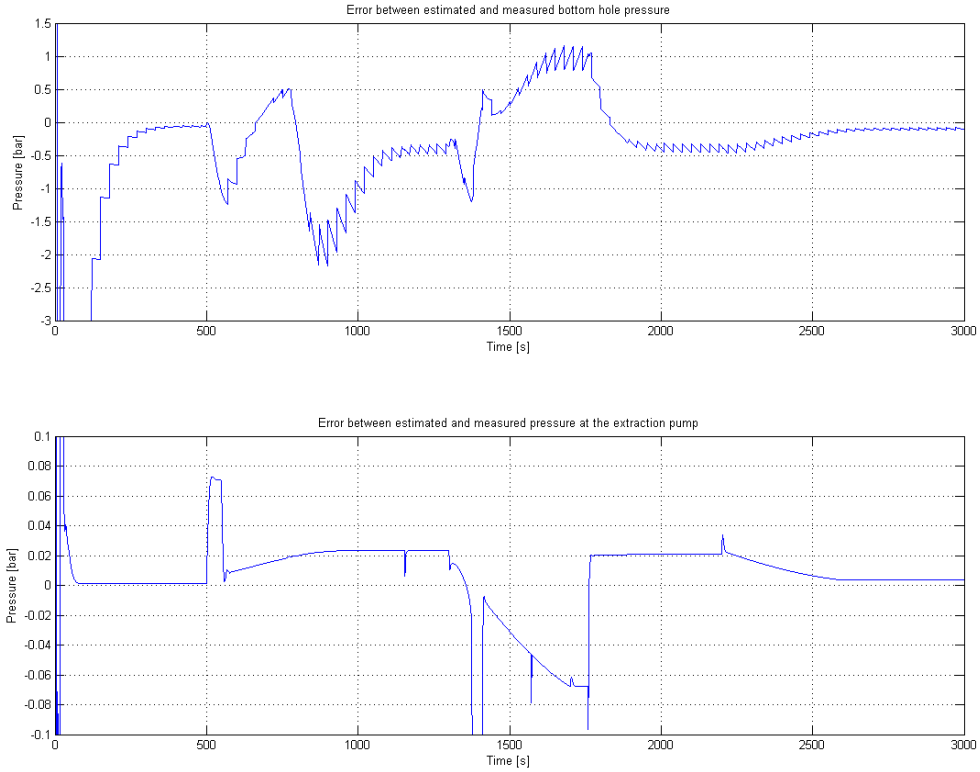

(b) The error between estimated and measured pressures

Figure 7.14: The pressures and error between estimated and measured pressures

The behaviour for the kalman filter was also tested when the different measurements was absent for some time. The flow in the system during the simulation was as in figure 7.13a. Figure 7.15 shows the pressures and estimated pressures, together with the error between the estimated and real pressure when the measurement of the pressure at the riserbottom was absent between 1000 and 1300 seconds and 2000 and 2300 seconds. Figure 7.16 shows the same plots for a case where the bottom hole pressure was not updated in the same intervals. It is clear that when the measurements are absent, the filter will be more inaccurate than when the measurements are continuously available from the extraction pump and every thirtieth second from the bottom hole pressure. The error in estimation of the pressures was more significant when the pressure measurement from the extraction pump was unavailable. This is believed to be caused by the fact that the slow update rate and the delay of the bottom hole pressure measurement gives more inaccurate estimates than the continuous measurement of the pressure at the extraction pump. The friction factor is not excitated in these simulations either, so the equation for the measurement of the pressure at the riserbottom contains both states that alter. Since the reliability and accuracy of the measurement at the extraction pump is believed to be much better than the mud pulse transmitted signal from the bottom hole pressure, the effect of absent bottom hole pressure is further simulated and results are shown in figure 7.17. The fact that the measurement at the extraction pump is most crucial is a positive factor for estimation in a real well. Figure 7.17 shows the estimated and real pressures together with the error between estimated and real pressures for different flows in the well when the bottom hole pressure measurement is absent between 1000 and 2800 seconds. The estimation of the bottom hole pressure shows promising results. The estimated pressure deviates by ca 10 bar at low flows into the well, but shows better performance when the flow is higher.

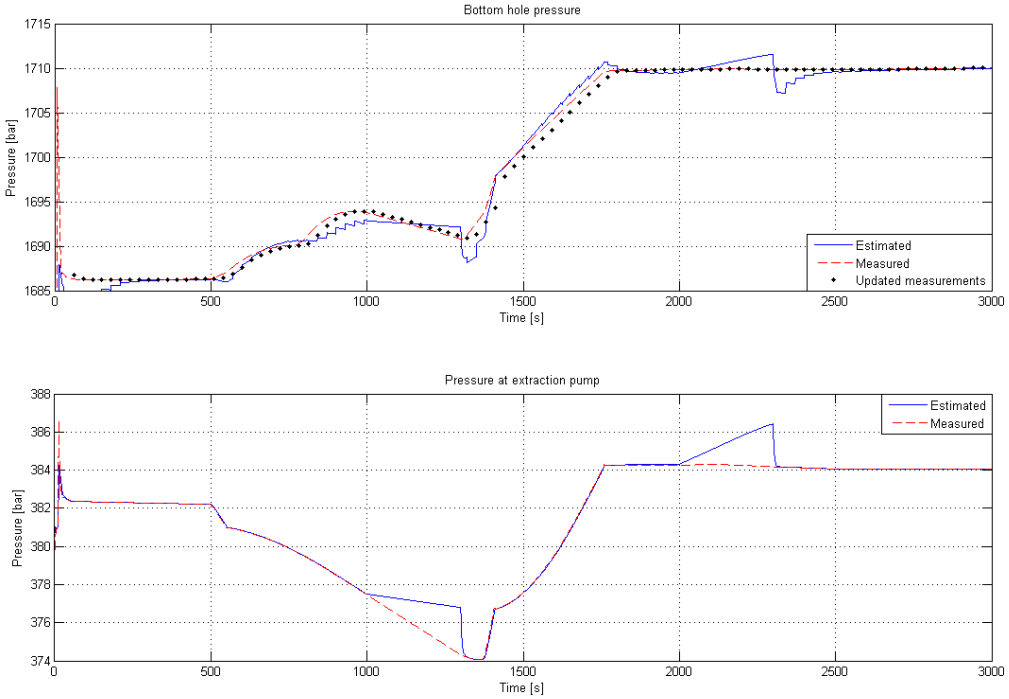

(a) The measured and estimated pressures

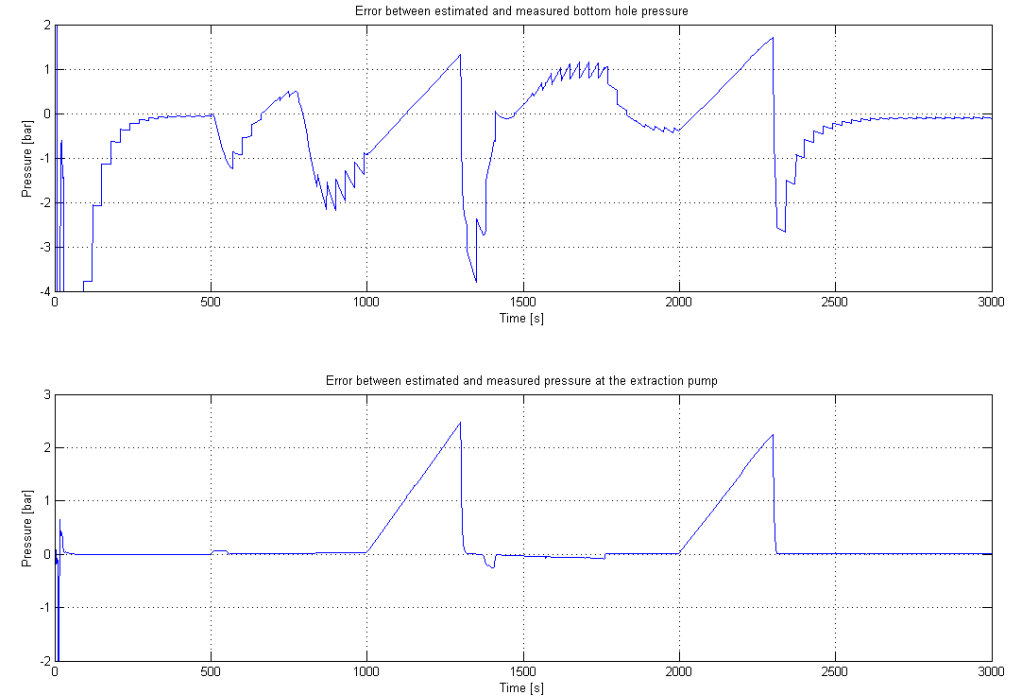

(b) The error between estimated and measured pressures

Figure 7.15: The pressures and error between estimated and measured pressures when the measurement from the riserbottom is absent

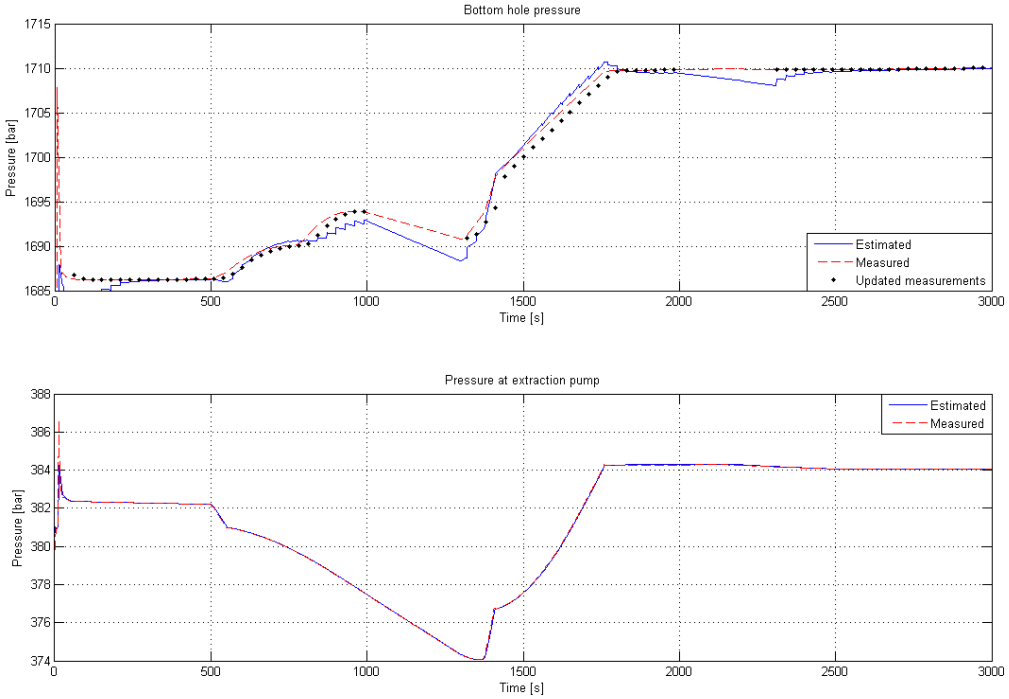

(a) The measured and estimated pressures

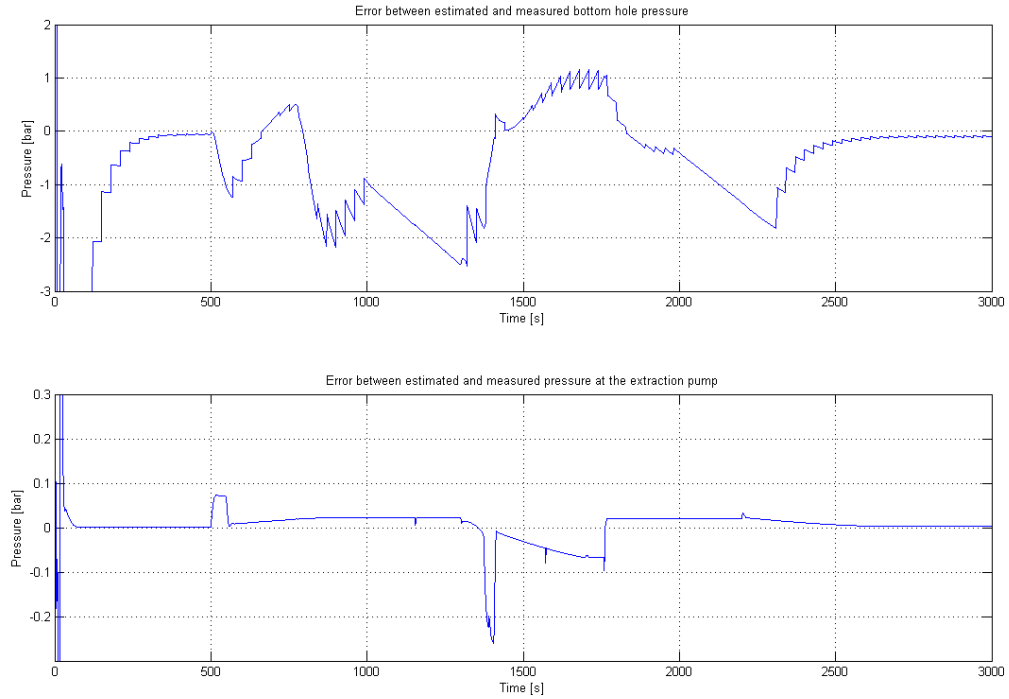

(b) The error between estimated and measured pressures

Figure 7.16: The pressures and error between estimated and measured pressures when the bottom hole pressure measurement is absent

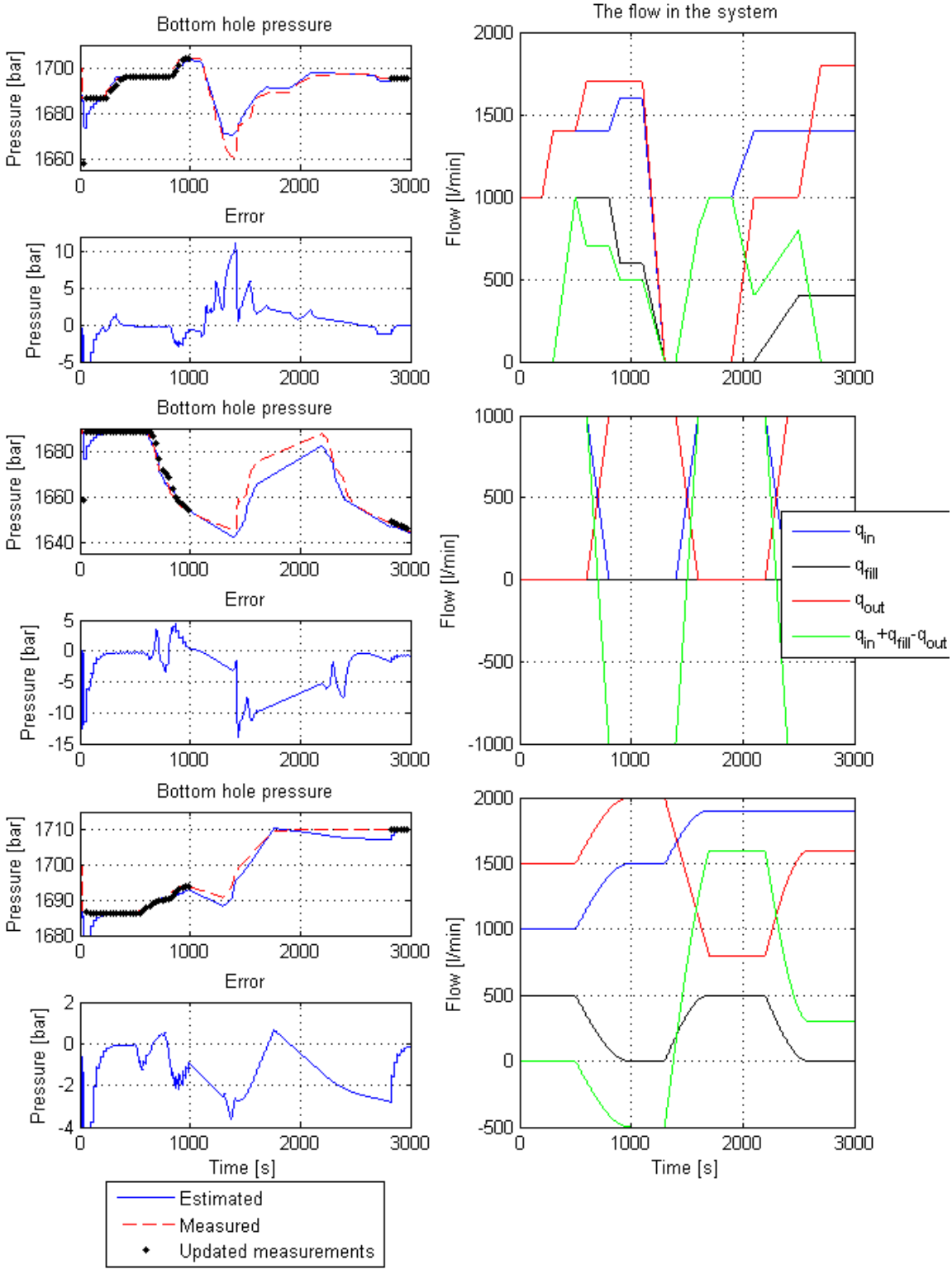

Figure 7.17: The bottom hole pressure for different flows

7.3 Use of different filters for different flows

A simulation using three different kalman filters and switching between them for different values of q_{in} to see if this could give better results by trying to estimate the friction contribution as a piecewise linear function as seen in section 4.3. As in previous simulations, the measurement for the bottom hole pressure arrived every thirtieth second, and each measurement was delayed by thirty seconds. The AGR system was simulated and the flow from figure 7.1a was used so that it was possible to compare this method against previously used simulations. But this estimation scheme did not give convergence for the friction factor in each filter either. The estimate of the bottom hole pressure is closer to the real pressure when the flow into the well is ramped down to zero as seen in figure 7.18a, but this is because of the initial values for the friction factors in the filters give better approximation of the friction contribution to the bottom hole pressure. This gives less deviation in the estimated values for the height of the mud and the mud weight (figure 7.18b), which in turn gives better estimate of the bottom hole pressure.

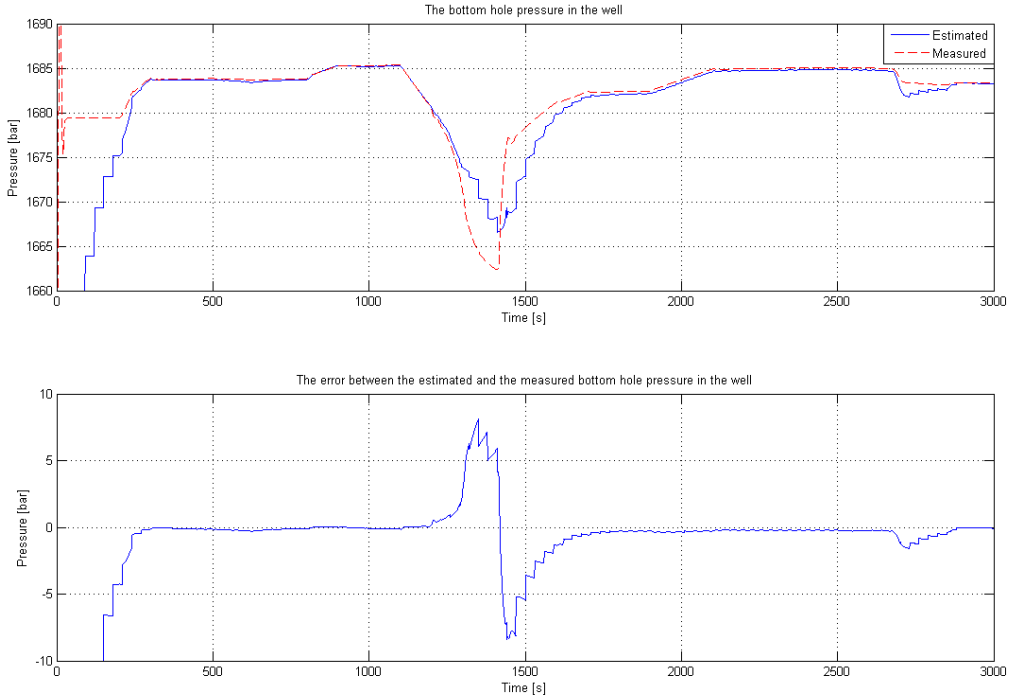

(a) The bottom hole pressure and the error between the estimated and real bottom hole pressure

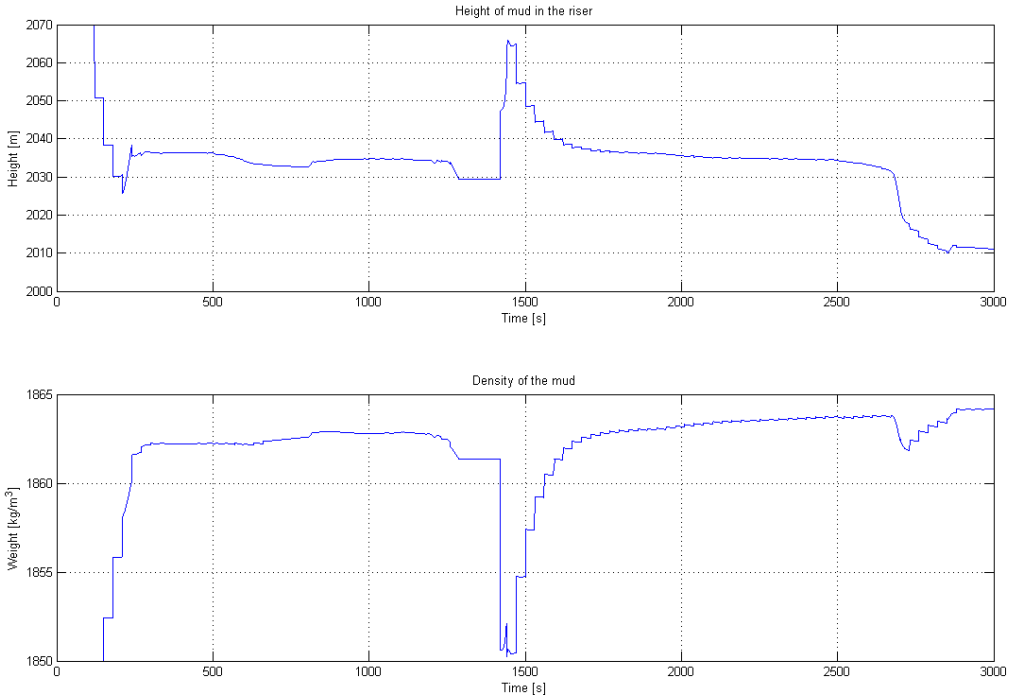

(b) The estimate for the height of mud in the riser and the mud weight

Figure 7.18: The bottom hole pressure and estimated states when estimating with different filters for different flows

Chapter 8

Control

During drilling, control of the pressure is of great importance as described in chapter 1. Two different cases were simulated to see how the well can be controlled by using the available manipulated variables. The first case was reference tracking during alteration of set point, and the second case was pressure control during pipe connection. For the second case, the flow into the system was decreased from 500 l/min to zero. After 1000 seconds, the flow into the system was ramped up to 500 l/min again. The reason for choosing the latter case, is that pipe connections must be performed when drilling with jointed drill pipes, to increase the reach of the string. Drill pipes has a nominal length of 9,6 meters, and is often connected in stands of three pipes which are jointed together in a pipe stand to save time during drilling. During the connection-procedure, the flow into the well has to be stopped. This leads to the loss of measurements from the MWD-tools, but also that the friction contribution to the bottom hole pressure disappears. Since pipe connections has to be performed ca every thirtieth meter, this is an important case to investigate for automatic control. The pumps in the systems were controlled by a PI-controller [13].

8.1 Control of the AGR system

In the first simulation the reference pressure was decreased with 5 bar every thousandth second from 1680 bar until it reached 1635 bar, and then increased at the same rate until it reached 1670 bar. In the first simulation, the bottom hole pressure was available every second, so that the control was performed on the measurement. The pressure in the well plotted against the reference pressure, the error between reference and real pressure and the flow in the well is shown in figure 8.1. In the second simulation, the measurement of the bottom hole pressure was available every thirtieth second, as in the simulation with delayed measurements in section 7.2. Therefore, the control was performed on the estimated value of the bottom hole pressure. Figure 8.2 shows the estimated states in the system (the friction factor is eliminated from the plots, as it does not converge). The error between the estimated and the measured pressures is shown in figure 8.3a. Figure 8.3b shows the pressure in the well together with the deviation from the set point and the flow through the pumps. As in previous simulations, the maximum pump rate is set to 2000 l/min. The flow into the well is constant at 1000 l/min, and the manipulated variable is the extraction pump. In both simulations, the PI regulator was tuned to achieve quick control, while reducing the overshoot as much as possible.

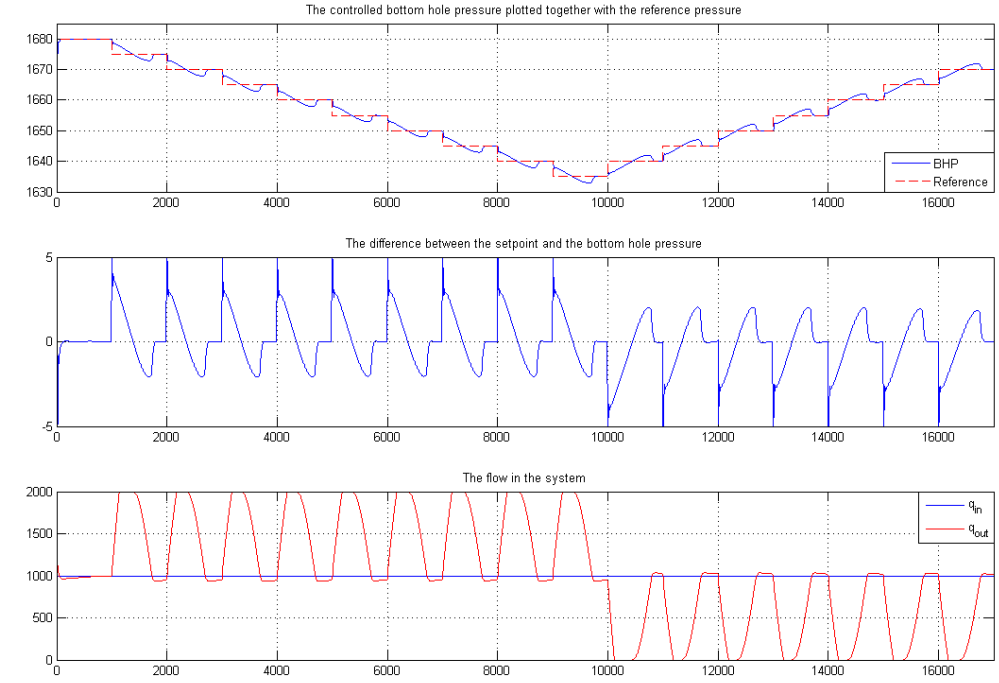

Figure 8.1: Plot of the bottom hole pressure and flow during continous update of the pressure measurements

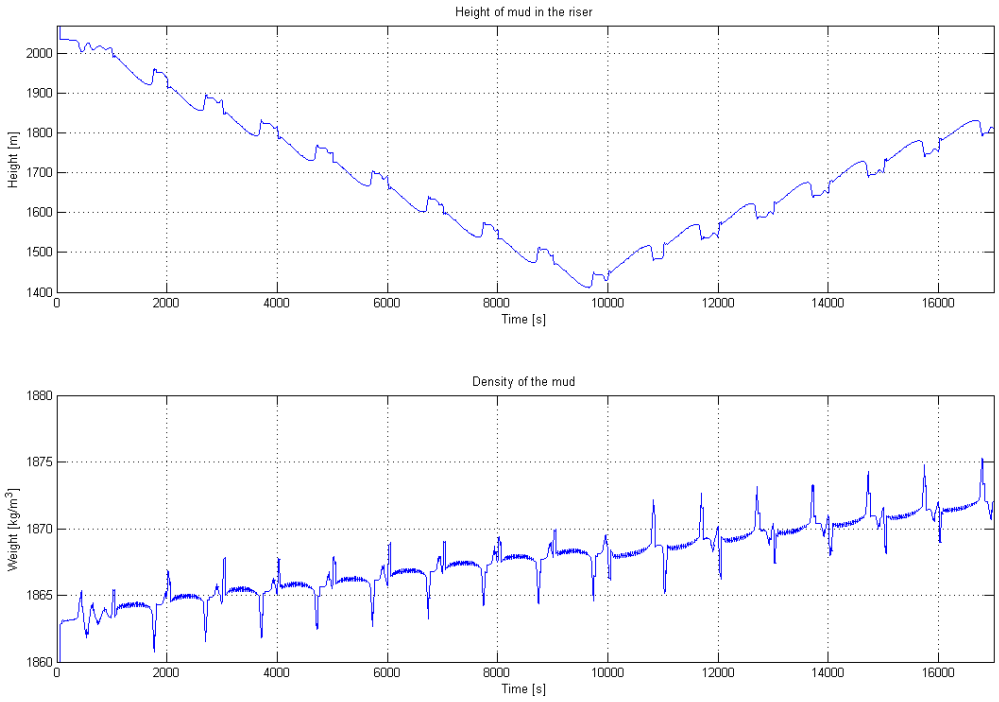

Figure 8.2: Plot of the estimated states during reference tracking with delayed measurement

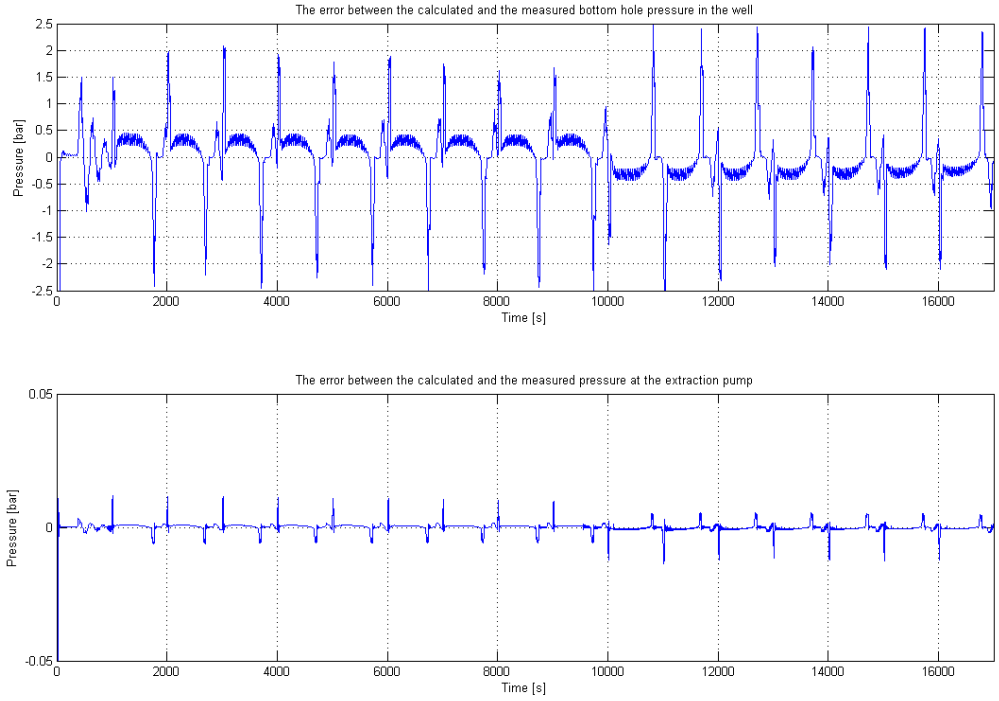

(a) Plot of the error between the measured and estimated pressures during reference tracking

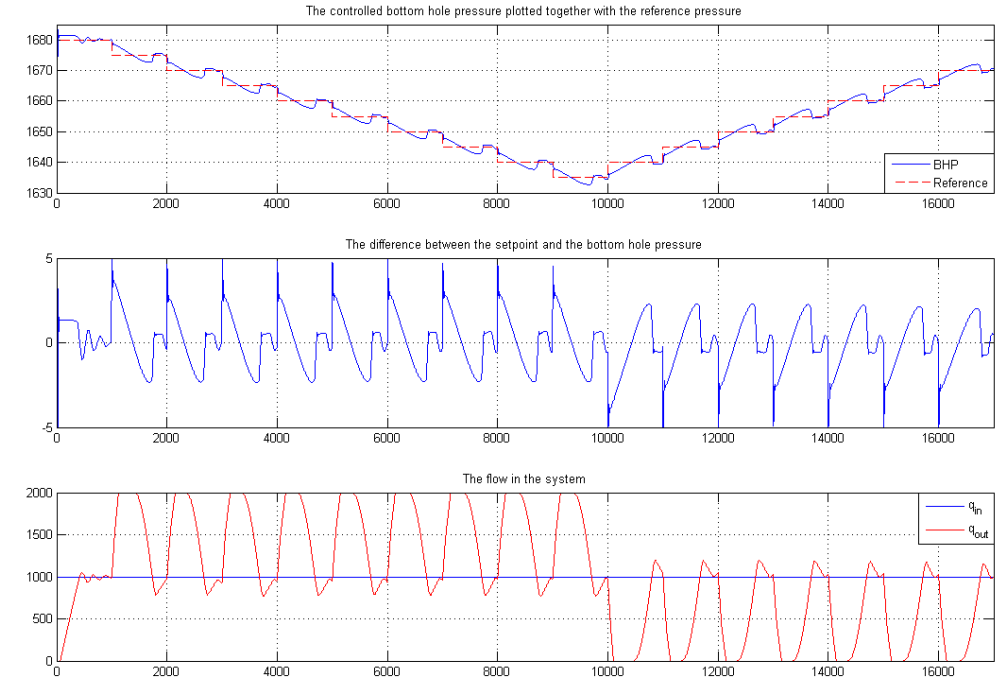

(b) Plot of the pressure, and flow during delayed update of the pressure measurements

Figure 8.3: Plots for the control case with delayed measurement

The pump hits it's saturation point of 2000 l/min in both simulation, which shows that this is a constraint which prevents faster control of the bottom hole pressure. For the simulation with control based on the estimated pressure, the control is not much worse than for the simulation with continous avaliable bottom hole pressure measurement. This is because the estimated pressure do not deviate much from the real pressure as seen from figure 8.3a. Since the flow into the system is steady and high, the problem with error in the friction factor is not so significant. The estimated height behaves as expected, following the alteration in pressure since the flow into the well is steady, but the flow out is controlled. Therefore, the alteration in pressure will depend on alteration in the height of mud in the riser, not the alteration in friction contribution.

8.2 Control of the ORS system

In the first scenario, the ability for reference tracking was tested. The reference pressure was lowered with 5 bar every 500 seconds from an initial value of 1680 bar to 1635 bar, and then increased to 1670 bar at the same rate. In the first simulation, the control was done directly on the measured bottom hole pressure. Figure 8.4 shows the pressure in the well plotted against the reference pressure, the error between the pressure and the reference pressure, and the flow in the well. It is clear from the figure that the controller will give the desired bottom hole pressure through the control of the extraction and annulus insertion pumps. There is however some overshoot in the pressure. This is because the system dynamics is slow. When the pump rate is updated, there is a delay from the time of the manipulation of the pumps to the effect in the bottom hole pressure. This leads to an excessive use of the two pumps, which, in a real case, may wear the the pumps more than necessary. A more advanced controller may help in this matter. In the second simulation, the control of the bottom hole pressure was done on the estimated bottom hole pressure from the extended kalman filter. In this simulation, the reference pressure was altered every 800 seconds. The bottom hole pressure measurement was a delayed update every thirtieth second. Figure 8.5a shows the difference between the estimated and measured pressures, while figure 8.5b shows the pressure in the well together with the deviation from the set point and the flow through the pumps. The pressure control for the first case when the control is done on the bottom hole pressure measurement show better performance. For the case where the control is done on the estimated pressure, the control is slower, and there is a problem for the controller to reach the correct pressure before the next alteration of the reference pressure when the reference switches from decreasing by 5 bar to increasing by 5 bar.

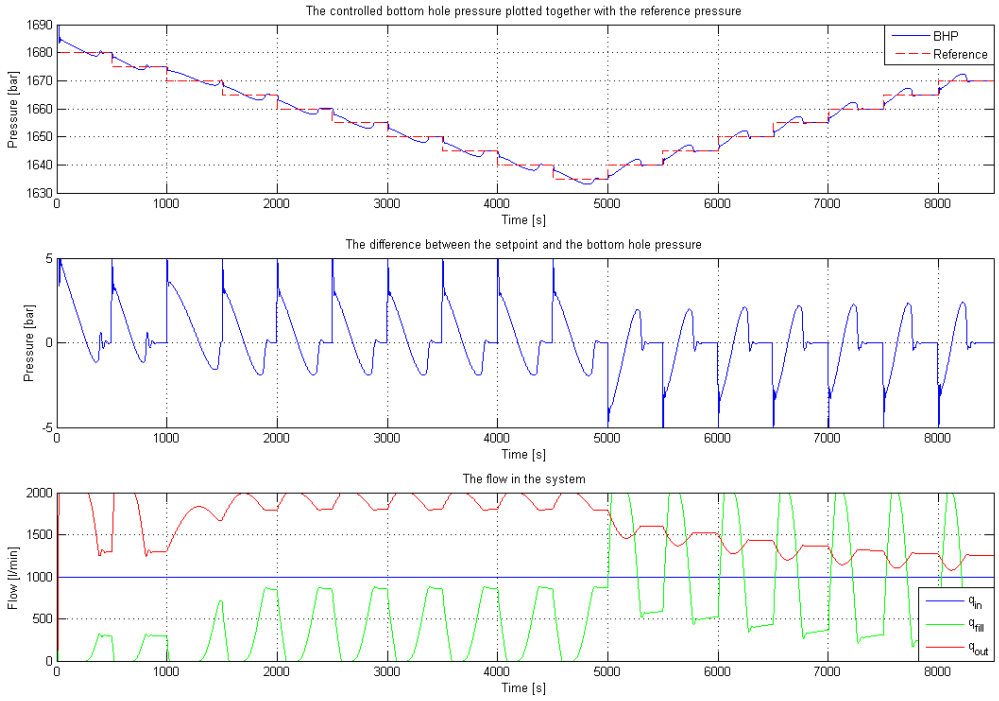

Figure 8.4: Plot of the pressure, and flow during continous update of the pressure measurements

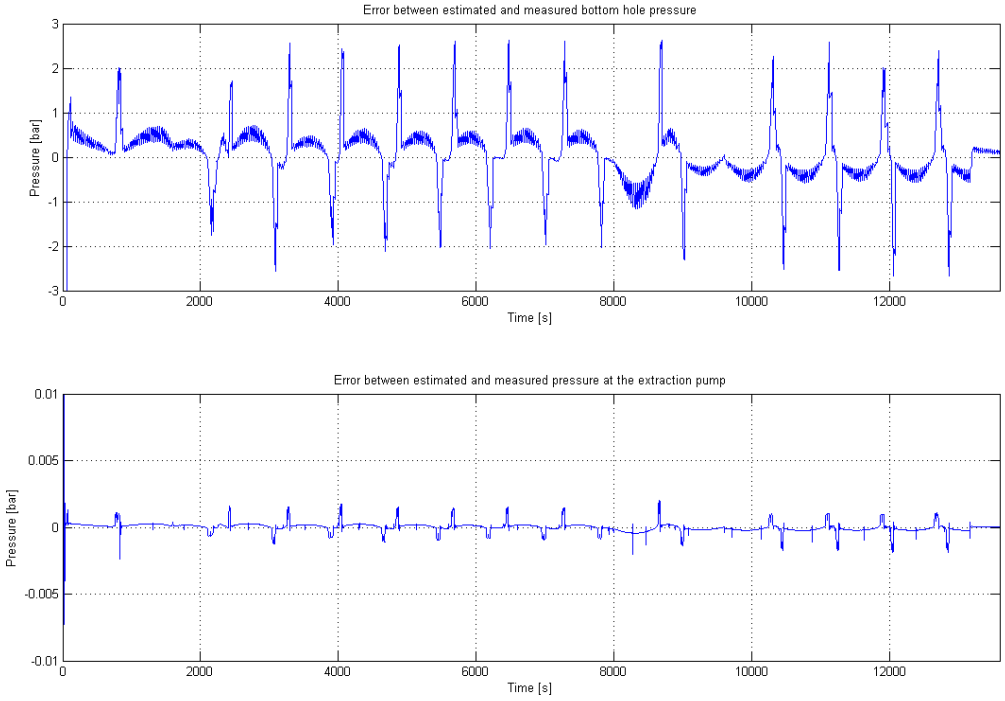

(a) Plot of the error between the measured and estimated pressures during reference tracking

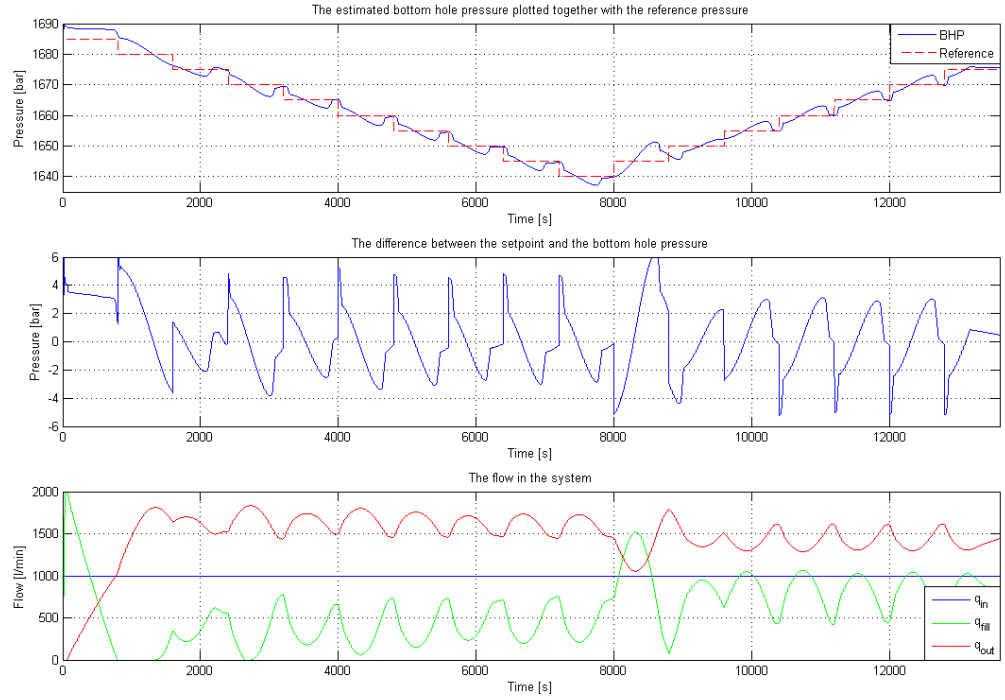

(b) Plot of the pressure, and flow during delayed update of the pressure measurements

Figure 8.5: Plots for the control case with delayed measurement

The second scenario for the ORS system is a simulated drill pipe connection. The flow into the drill string is ramped down from 500 l/min to zero, and then kept at zero during the connection. Thereafter, the flow into the system is ramped up to 500 l/min again. For the first simulation, the control is done directly on the measured bottom hole pressure. Figure 8.6 shows the pressure in the well plotted against the reference pressure, the error between the pressure and the reference pressure, and the flow in the well. To test the performance of the pressure controller during more realistic condition, the control was done on the estimated pressures from the kalman filter with update of the bottom hole pressure every thirtieth second. Figure 8.7a shows the error between estimated and measured pressures in the system Figure 8.7b shows the pressure plotted together with the reference pressure, the deviation from the reference pressure and the flow in the system. For both simulation the desired pressure is set to 1660 bar during the connection.

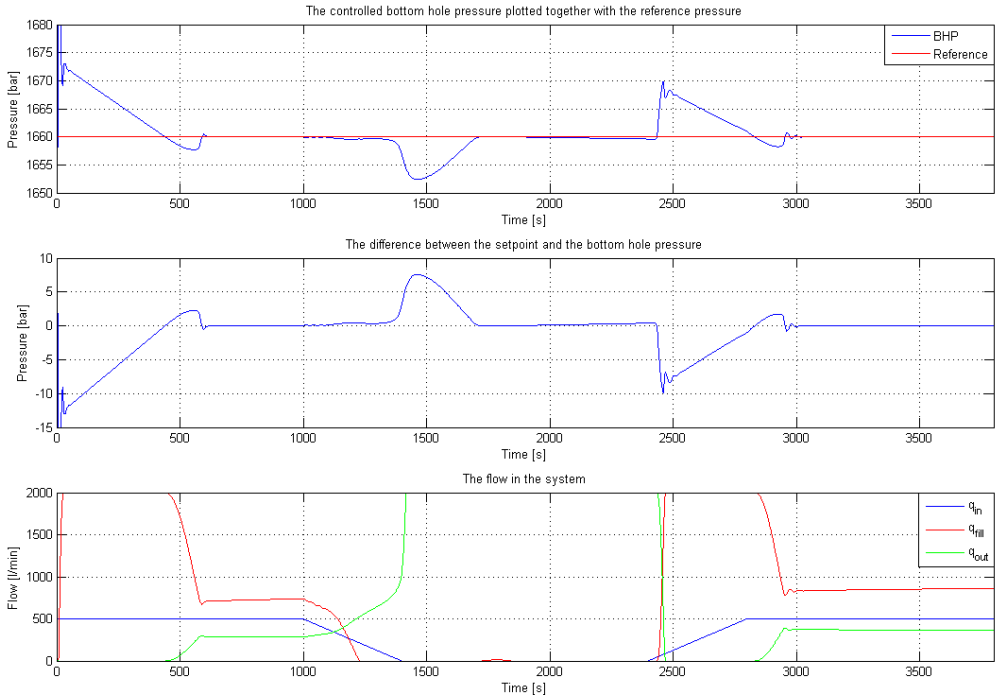

Figure 8.6: Plot of the pressure and flow during continous update of the pressure measurements

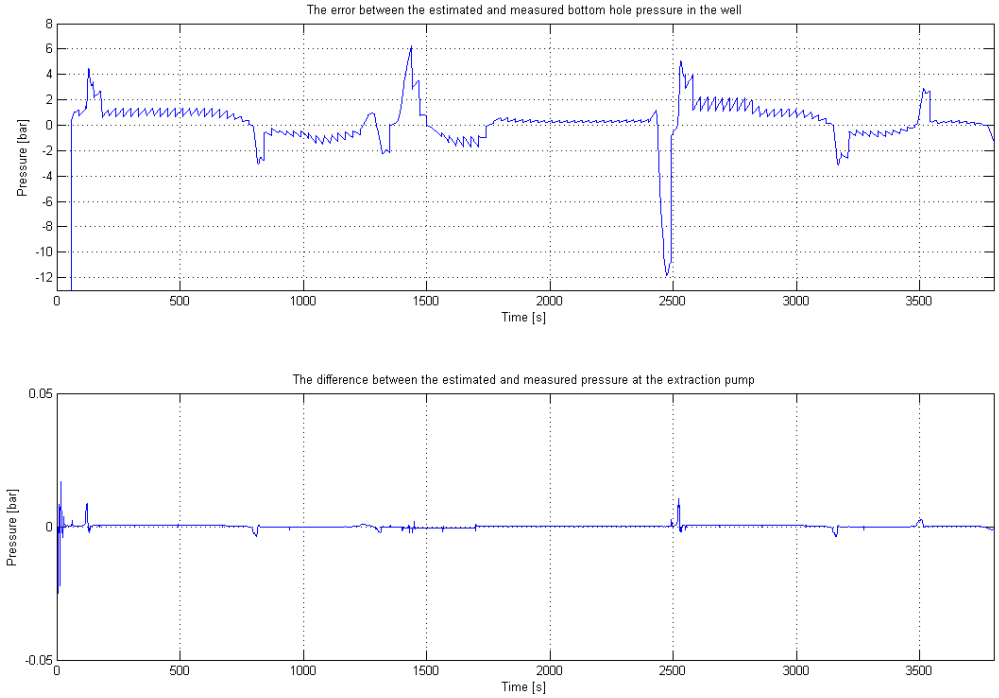

(a) Plot of the error between the measured and estimated pressures during pipe connection

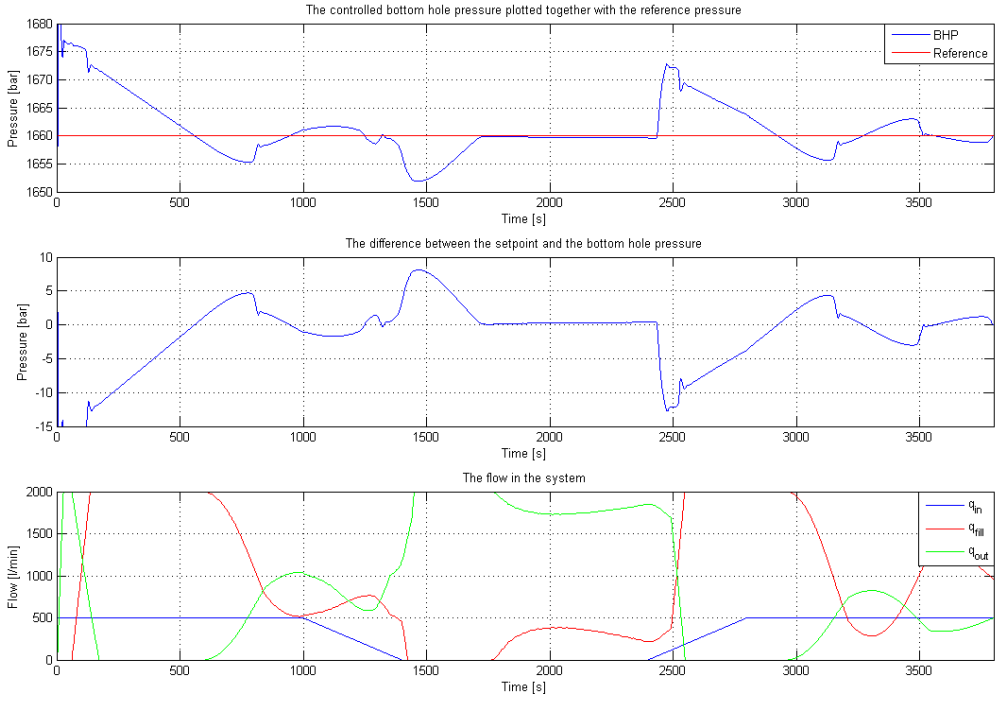

(b) Plot of the pressure, and flow for a simulated pipe connection during delayed update of the pressure measurements

Figure 8.7: Plots for the control case with delayed measurement

The results show that the bottom hole pressure will deviate somewhat from the desired pressure during a pipe connection. This is because of the delay from the manipulation of the pumps until the change in bottom hole pressure, and the fact that the pumps hits their saturation pump during the simulation. The control of the system is slow, so there will be problematic to compensate for the absence of friction loss when the main pump is ramped down to zero. This has to be compensated for by higher mud level in the riser. The bottom hole pressure deviates more than 10 bar from the set point when the main pump is ramped up again. This might be a problem if the pressure margins are very narrow, but since the bottom hole pressure is so extremely high in this well, the percent wise deviation from the set point is low. If the pressure measurements for the bottom hole pressure is set to be unavailable at low flows (set to below 400 l/min), figure 8.8 shows the pressure and flows in the system for the same case as simulated above. The control of the pumps are done on the estimated pressure in this case. The bottom hole pressure measurement is absent for 1650 seconds, and in this time period the states and bottom hole pressure estimate is updated based on the previous estimate of the bottom hole pressure and the measured pressure at the extraction pump. Because of the error between the estimated and real pressure and the fact that the control is done based on the estimated bottom hole pressure, the maximum deviation for the bottom hole pressure from the reference pressure is in fact lower than in previous case. This is because there is an considerable error between the estimated and real bottom hole pressure.

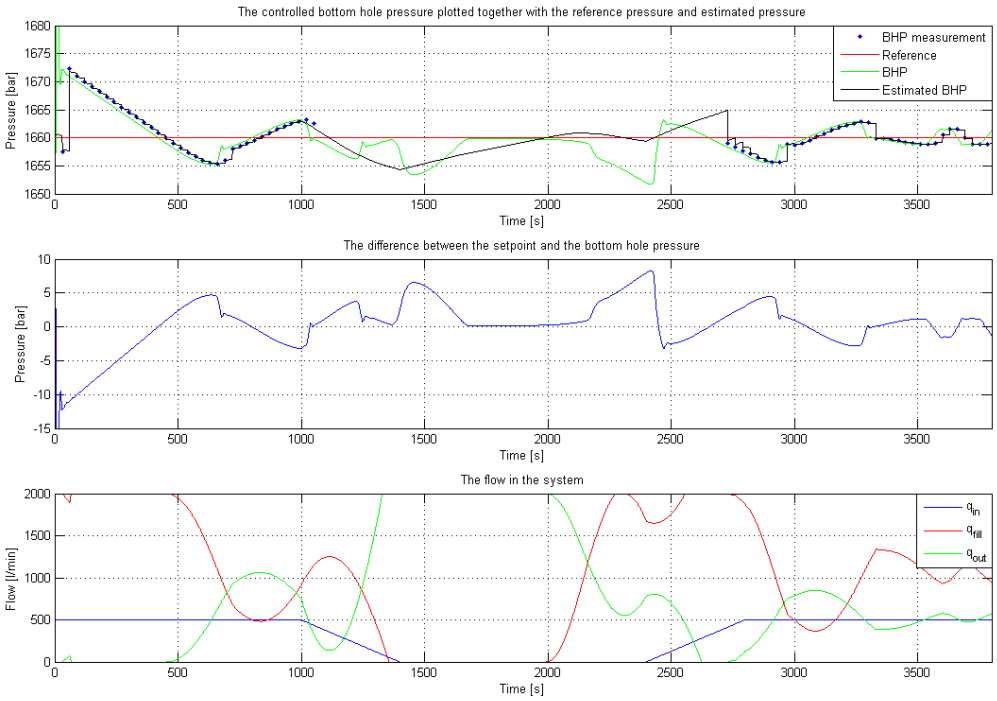

Figure 8.8: Plot of the pressure, and flow for a simulated pipe connection during delayed update of the pressure measurements with missing measurements for low flows

Chapter 9

Conclusions and future work

9.1 Conclusions

The simplified model for the dual gradient drilling systems shows weaknesses in estimation of friction. This is because the friction contribution to the bottom hole pressure is so marginal compared to the hydrostatic contribution to the bottom hole pressure. Since the friction parameter is not excitated, the value for the friction contribution will be erroneous, and this will influence the correctness of the estimate of the other states in the model. Different friction models was tested, but none gave very accurate estimates for the bottom hole pressure during low flows, as none of the parameters regarding the friction would alter during the simulations, and would therefore not converge against reasonable values. In the nominal testing, it was shown that it is possible to get all states to converge to their real values if the flow is sufficiently increased. This shows that if the friction contribution in the well is larger, the model might have a better fit against real values. Since it was impossible to get excitation of the friction factor parameter for the kalman filter in both nominal testing and testing against WeMod during normal flow conditions, it is believed that the extended kalman filter works as it is supposed to, but not as desired. The variation in bottom hole pressure for changes in pump rate is surprisingly low for this well, so the model might fit other wells with higher friction loss compared to hydrostatic pressure better. That being said, the flow through the well had to be extremely high in the nominal testing to get correct value for the friction parameter. When the friction is modelled as in the linear approximation in section 4.3, the bottom hole pressure estimate will be closer to the real pressure when the bottom hole pressure measurement is delayed, but the friction forces does not seem to behave exactly as the piecewise linear model, so the bottom hole pressure estimate will be erroneous for this simulation also. The kalman filter gave good estimate of the bottom hole pressure even when the bottom hole pressure measurement was absent for long periods. When the flow in the system was high, the estimate would deviate less than 4 bar from the real pressure even if the measurement was absent for most of the simulation.

A PI-controller is used to control the bottom hole pressure in the well during reference tracking and simulated pipe connection. The system dynamics are slow, since drilling fluid has to be extracted or pumped into the riser to lower or heighten the pressure and the pumps will hit their saturation point during the control cases. For the simulated pipe connection, the problem with the rapid alteration of the friction contribution at low flows, and the total absence of friction contribution at zero flow, leads to quite large deviation from the set point.

9.2 Future work

Since there are problems to estimate the friction parameter in the simplified model for this well, there is a need to test the model against other wells to see if the model will give better approximations in wells where the bottom hole pressure alter more when the flow is increased. Testing of the model against measurements done in a real well would show how this model will behave in real cases. If log data for typical drilling scenarios is obtained, testing of the model against these will reveal strengths and weaknesses of the estimation scheme.

If a method for estimating the friction contribution to the bottom hole pressure is found, it is believed that the model will give good estimation of the bottom hole pressure, even when this measurement is rarely updated and time delayed or absent for some time, since the error between the estimated and real bottom hole pressure is small for high flows when the friction contribution error is smaller.

The model only considers one phase flow, but in a real well, the flow can consist of cuttings and gas as well. Also, influx from the reservoir or loss of fluid from the well is not considered in the simulations, and this is something that should be investigated.

The model derived for the dual gradient drilling systems in this thesis is very simple. Deriving a new mathematical model with the possibility of estimating different parameters is something that should be considered. This can also lead to better estimates for the states and measurements considered in the existing model.

Bibliography

[1] Lars Imsland. *Modeling of hydraulics for adaptive pressure estimation, 2008*

[2] Pål Skalle. *Pressure control during drilling.* Tapir akademisk forlag, 2005.

[3] Schlumberger Oilfield Glossary, *http://www.glossary.oilfield.slb.com/*

[4] Neal J. Adams, Tommie Charrier. *Drilling Engineering. A Complete Well Planing Approach.* PennWell Books, 1985.

[5] Jean-Paul Nguyen. *Drilling.* Institut Francais du petrole publications, 1996.

[6] Øyen, Rogvin, Søgaard, Vea, Valstad. *Økt utvinning ved hjelp av integrerte operasjoner, Wired Drill Pipe på Gullfaks.* Project, NTNU - Norwegian University of Science and Technology, 2008.

[7] Don Hannegan. *Managed pressure drilling, SPE Advanced Drilling Technology and Well Construction Textbook*, 2007

[8] Matthew Daniel Martin. *Managed Pressure Drilling Techniques and Tools.* Master's thesis, Texas AM University, 2006

[9] Frank M. White. *Fluid Mechanics.*McGraw-Hill, 2008.

[10] Lennart Ljung. *System Identification. Theroy for the user.* Prentice Hall, 1999.

[11] Robert Grover Brown, Patrick Y. C. Hwang. *Introduction To Random Signals And Applied Kalman Filtering.* John Wiley and Sons, 1997.

[12] Ø. Breyholtz, G. Nygaard, E. H. Vefring. *Dual Gradient Drilling Concept Simulator using WeModForMatlab.* International Research Institute of Stavanger, 2008

[13] Jens G. Balchen, Trond Andresen, Bjarne A. Foss. *Reguleringsteknikk.* Institutt for teknisk kybernetikk, NTNU, 2003.

[14] Øyvind Nistad Stamnes. *Adaptive observer for bottomhole pressure during drilling.* Master's thesis, NTNU - Norwegian University of Science and Technology, 2007.

[15] Øyvind Breyholtz. *Nonlinear Model Predictive Pressure Control during Drilling Operations.* Master's thesis, NTNU - Norwegian University of Science and Technology, 2008.

[16] Thomas Rognmo. *Evaluation of Kalman filters for estimation of the annular bottomhole pressure during drilling.* Master's thesis, NTNU - Norwegian University of Science and Technology, 2008.

[17] Petros Ioannou, Jing Sun. *Robust Adaptive Control.* 1998.

[18] Jay A. Farrell, Matthew Barth. *The Global Positioning System Inertial Navigation*. McGraw Hill,1999.

[19] Neil Forrest, Tom Bailey, Don Hannegan. *Subsea Equipment for Deep Water Drilling Using Dual Gradient Mud System*. SPE/IADS 67707, 2001.

[20] K.L. Smith, A.D. Gault, D.E. Witt, C.E. Weddle. *SubSea MudLift Drilling Joint Industry Project: Delivering Dual Gradient Drilling Technology to Industry*. SPE 71357, 2001.

[21] J. P. Schumacher, J. D. Dowell, L. R. Ribbeck, J. C. Eggemeyer. *Subsea Mudlift Drilling: Planning and Preparation for the First Subsea Field Test of a Full-Scale Dual Gradient Drilling System at Green Canyon 136, Gulf of Mexico*. SPE71358, 2001.

[22] J. C. Eggemeyer, M. E. Akins, R. Brainard, R. A. Judge, C. P. Peterman, L. J. Scavone, K. S. Thethi. *SubSea MudLift Drilling: Design and Implementation of a Dual Gradient Drilling System*. SPE71359, 2001.

[23] Børre Fossli, Sigbjørn Sangesland. *Managed Pressure Drilling for Subsea Applications; Well Control Challenges in Deep Waters*. SPE/IADC 91633, 2004.

[24] Børre Fossli. *PRD12,000 Drill Ship; increasing Efficiency in Deep Water Operations*. SPE/IADC 112388, 2008.

[25] Mikolaj Stanislawek. *Analysis of alternative well control methods for dual density deepwater drilling*. Master's thesis, Louisiana State University, 2004.

[26] J.J. Schubert, H.C. Juckam-Wold, J. Choe. *Well-Control Procedures for Dual-Gradient Drilling as Compared to Conventional Riser Drilling*. SPE, 2006.

[27] Robert P. Herrmann, John M. Shaughnessy. *Two Mehods for Achieving a Dual Gradient in Deepwater*. SPE, 2001.

[28] Neil Forrest, Tom Bailey, Don Hannegan. *Subsea Equipment for Deep Water Drilling Using Dual Gradient Mud System*. SPE, 2001.

[29] J. C. Eggemeyer, M. E. Akins, R. R. Brainard, R. A. Judge, C. P. Peterman, L. J. Scavone, K. S. Thethi *SubSea MudLift Drilling: Design and Implementation of a Dual Gradient Drilling System*. SPE, 2001.

[30] Mohinder S. Grewal, Angus P. Andrews. *Kalman filtering : theory and practice using MATLAB*.Wiley, 2008.

[31] Dan Simon. *Optimal state estimation : Kalman, H [infinity] and nonlinear approaches*. Wiley-Interscience, 2006.

[32] Eli Brookner. *Tracking and Kalman filtering made easy*. Wiley, 1998.

Appendix A

Kalman filter theory

The following chapter describes the discrete Kalman filter and how it can be utilized to estimate states, disturbances and parameters of a set of non-linear difference equations.

A.1 Discretization of model

To implement a discrete Kalman filter, the model considered needs to be discrete.

A.2 Kalman filter theory

The Kalman filter provides a recursive solution to the linear optimal filtering problem, and is rooted in the state-space formulation of linear dynamical systems. It applies to stationary as well as non stationary environments. Each state is computed from the previous estimate and the new input data, and thus the required storage space is limited to the previous estimate. In addition to eliminating the need for storing the entire past observed data, the Kalman filter is computationally more efficient than computing the estimate directly from the entire past observed data at each step of the filtering process. This chapter describes the deviation of the equations for the discrete Kalman filter, and further the extension to the unscented Kalman filter.

A.3 Discrete Kalman filter

Suppose a process equation is given by

$$x_{k+1} = F_{k+1,k}x_k + w_k \tag{A.1}$$

where $F_{k+1,k}$ is the transition matrix taking the state x_k from time k to time k + 1. w_k is the process noise, and it is assumed to be white and Gaussian, with zero mean and with covaraince matrix defined by

$$E[w_n w_k^T] = \begin{cases} Q_k, n = k \\ 0, n \neq k \end{cases} \tag{A.2}$$

The measurement equation is given by

$$y_k = H_k x_k + v_k \tag{A.3}$$

where y_k is the measurements at time k and H_k is the measurement matrix. The measurement noise v_k is assumed to be additive, white, and Gaussian, with zero mean and with covairance matrix defined by

$$E[v_n v_k^T] = \begin{cases} R_k, n = k \\ 0, n \neq k \end{cases} \tag{A.4}$$

The measurement noise v_k is uncorrelated with the process noise w_k. The dimension of the measurement space is denoted by N.

Suppose that a measurement on a linear dynamical system, described by A.1 and A.3 has been made at time k. The requirement is to use the information contained in the new measurement y_k to update the estimate of the unknown state x_k. If $\hat{x}_k^-$ denotes the a priori estimate of the state which is avaliable at time k, we may express the a posteriori estimate $\hat{x}_k$ as a linear combination of the a priori estimate and the new measurement with a linear estimator as the objective,.

$$\hat{x}_k = G_k^{(l)} \hat{x}_k^- + G_k y_k \tag{A.5}$$

where the matrices $G_k^{(l)}$ and G_k has to be determined. The state-error vector is defined by

$$\tilde{x}_k = x_k - \hat{x}_k \tag{A.6}$$

and by applying the principle of orthogonality to this equation, we may write

$$E[\tilde{x}_k y_i^T] = 0, i = 1, 2, ..., k-1 \tag{A.7}$$

using equations A.3, A.5 and A.6 in A.7, we get

$$E[(x_k - G_k^{(l)} \hat{x}_k^- - G_k H_k x_k - G_k w_k) y_i^T] = 0, i = 1, 2, ..., k-1 \tag{A.8}$$

A.4 Extended Kalman Filter

The EKF approach is to apply the standard Kalman filter (for linear systems) to nonlinear systems with additive white noise by continually updating a linearization around the previous state estimate, starting with an initial guess. In other words, we only consider a linear Taylor approximation of the system function at the previous state estimate and that of the observation function at the corresponding predicted position. This approach gives a simple and efficient algorithm to handle a nonlinear model. However, convergence to a reasonable estimate may not be obtained if the initial guess is poor or if the disturbances are so large that the linearization is inadequate to describe the system.

If we consider the system model

$$x_k = f_{k-1}(x_{k-1}, u_{k-1}, w_{k-1}) \tag{A.9}$$
$$y_k = h_k(x_k, v_k) \tag{A.10}$$
$$w_k = (0, Q_k) \tag{A.11}$$
$$v_k = (0, R_k) \tag{A.12}$$

By performing a Taylor series expansion of the state equation around $x_{k-1} = \hat{x}^+_{k-1}$ and $w_{k-1} = 0$, we obtain:

$$\begin{aligned} x_k &= f_{k-1}(\hat{x}^+_{k-1}, u_{k-1}, 0) + \frac{\partial f_{k-1}}{\partial x}|_{\hat{x}^+_{k-1}}(x_{k-1} - \hat{x}^+_{k-1}) + \frac{\partial f_{k-1}}{\partial w}|_{\hat{x}^+_{k-1}} w_{k-1} \\ &= f_{k-1}(\hat{x}^+_{k-1}, u_{k-1}, 0) + F_{k-1}(x_{k-1} - \hat{x}^+_{k-1}) + L_{k-1}w_{k-1} \\ &= F_{k-1}x_{k-1} + [f_{k-1}(\hat{x}^+_{k-1}, u_{k-1}, 0) - F_{k-1}\hat{x}^+_{k-1}]L_{k-1}w_{k-1} \\ &= F_{k-1}x_{k-1} + \tilde{u}_{k-1} + \tilde{w}_{k-1} \end{aligned} \tag{A.13}$$

where $F_{k-1} = \frac{\partial f_{k-1}}{\partial x}|_{\hat{x}^+_{k-1}}$ and $L_{k-1} = \frac{\partial f_{k-1}}{\partial w}|_{\hat{x}^+_{k-1}}$. The known signal $\tilde{u}_k$ and the noise signal $\tilde{w}_k$ are defined as

$$\tilde{u}_k = f_k(\hat{x}^+_k, u_k, 0) - F_k\hat{x}^+_k \tag{A.14}$$
$$\tilde{w}_k \sim (0, L_kQ_kL_k^T) \tag{A.15}$$

The measurement equation is linearized around $x_k = \hat{x}^-_k$ and $v_k = 0$ and gives

$$\begin{aligned} y_k &= h_k(\hat{x}^-_k, 0) + \frac{\partial h_k}{\partial x}|_{\hat{x}^-_k}(x_k - \hat{x}^-_k) + \frac{\partial h_k}{\partial v}|_{\hat{x}^-_k} v_k \\ &= h_k(\hat{x}^-_k, 0) + H_k(x_k - \hat{x}^-_k) + M_kv_k \\ &= H_kx_k + [h_k(\hat{x}^-_k, 0) - H_k\hat{x}^-_k] + M_kv_k \\ &= H_kx_k + z_k + \tilde{v}_k \end{aligned} \tag{A.16}$$

where $H_k = \frac{\partial h_k}{\partial x}|_{\hat{x}^-_k}$ and $M_k = \frac{\partial h_k}{\partial v}|_{\hat{x}^-_k}$. The known signal z_k and the noise signal $\tilde{v}_k$ are defined as

$$z_k = h_k(\hat{x}^-_k, 0) - H_k\hat{x}^-_k \tag{A.17}$$
$$\tilde{v}_k \sim (0, M_kR_kM_k^T \tag{A.18}$$

This gives a linear state-space system in equation A.14 and a linear measurement equation in equation A.17. The standard Kalman filter equations can then be applied to estimate the state. For the discrete time extended Kalman filter, the equations will then be given as

$$P_k^- = F_{k-1}P_{k-1}^+F_{k-1}^T + L_{k-1}Q_{k-1}L_{k-1}^T \tag{A.19}$$
$$K_k = P_k^- H_k^T (H_k P_k^- H_k^T + M_k R_k M_k^T)^{-1} \tag{A.20}$$
$$\hat{x}_k^- = f_{k-1}(\hat{x}_{k-1}^+, u_{k-1}, 0) \tag{A.21}$$
$$z_k = h_k(\hat{x}_k^-, 0) - H_k\hat{x}_k^- \tag{A.22}$$
$$\hat{x}_k^+ = \hat{x}_k^- + K_k(y_k - H_k\hat{x}_k^- - z_k) \tag{A.23}$$
$$= \hat{x}_k^- + K_k[y_k - h_k(\hat{x}_k^-, 0)] \tag{A.24}$$
$$P_k^+ = (I - K_k H_k)P_k^- \tag{A.25}$$